Research Project Number TPF-5(193) Supplement #130

ENERGY ANALYSIS OF VEHICLE-TO-CABLE BARRIER IMPACTS

Submitted by

Jennifer Schmidt, Ph.D., E.I.T.
Post-Doctoral Research Associate

Curt L. Meyer, M.S.M.E., E.I.T.
Former Research Associate Engineer

Karla A. Lechtenberg, M.S.M.E., E.I.T.
Research Associate Engineer

Ronald K. Faller, Ph.D., P.E.
Research Associate Professor
Interim MwRSF Director

Robert W. Bielenberg, M.S.M.E., E.I.T.
Research Associate Engineer

Cody S. Stolle, Ph.D., E.I.T.
Post-Doctoral Research Associate

Dean L. Sicking, Ph.D., P.E.
Emeritus Professor
Former MwRSF Director

John D. Reid, Ph.D.
Professor

MIDWEST ROADSIDE SAFETY FACILITY
Nebraska Transportation Center
University of Nebraska-Lincoln
130 Whittier Research Center
2200 Vine Street
Lincoln, Nebraska 68583-0853
(402) 472-0965

Submitted to

NEW YORK STATE DEPARTMENT OF TRANSPORTATION
50 Wolf Road, 6th Floor
Albany, New York 68502

MwRSF Research Report No. TRP-03-283-13

June 11, 2013

TECHNICAL REPORT DOCUMENTATION PAGE

1. Report No. TRP-03-283-13	2.	3. Recipient's Accession No.	
4. Title and Subtitle Energy Analysis of Vehicle-to-Cable Barrier Impacts		5. Report Date June 11, 2013	
		6.	
7. Author(s) Schmidt, J.D., Meyer, C.L., Lechtenberg, K.A., Faller, R.K., Bielenberg, R. W., Stolle, C.S., Reid, J.D., and Sicking, D.L.		8. Performing Organization Report No. TRP-03-283-13	
9. Performing Organization Name and Address Midwest Roadside Safety Facility (MwRSF) Nebraska Transportation Center University of Nebraska-Lincoln 130 Whittier Research Center 2200 Vine Street Lincoln, Nebraska 68583-0853		10. Project/Task/Work Unit No.	
		11. Contract or Grant No. TPF-5(193) Supplement #130	
12. Sponsoring Organization Name and Address New York State Department of Transportation 50 Wolf Road, 6th Floor Albany, New York 68502		13. Type of Report and Period Covered Final Report: 2010 – 2013	
		14. Sponsoring Agency Code	
15. Supplementary Notes Prepared in cooperation with U.S. Department of Transportation, Federal Highway Administration.			

16. Abstract

An accident reconstruction technique was developed for estimating the energy absorbed during an impact with a cable barrier system as well as the initial impact velocity. The kinetic energy absorbed during a cable barrier system impact is comprised of several components: (1) plastic deformation/rotation of posts in a rigid foundation or soil foundation; (2) vehicle-ground interaction; (3) internal cable energy; and (4) frictional losses during vehicle-barrier interaction. The energy absorbed by deforming the J-bolt clips was analyzed and determined to be negligible for this study. Charts were developed that estimate the energy absorbed by deforming S3x5.7 (S76x8.5) cable line posts based on the soil condition, deformed post orientation, and deformed post height above the ground. Charts were also developed relating the cable tension to the cable energy absorbed versus the lateral deflection of the vehicle and the frictional energy versus the vehicle's distance traveled for both a straight cable system and an exterior-curved cable system. However, without additional crash testing to verify the relationships, these charts are only applicable to the cable barrier systems for which the full-scale crash tests were conducted. In the straight system impact, the vehicle's estimated initial velocity using the reconstruction technique was 55.1 mph ± 3.0 mph (88.7 km/h ± 4.9 km/h), and the actual velocity of the vehicle was 61.6 mph (99.1 km/h). In one curved system impact, the vehicle's estimated initial velocity was 61.0 mph ± 0.3 mph (98.1 km/h ± 0.4 km/h), and the actual velocity of the vehicle was 61.6 mph (99.1 km/h). In another curved system impact, the vehicle's estimated initial velocity was 63.2 mph ± 2.4 mph (101.6 km/h ± 3.7 km/h), and the actual velocity of the vehicle was 63.1 mph (101.6 km/h). Future improvements for the cable barrier system accident reconstruction procedure are discussed.

17. Document Analysis/Descriptors Highway Safety, Crash Test, Roadside Appurtenances, Accident Reconstruction, Energy Analysis, Cable Barrier System, and Speed Determination		18. Availability Statement No restrictions. Document available from: National Technical Information Services, Springfield, Virginia 22161	
19. Security Class (this report) Unclassified	20. Security Class (this page) Unclassified	21. No. of Pages 92	22. Price

DISCLAIMER STATEMENT

This report was completed with funding from the New York State Department of Transportation. The contents of this report reflect the views and opinions of the authors who are responsible for the facts and the accuracy of the data presented herein. The contents do not necessarily reflect the official views or policies of the New York State Department of Transportation nor the Federal Highway Administration, U.S. Department of Transportation. This report does not constitute a standard, specification, regulation, product endorsement, or an endorsement of manufacturers.

UNCERTAINTY OF MEASUREMENT STATEMENT

The Midwest Roadside Safety Facility (MwRSF) has determined the uncertainty of measurements for several parameters involved in standard full-scale crash testing and non-standard testing of roadside safety features. Information regarding the uncertainty of measurements for critical parameters is available upon request by the sponsor and the Federal Highway Administration.

ACKNOWLEDGEMENTS

The authors wish to acknowledge several sources that made a contribution to this project: (1) the New York State Department of Transportation for sponsoring this project; and (2) MwRSF personnel for constructing the barriers and conducting the crash tests.

Acknowledgement is also given to the following individuals who made a contribution to the completion of this research project.

Midwest Roadside Safety Facility

J.C. Holloway, M.S.C.E., E.I.T., Test Site Manager
S.K. Rosenbaugh, M.S.C.E., E.I.T., Research Associate Engineer
A.T. Russell, B.S.B.A., Shop Manager
K.L. Krenk, B.S.M.A., Maintenance Mechanic
S.M. Tighe, Laboratory Mechanic
D.S. Charroin, Laboratory Mechanic
Undergraduate and Graduate Research Assistants

New York State Department of Transportation

Lyman L. Hale III, Senior Engineer
Pratip Lahiri, P.E., Standards and Specifications Section
Robert Lohse, Design Quality Assurance Bureau
James Turley, Design Quality Assurance Bureau

TABLE OF CONTENTS

LIST OF FIGURES

LIST OF TABLES

1 INTRODUCTION

1.1 Introduction

The New York State Department of Transportation has received requests from New York State police investigators regarding the amount of energy that is absorbed during the process of "flattening" a standard cable barrier weak post. The energy absorbed through the deformation/rotation of posts can aid in accident reconstructions, particularly as it relates to determining initial impact velocity. The kinetic energy of a vehicle, which is directly related to the velocity, decreases in a run-off-road crash through rolling resistance, braking, sliding, deformation or fracture of impacted objects, friction, and other factors. Therefore, quantifying the energy absorbed through each of these events can help reconstruct the initial velocity of the vehicle through the principle of the conservation of energy. However, determining if or when these events happened and the amount of energy absorbed through each event can be difficult to quantify.

1.2 Objective

The objective of this study was to develop a procedure for estimating the vehicle's initial velocity and the energy absorbed during a vehicular impact with a cable guardrail system. The vehicle's energy dissipation is to be investigated as a function of time and various events.

1.3 Scope

The research study was accomplished by completing a series of tasks. First, quantifiable energy-absorbing components or events were identified. Evaluation of each system component was completed. A reconstruction procedure was developed and analyzed for estimating the total quantifiable energy absorbed during a vehicle impact with a barrier system and subsequently the initial velocity of the vehicle. Recommendations for improving the predictive reconstruction procedure were made. Several full-scale crash tests, including those conducted on curved, low-

tension, three-cable barrier systems detailed in Volume I [1], were used to validate the methods proposed in this report.

2 ENERGY ABSORPTION PARAMETERS

Due to the difficulty gathering values and other values considered insignificant, the study focused on five energy-absorbing events:

1. plastic deformation/rotation of posts in a rigid foundation or soil;
2. internal cable losses;
3. vehicle-ground interaction;
4. vehicle-barrier frictional interaction; and
5. cable-to-post attachment deformation.

The analysis was limited to low-tension cable barriers. As such, all posts considered in this study were S3x5.7 (S76x8.5) steel line posts, and all cable-to-post attachments were 5/16-in. (8-mm) J-bolts. Previous studies pertaining to cable barrier systems and components conducted at the Midwest Roadside Safety Facility (MwRSF) were utilized during the crash investigation and analysis phase of this project. In particular, several full-scale crash tests have been performed on cable barrier systems [1-2]. In addition, the MwRSF has also conducted component tests on S3x5.7 (S76x8.5) posts [3-5] and J-bolts [6]. Finally, a finite element analysis of cable wire rope was also used [7].

2.1 Plastic Deformation/Rotation of Posts

A plastic hinge is commonly formed at the groundline as cable barrier line posts are deformed. Kinetic energy is absorbed by plastic flow in the hinge location. The amount of energy is dependent on the soil/foundation, post material, the direction of bending (strong or weak axis), and the lateral deflection of the post.

Line posts in low-tension, three-cable barrier systems are typically ASTM A36 S3x5.7 (S76x8.5) steel posts. The A36 steel specification has a minimum yield strength of 36 ksi (248 MPa), but the material typically has yield strengths varying from 46 ksi to 56 ksi (317 MPa to

386 MPa) depending on the manufacturer. Since ASTM A992 rolled shapes have become more common than ASTM A36 rolled shapes, many new S3x5.7 (S76x8.5) steel posts may be fabricated with ASTM A992 steel. The ASTM A992 material specification has a minimum yield strength of 50 ksi (345 MPa) and a maximum yield strength specification of 65 ksi (450 MPa). The energy absorbed by the post will increase when the yield strength of the steel is higher. However, for line posts already in cable barrier installations, the yield strengths would be difficult to determine.

In prior research studies, MwRSF conducted dynamic component testing with a bogie vehicle in which force vs. lateral deflection was determined for S3x5.7 (S76x8.5) cable line posts at various impact angles [3-5]. The post testing setup and methodology is described in Appendix A. The mill certifications containing the yield strength and ultimate strength for these tests were not available, but the data is assumed to be representative of ASTM A36 steel cable barrier system posts. The posts were tested in rigid sleeves at 0, 60, 75, and 90 degree angles in test series CMPB [3] and CCP [4]. The posts also were tested in a compacted, crushed limestone soil material at 0, 82.5, and 90 degree angles in test series CMPB [3] and CPB [5]. Angles were measured from the direction of a weak-axis impact (i.e., 0 degrees = weak-axis impact, 90 degrees = strong-axis impact). In a strong-axis post impact, or where the post is bent backward from cable loading, the post will usually twist from a 90 orientation after some time, so it can be difficult to determine the correct deformed post orientation. The dynamic component tests were used to determine the energy absorption of S3x5.7 (S76x8.5) cable barrier line posts.

The S3x5.7 (S76x8.5) is often deemed a weak post in highway guardrail systems, which means the post usually deforms before there is much post rotation in soil. Therefore, the energy absorbed by the S3x5.7 (S76x8.5) post in soil in weak-axis impacts is similar to the energy absorbed by the post in a rigid sleeve. Since most of the New York State cable barrier systems

are installed in soil that may be frozen four months out of the year, often with a thick layer of asphalt at the surface for vegetation control, the posts will usually behave similar to the posts in rigid sleeves. However, in strong-axis impacts, the soil may be displaced. If the posts are installed in soil with no asphalt overlay, the energy absorbed by the posts may be lower. The energy absorption due to the plastic deformation/rotation of the S3x5.7 (S76x8.5) posts in both rigid sleeves and in soil were analyzed.

2.1.1 S3x5.7 (S76x8.5) Posts Embedded in a Rigid Sleeve

Four tests were conducted on S3x5.7 (S76x8.5) steel posts embedded in a rigid sleeve. The bogie impacted the posts at a speed of approximately 20 mph (32.2 km/h) and at a height of 21.7 in. (550 mm) above the ground. However, the angle of impact varied from test to test as shown in Table 1. The force vs. deflection and energy vs. deflection results are shown in Figures 1 through 4 for test nos. CCP-5, CMPB-5, CMPB-4, and CMPB-6, respectively.

Table 1. Summary of S3x5.7 (S76x8.5) Posts Embedded in Rigid Sleeve

Test No.	Impact Height in. (mm)	Impact Speed mph (km/h)	Impact Angle degrees	Reference
CCP-5	21.7 (550)	20.1 (32.3)	0 (weak axis)	4
CMPB-5	21.7 (550)	20.7 (30.3)	60	3
CMPB-4	21.7 (550)	21.6 (34.8)	75	3
CMPB-6	21.7 (550)	19.8 (32.2)	90 (strong axis)	3

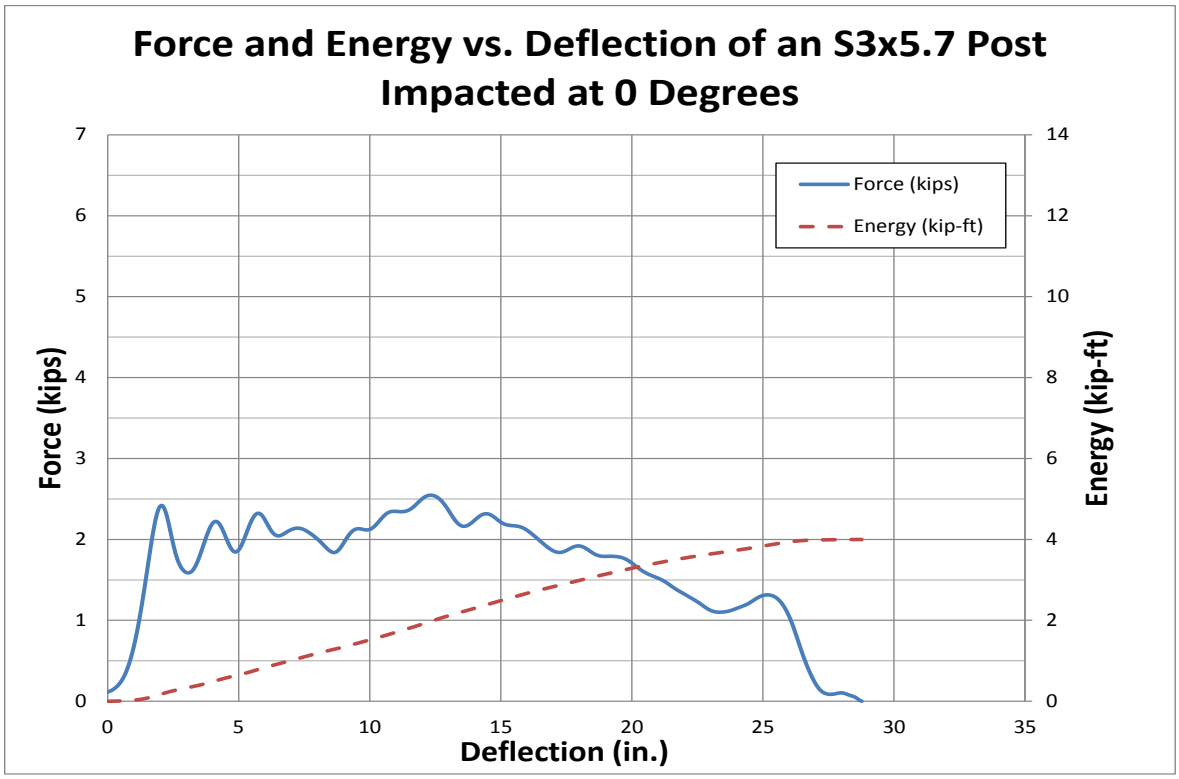

Figure 1. Test No. CCP-5 Results – 0 Degree (Weak Axis) Impact in Sleeve

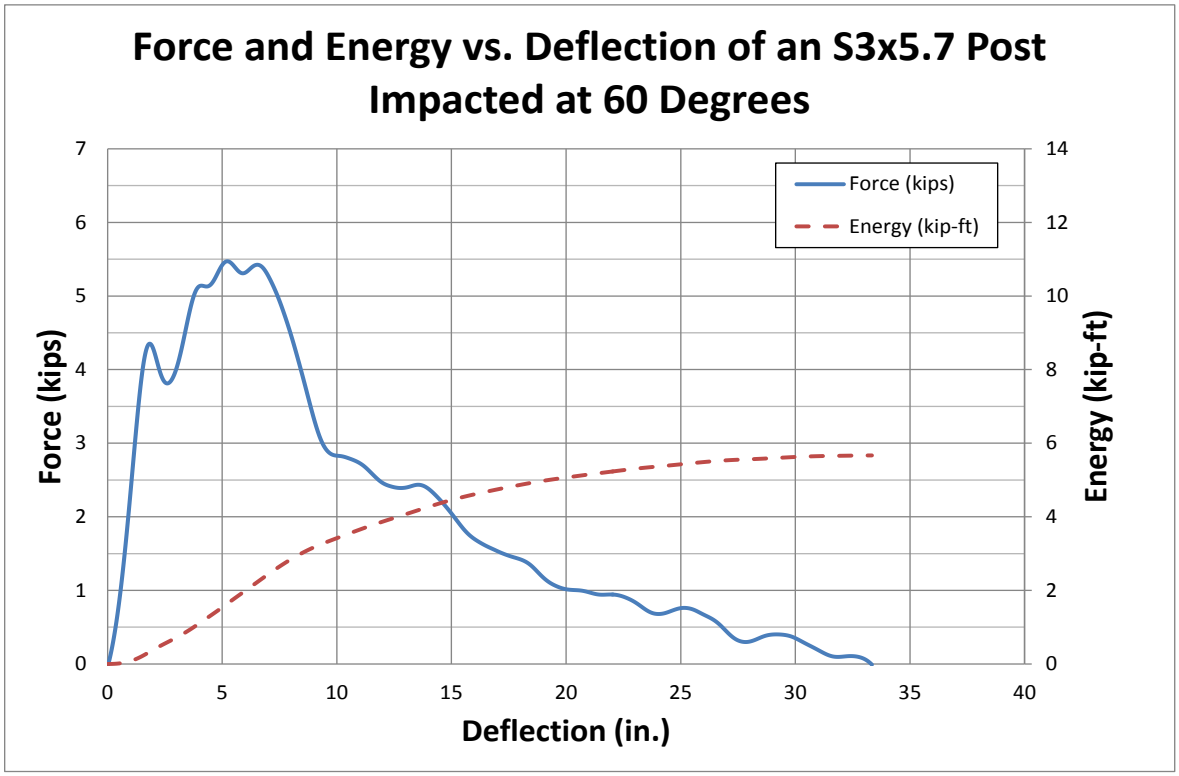

Figure 2. Test No. CMPB-5 Results – 60 Degree Impact in Sleeve

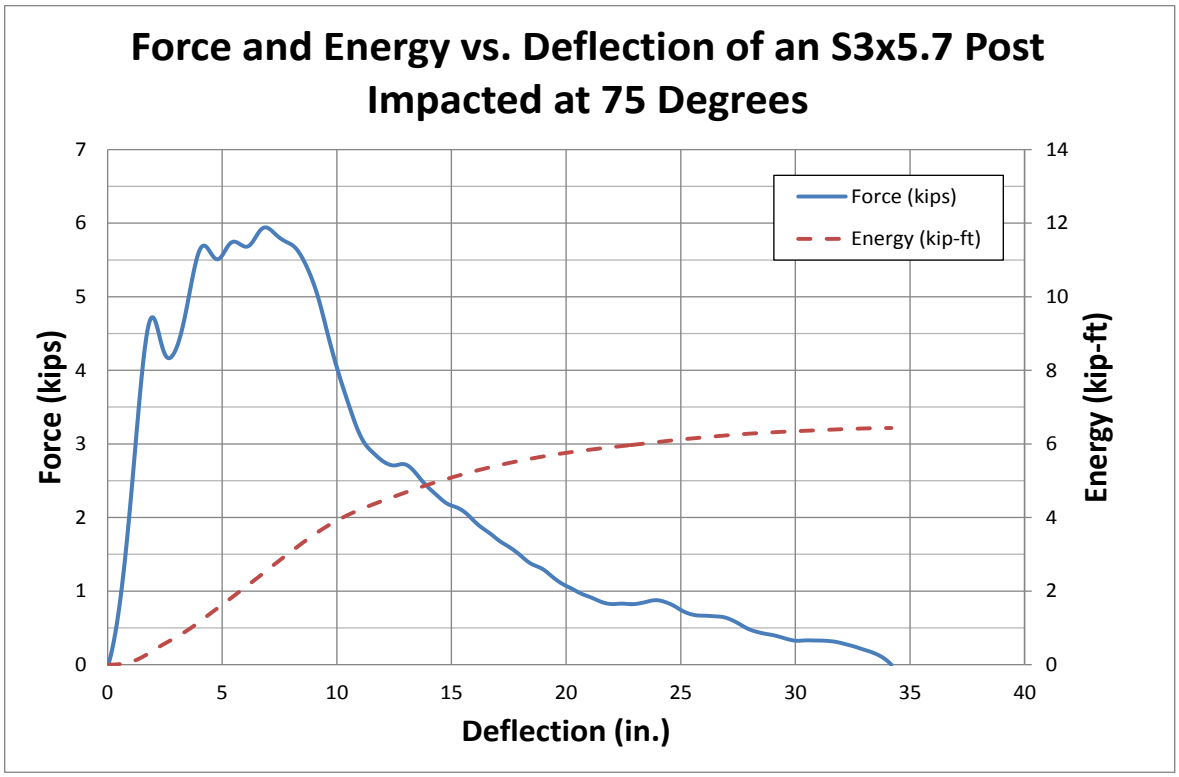

Figure 3. Test No. CMPB-4 Results – 75 Degree Impact in Sleeve

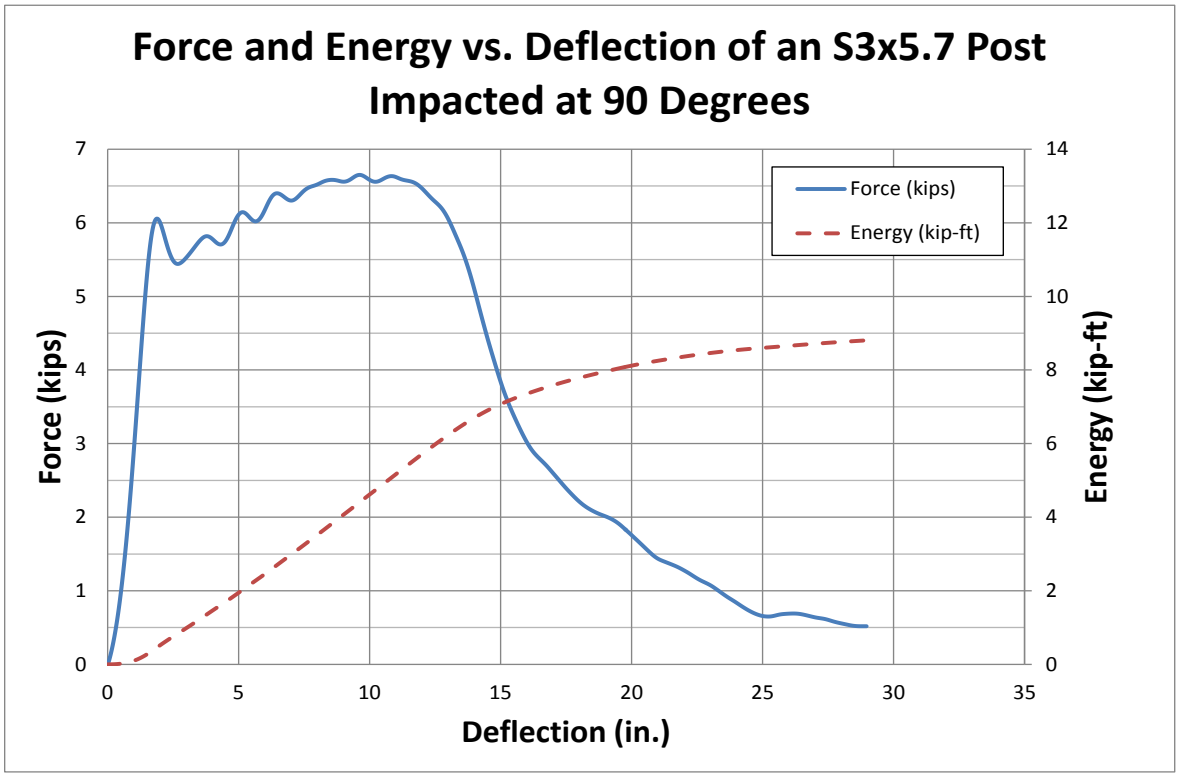

Figure 4. Test No. CMPB-6 Results – 90 Degree (Strong Axis) Impact in Sleeve

2.1.2 S3x5.7 (S76x8.5) Posts Embedded in Soil

Three tests were conducted on S3x5.7 (S76x8.5) steel posts embedded 30 in. (762 mm) in soil. In all tests, the bogie impacted the posts at a speed of approximately 20 mph (32.2 km/h). In test no. CPB-6, the bogie impacted the post at a height of 27 in. (686 mm) above the ground. In test nos. CMPB-15 and CMPB-14, the bogie impacted the posts at a height of 21.7 in. (550 mm) above the ground. The angle of impact varied from test to test as shown in Table 2. The force vs. deflection and energy vs. deflection results are shown in Figures 5 through 7 for test nos. CPB-6, CMPB-15, and CMPB-14, respectively. The bogie used in test no. CPB-6 was not completely rigid, so the force curve had vibrations.

Table 2. Summary of S3x5.7 (S76x8.5) Posts Embedded in Soil

Test No.	Impact Height in. (mm)	Impact Speed mph (km/h)	Impact Angle degrees	Reference
CPB-6	27 (686)	20.0 (32.2)	0 (weak axis)	5
CMPB-15	21.7 (550)	20.1 (32.3)	82.5	3
CMPB-14	21.7 (550)	21.6 (34.8)	90 (strong axis)	3

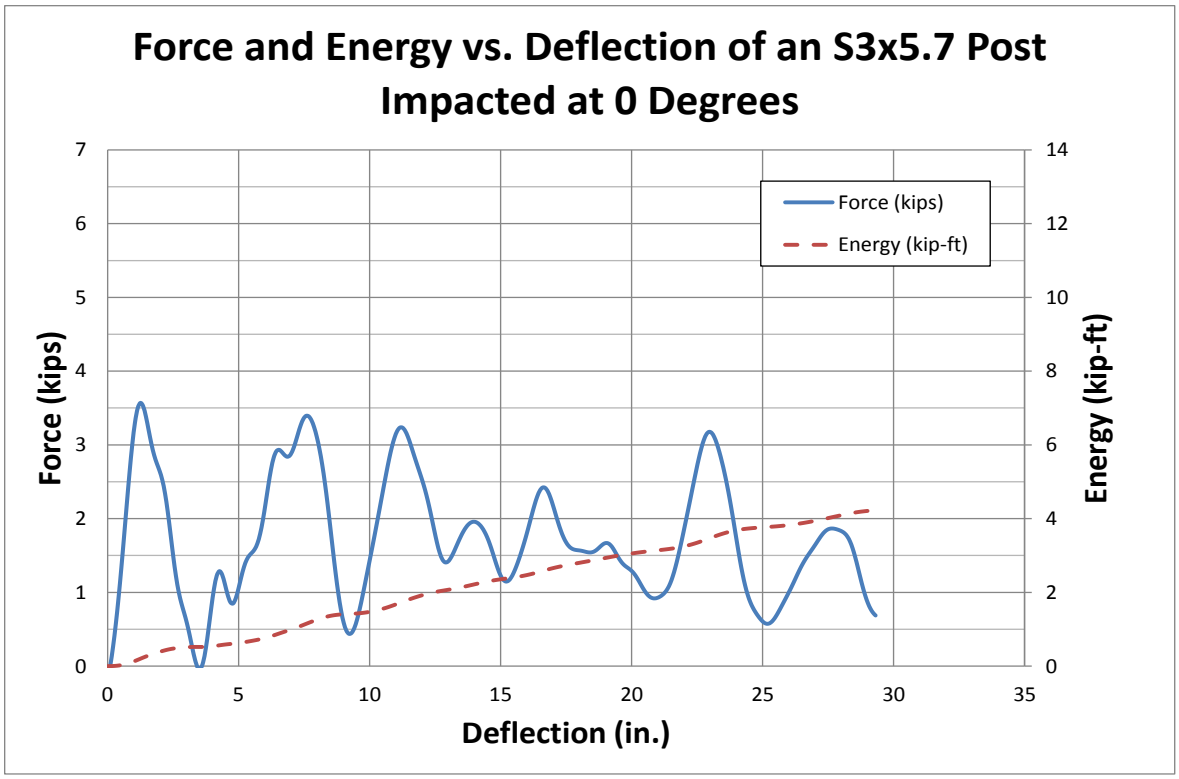

Figure 5. Test No. CPB-6 Results – 0 Degree (Weak Axis) Impact in Soil

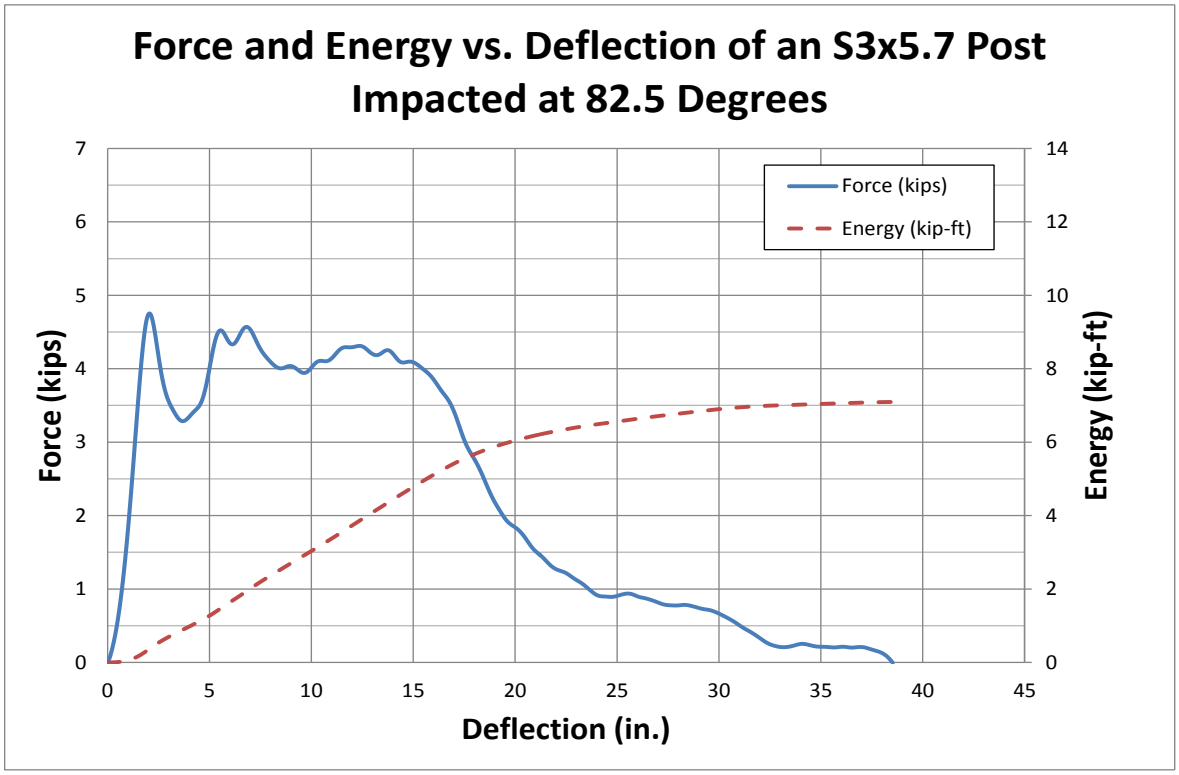

Figure 6. Test No. CMPB-15 Results – 82.5 Degree Impact in Soil

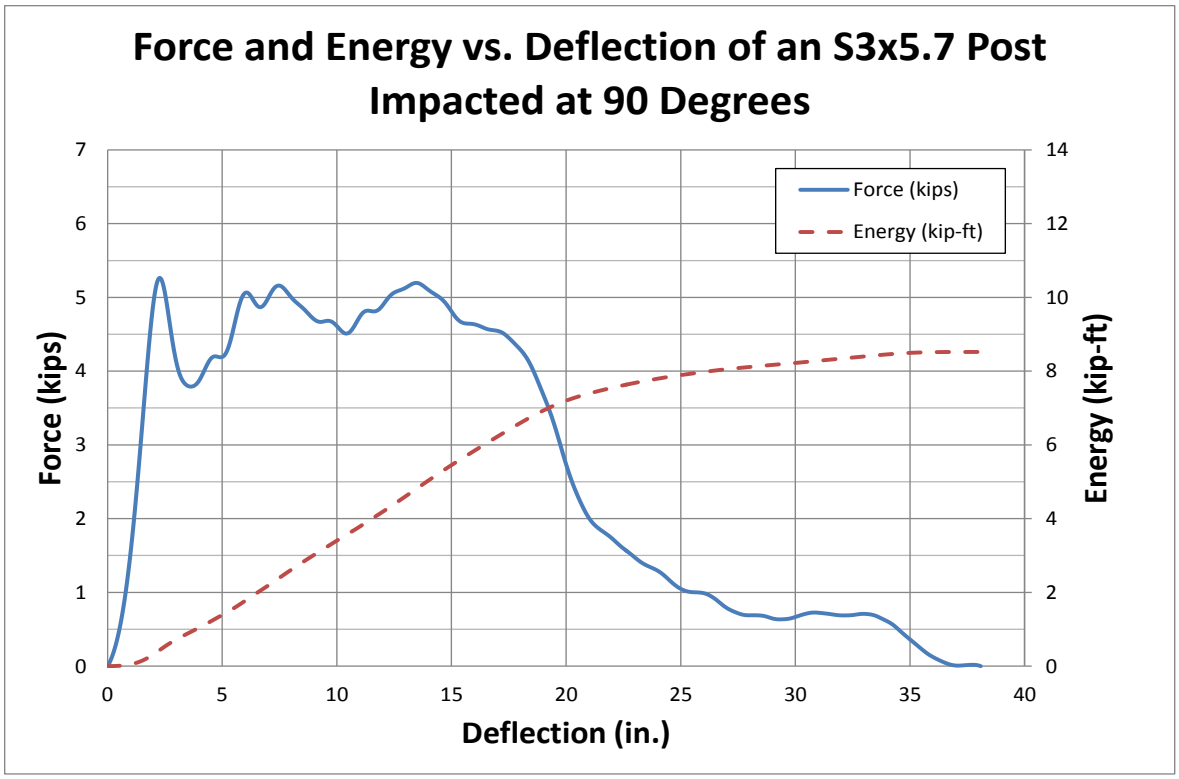

Figure 7. Test No. CMPB-14 Results – 90 Degree (Strong Axis) Impact in Soil

If the cable barrier line posts are installed in soil, or if the asphalt layer allows the posts to rotate at groundline, the energy absorbed by each post will decrease. Comparisons of the energy vs. deflection of S3x5.7 (S76x8.5) posts embedded in soil and rigid sleeves are shown in Figures 8 and 9 for impacts at 0 and 90 degrees, respectively. A vehicle impacting at a 0-degree angle (i.e. vehicle parallel to the system) would be more common. At this angle, there is a minimal difference in the energy absorption over 29 in. (737 mm) of deflection. For a 90-degree impact angle, 25% less energy can be absorbed by an S3x5.7 (S76x8.5) post in soil compared to a rigid sleeve. When the post rotates in soil, less energy is absorbed than through plastic deformation of posts.

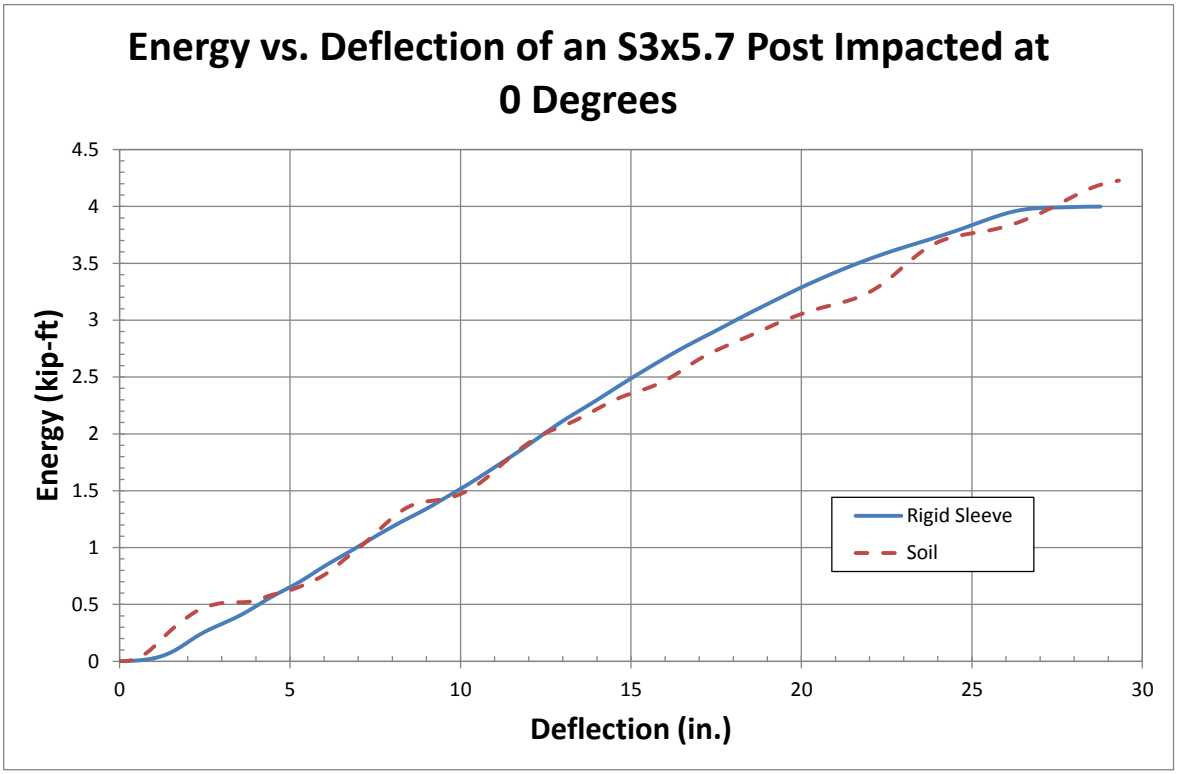

Figure 8. Energy vs. Deflection – S3x5.7 (S76x8.5) Post in Soil and Rigid Sleeve – 0 Degrees

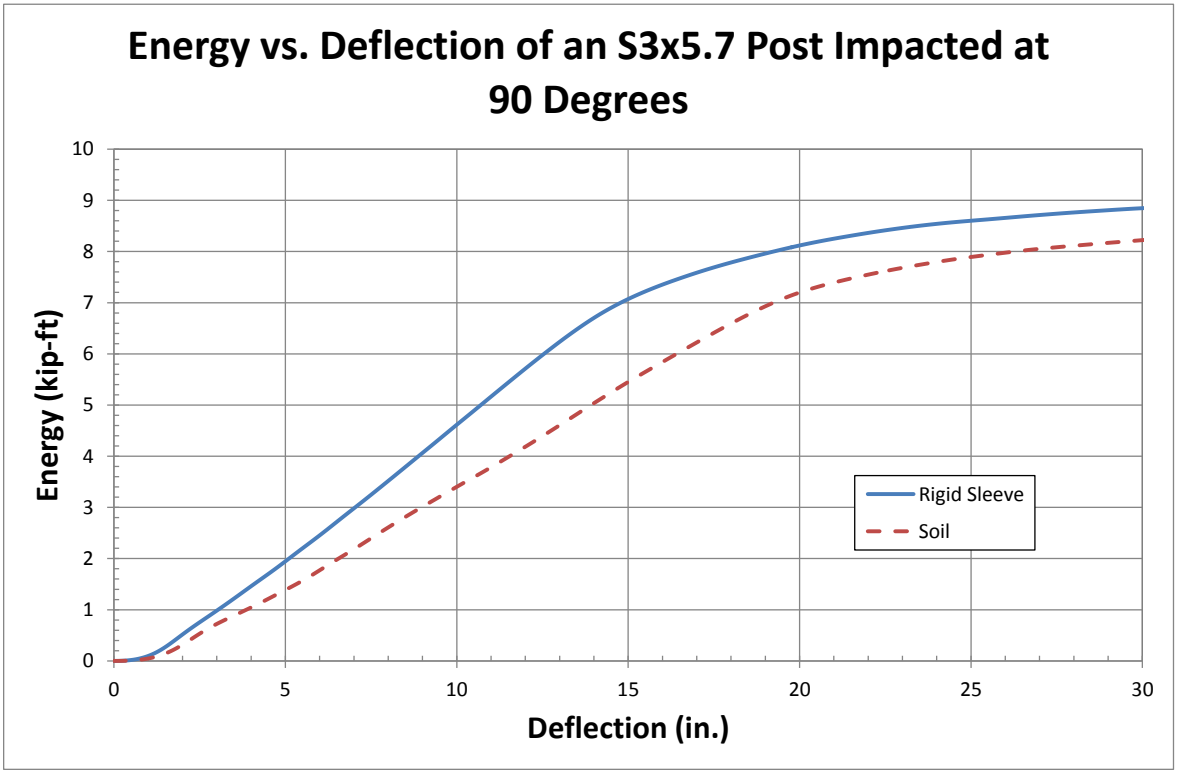

Figure 9. Energy vs. Deflection – S3x5.7 (S76x8.5) Post in Soil and Rigid Sleeve – 90 Degrees

2.1.3 Data Transformation

In order to use the data shown in Figures 1 through 7, the deflection of the post along its impact angle axis would need to be measured. This may be difficult to measure after an impact event. Therefore, to simplify the measurement for the accident reconstructionist, the post deflections were converted into deformed heights above the ground. The energy absorption of the deformed S3x5.7 (S76x8.5) cable post can then be determined by measuring the deformed post height and estimating the deformed post orientation.

According to the NYSDOT, installed cable barrier line posts may vary in height from 28 in. to 33 in. (711 mm to 838 mm). The 30-in. (762-mm) post height is the standard height for the New York State curved cable system, but it was also recommended to use a 32-in. (813-mm) post height for installations on large radii curves (e.g. 440 ft (134 m)) [1]. The 33-in. (838-mm) post height has been installed previously and may currently exist on roadsides. Further, variations in post height may develop in service or due to soil erosion or overlays.

A diagram of a deforming post is shown in Figure 10. Assuming the posts yield at groundline and that the upper portion of the post rotates about the hinge point, the bogie's maximum lateral deflection that could occur is equal to the bogie impact height. The energy absorption of the posts in rigid sleeves versus bogie's lateral deflection (up to 21.7 in. (550 mm)) along the impact axis orientation is shown in Figure 11. However, the contact height on the post varies as the post is bent, and this is not accounted for in the analysis. Therefore, post deflections exceeded the 21.7 in. (550 mm) post impact height, as shown in Figures 1 through 7. The lateral deflections at the bogie impact height were converted to lateral deflections at the top of the post assuming a groundline yield rotation point of the post and the geometry of similar triangles. Using the dimensions of the installed post height and lateral deflection at the top of the post, the deformed post height above the ground was calculated. The final deformed height of the post

never reached zero (flat on the ground), but the energy changed minimally when the height of the post was 0 to 10 in. (0 to 254 mm) above the ground. Energy vs. deformed post height above the ground at impact angles from 0 to 90 degrees in rigid sleeves are shown in Figures 12 through 17 for installed post heights from 28 in. to 33 in. (711 mm to 838 mm), respectively. The energy absorption of the posts in soil versus the lateral deflection along the impact axis orientation is shown in Figure 18. Energy vs. deformed post height above the ground at impact angles from 0 to 90 degrees in soil are shown in Figures 19 through 24 for installed post heights from 28 in. to 33 in. (711 mm to 838 mm), respectively. The soil charts should be used if soil gaps are present around the base of the post that implies the post rotated before the plastic deformation began. The data can be extrapolated for other deformed post orientations. The post height should be measured from the ground to the top of front flange of the post.

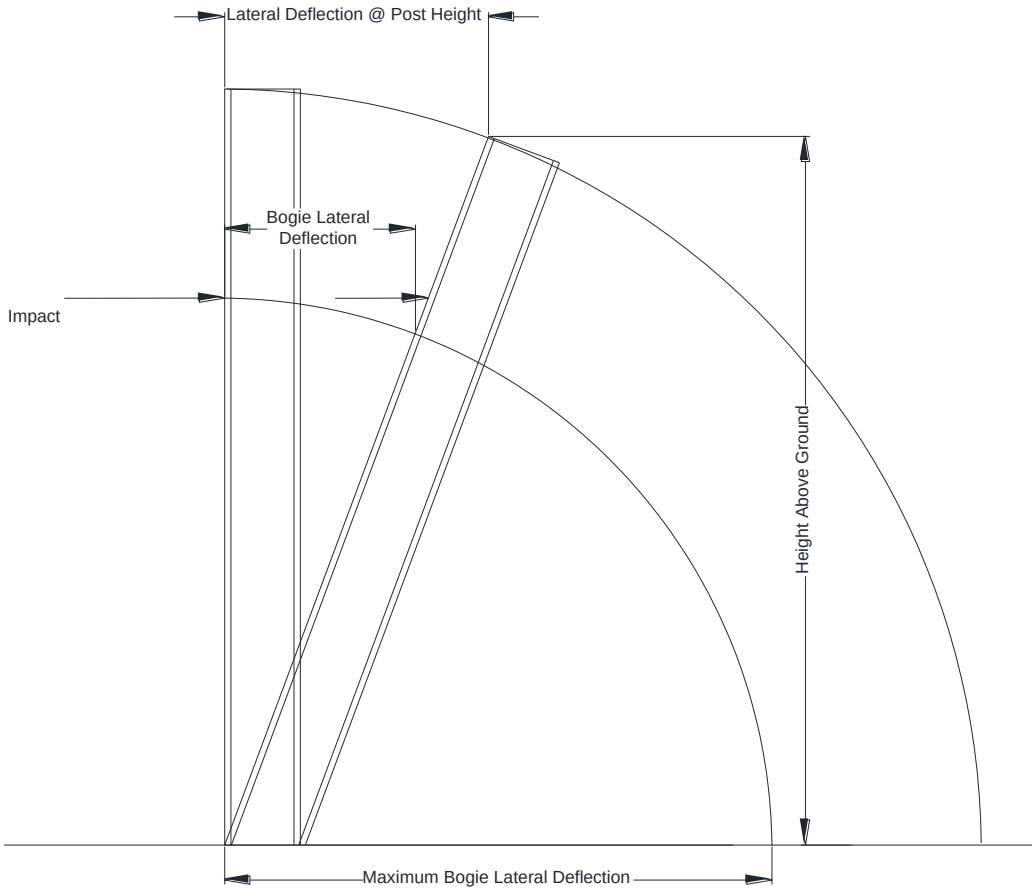

Figure 10. Deforming Post Diagram

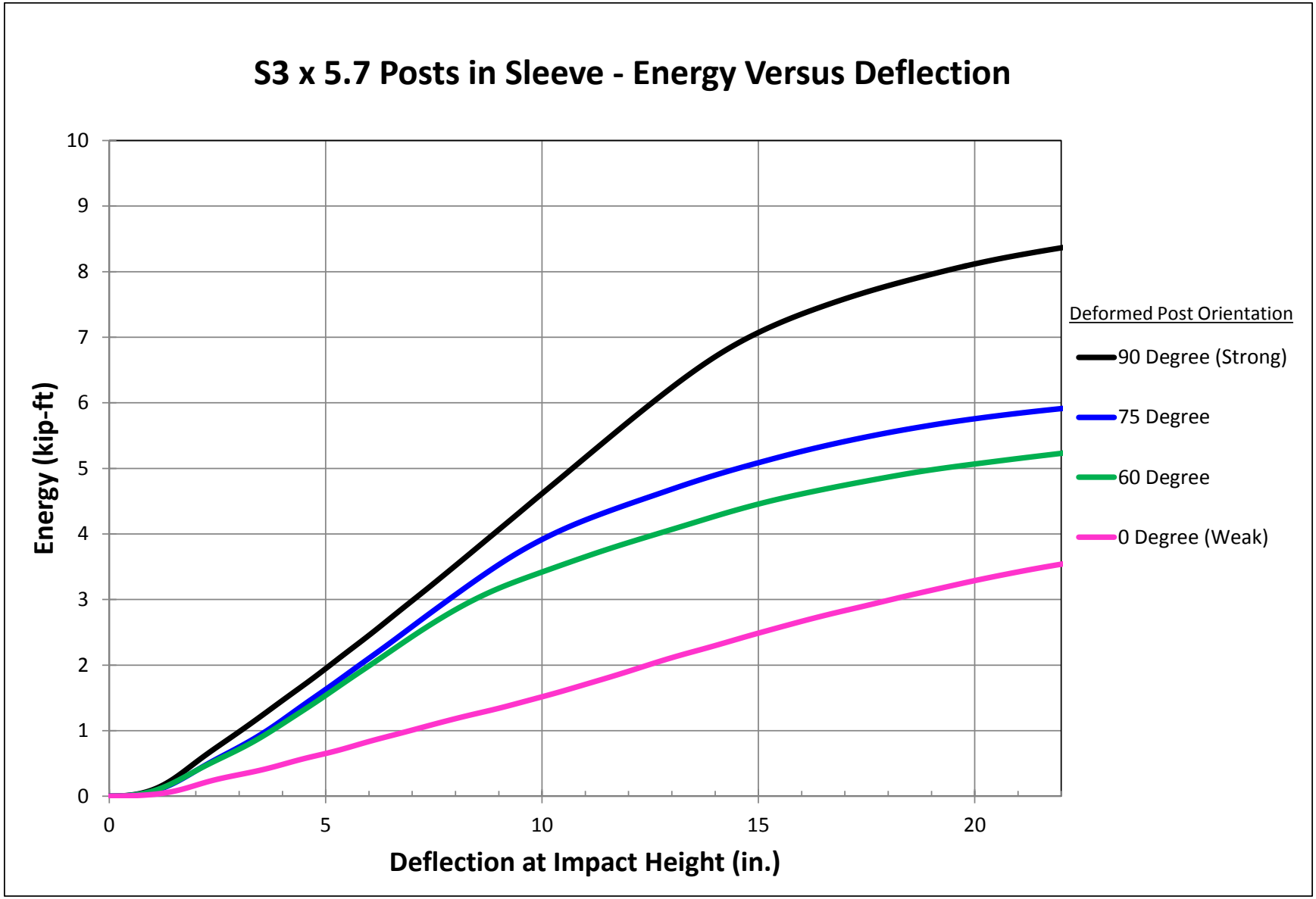

Figure 11. Energy vs. Deflection – S3x5.7 (S76x8.5) Posts in Concrete Sleeve

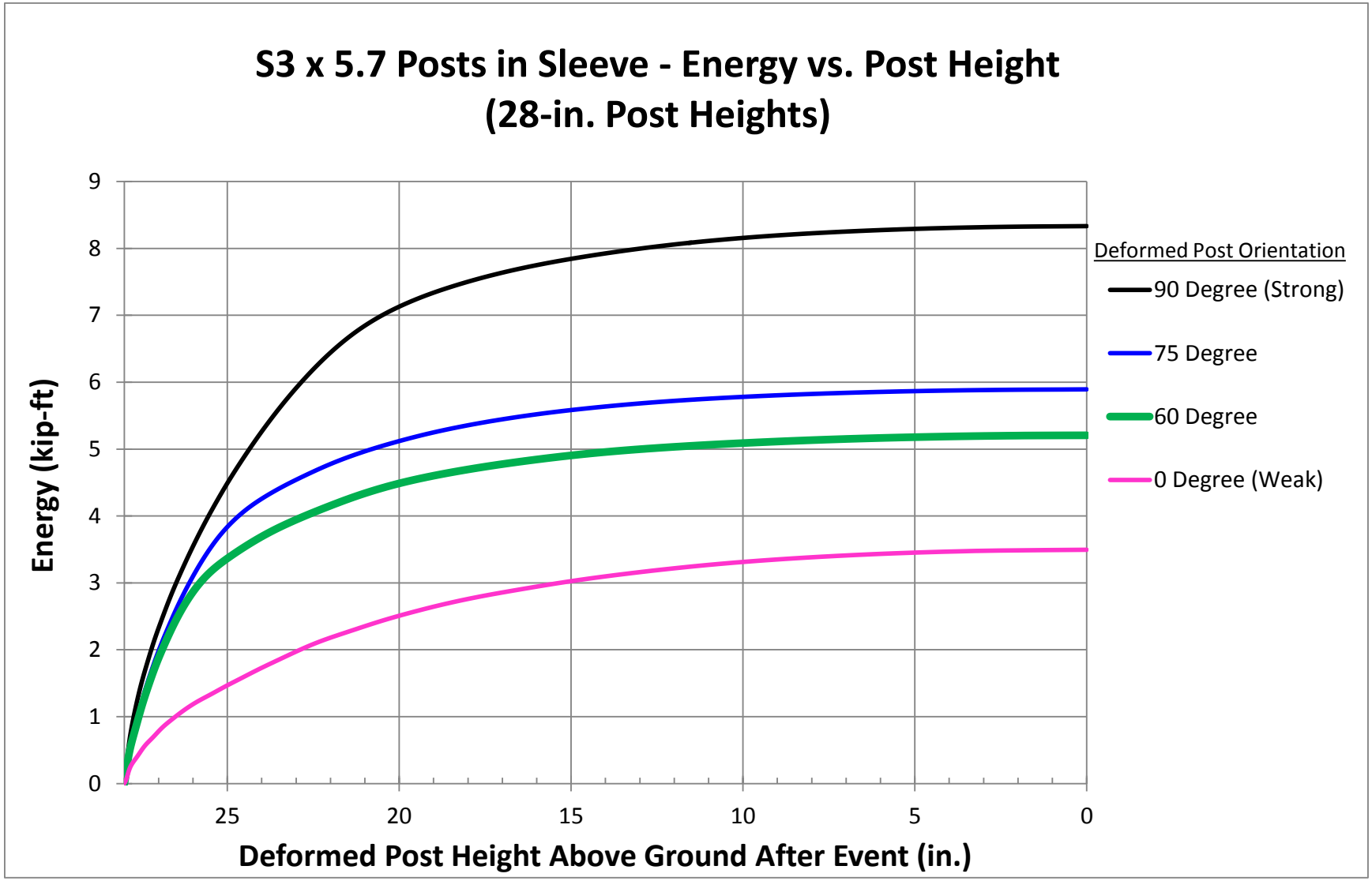

Figure 12. Energy vs. Deformed Post Height – S3x5.7 (S76x8.5) Posts in Concrete Sleeve - Post Height 28 in. (711 mm)

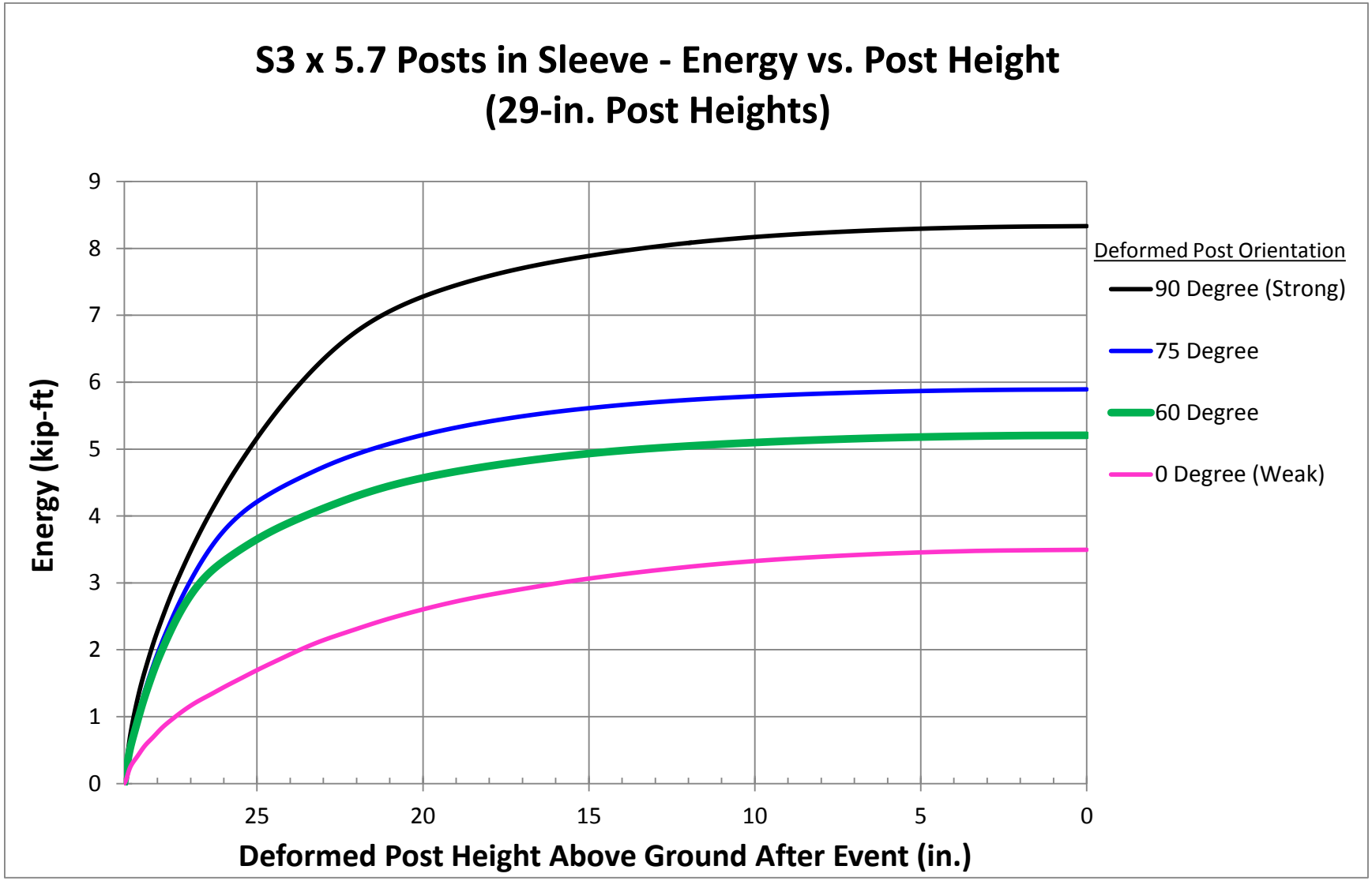

Figure 13. Energy vs. Deformed Post Height – S3x5.7 (S76x8.5) Posts in Concrete Sleeve - Post Height 29 in. (737 mm)

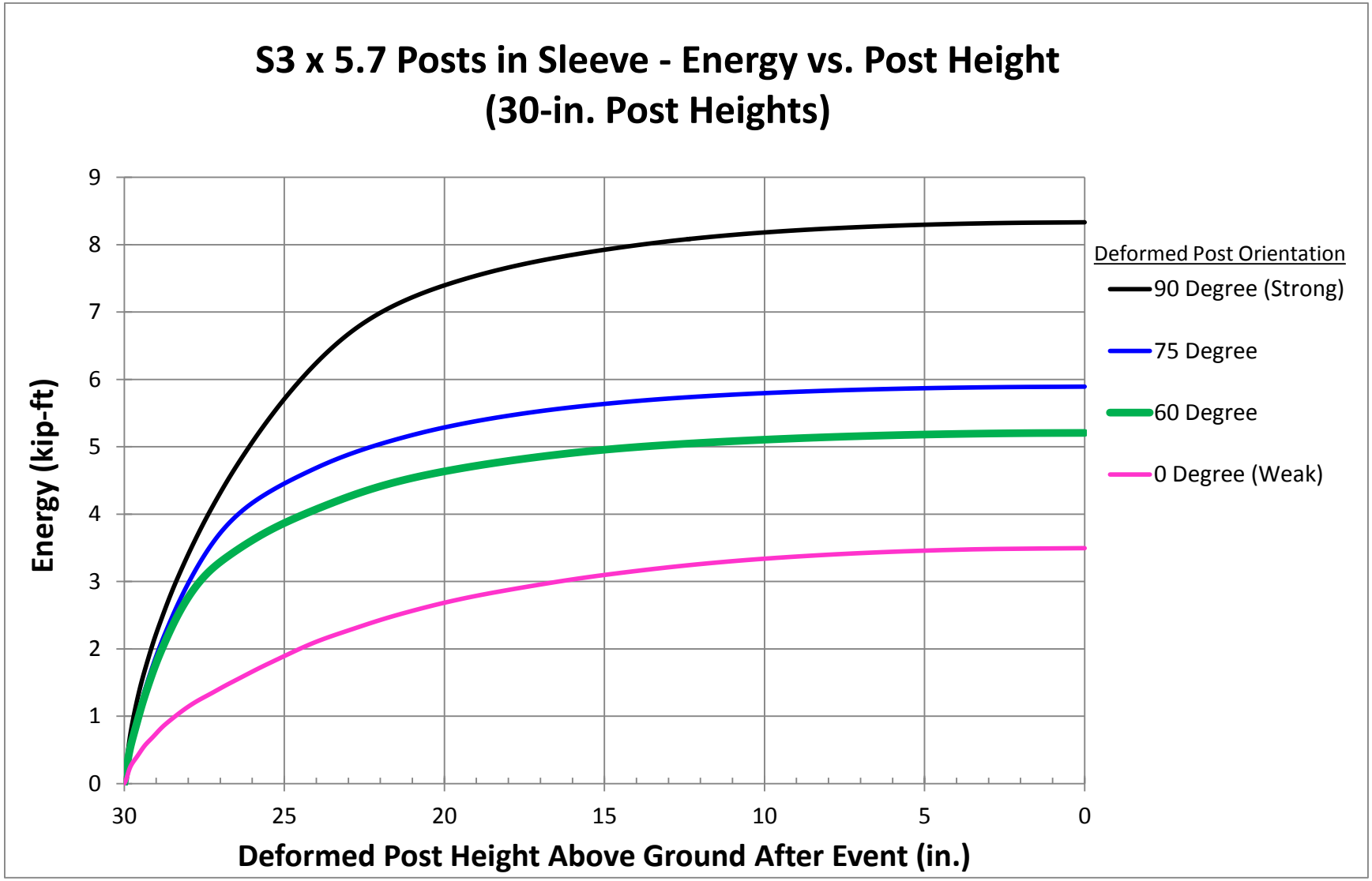

Figure 14. Energy vs. Deformed Post Height – S3x5.7 (S76x8.5) Posts in Concrete Sleeve - Post Height 30 in. (762 mm)

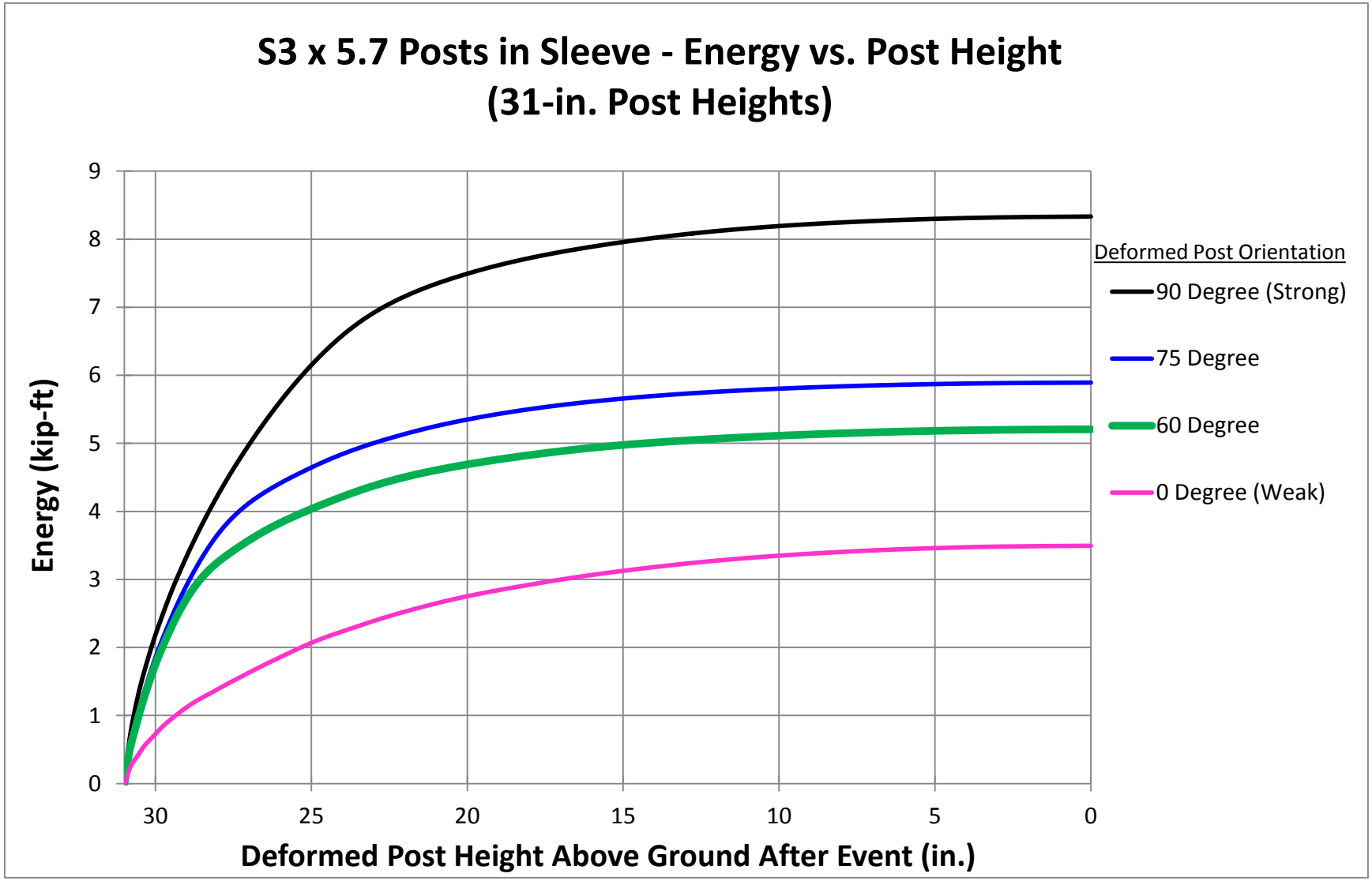

Figure 15. Energy vs. Deformed Post Height – S3x5.7 (S76x8.5) Posts in Concrete Sleeve - Post Height 31 in. (787 mm)

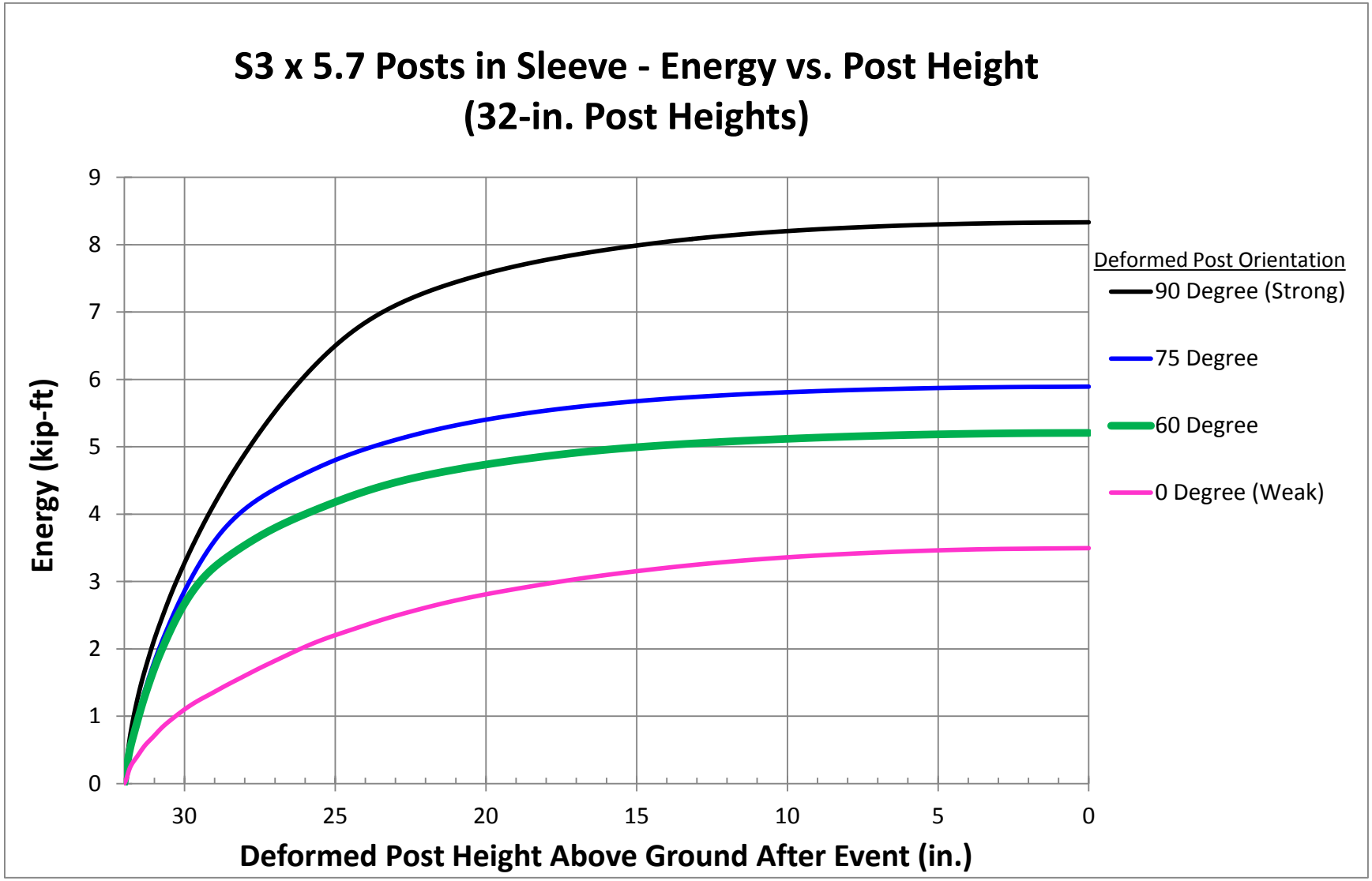

Figure 16. Energy vs. Deformed Post Height – S3x5.7 (S76x8.5) Posts in Concrete Sleeve - Post Height 32 in. (813 mm)

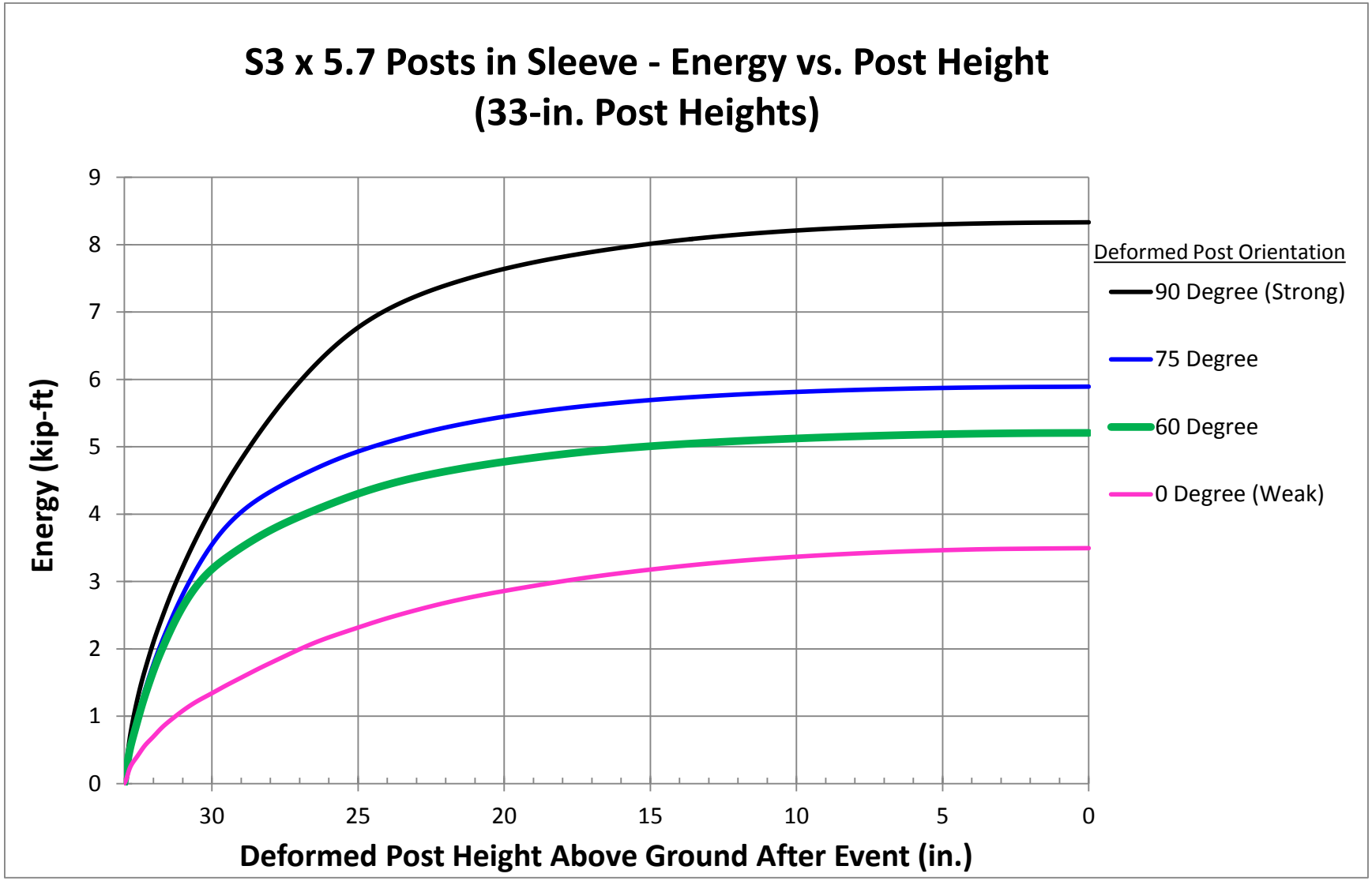

Figure 17. Energy vs. Deformed Post Height – S3x5.7 (S76x8.5) Posts in Concrete Sleeve - Post Height 33 in. (838 mm)

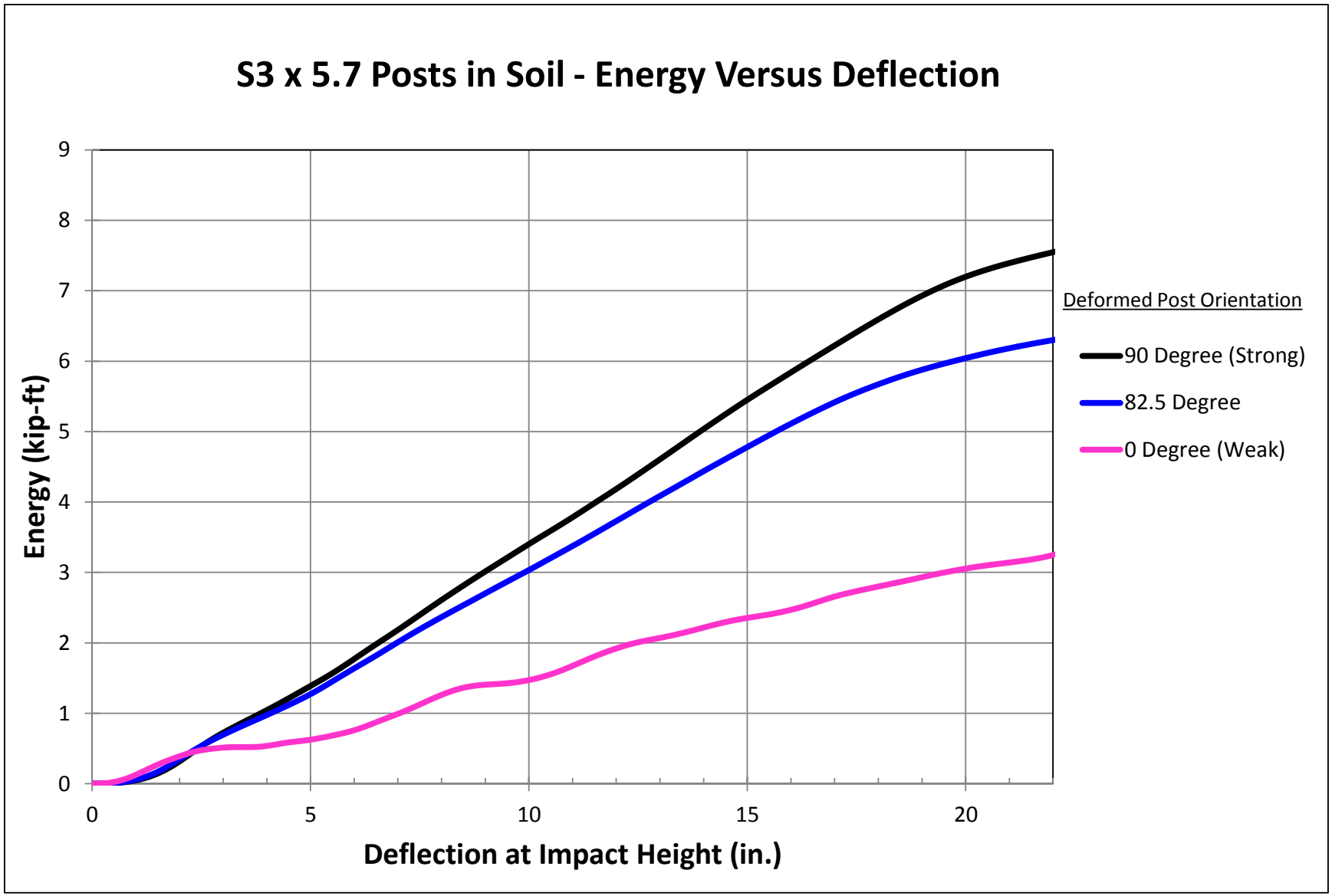

Figure 18. Energy vs. Deflection S3x5.7 (S76x8.5) Posts in Soil

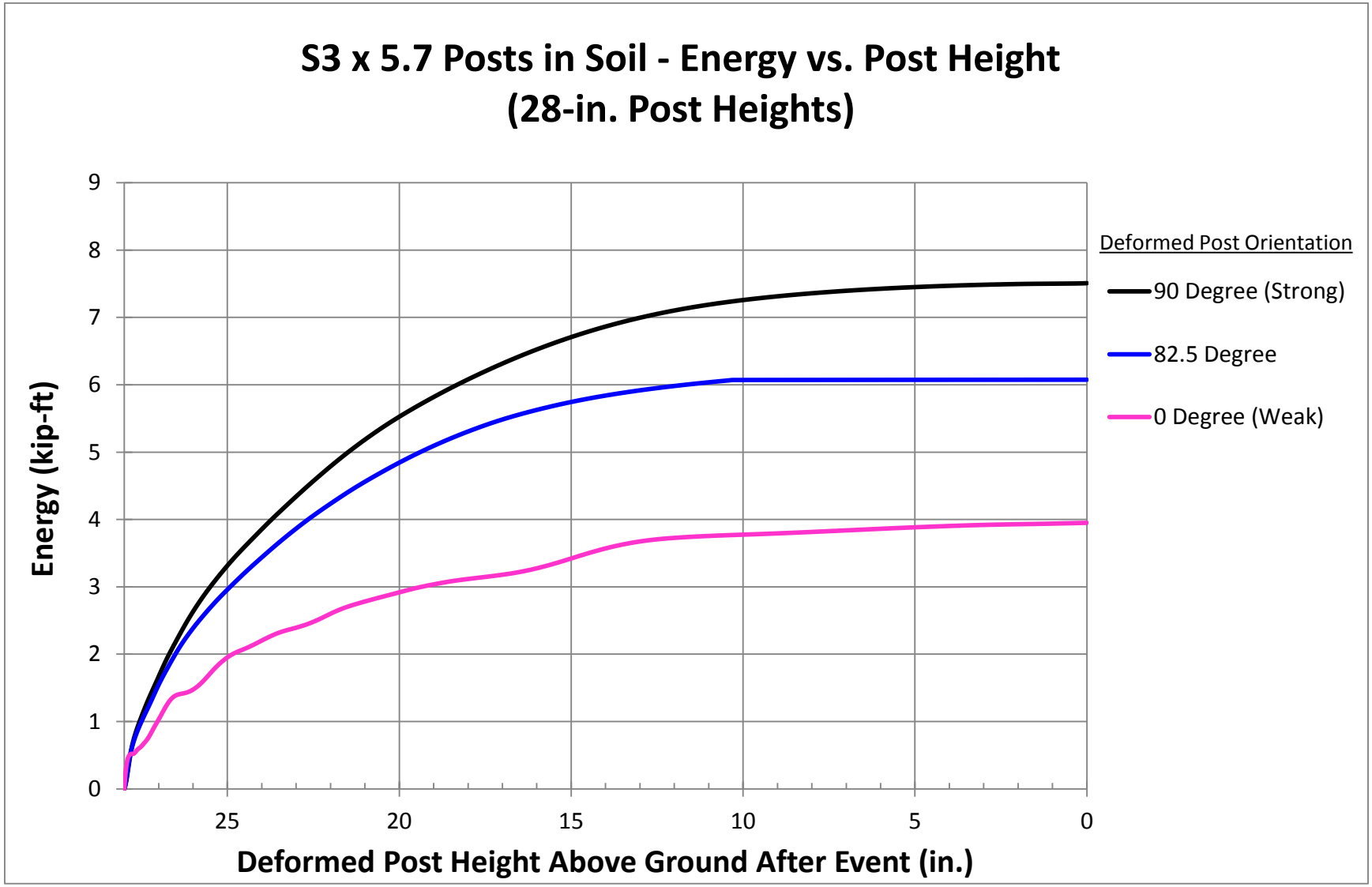

Figure 19. Energy vs. Deformed Post Height – S3x5.7 (S76x8.5) Posts in Soil - Post Height 28 in. (711 mm)

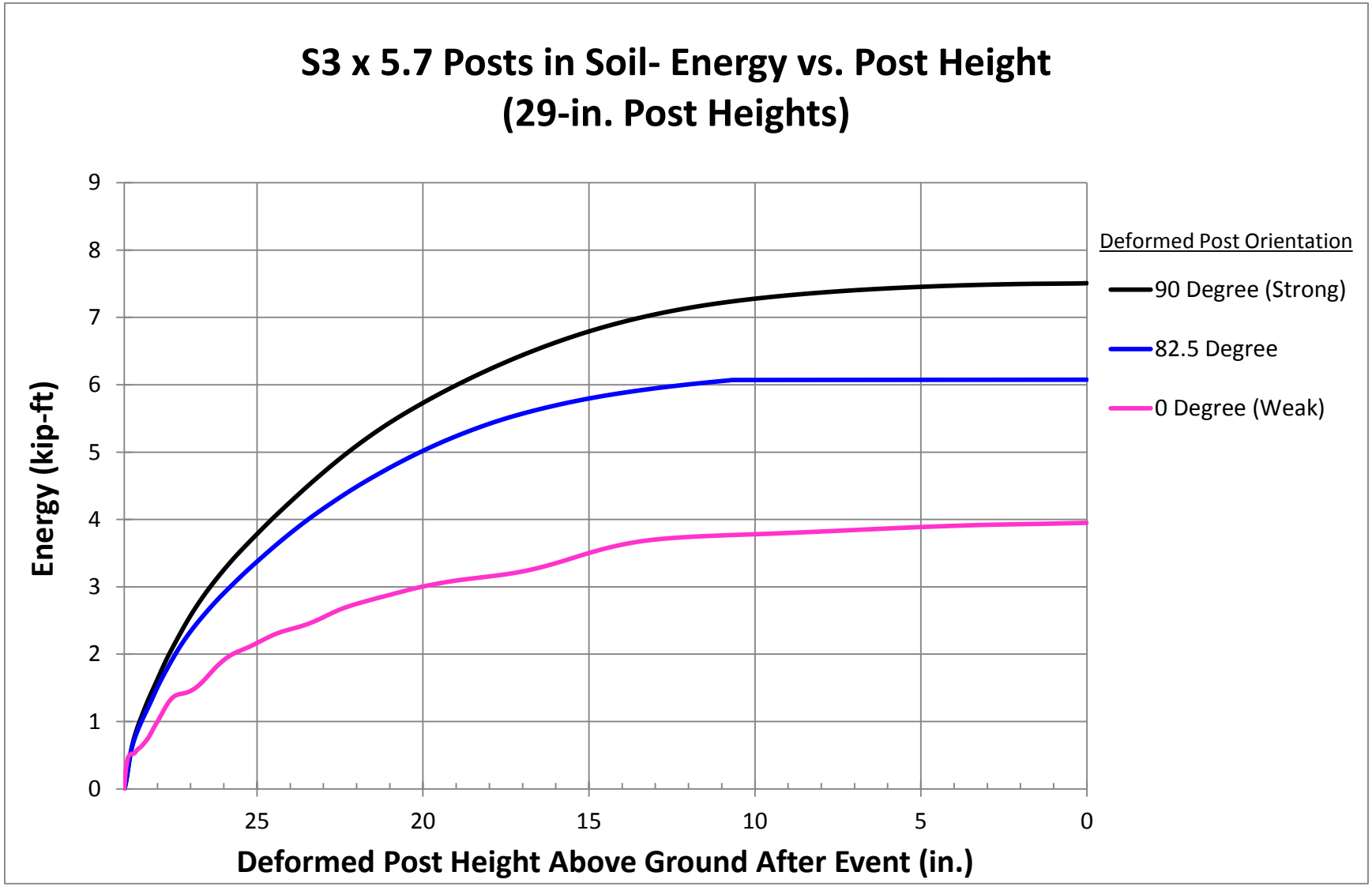

Figure 20. Energy vs. Deformed Post Height – S3x5.7 (S76x8.5) Posts in Soil - Post Height 29 in. (737 mm)

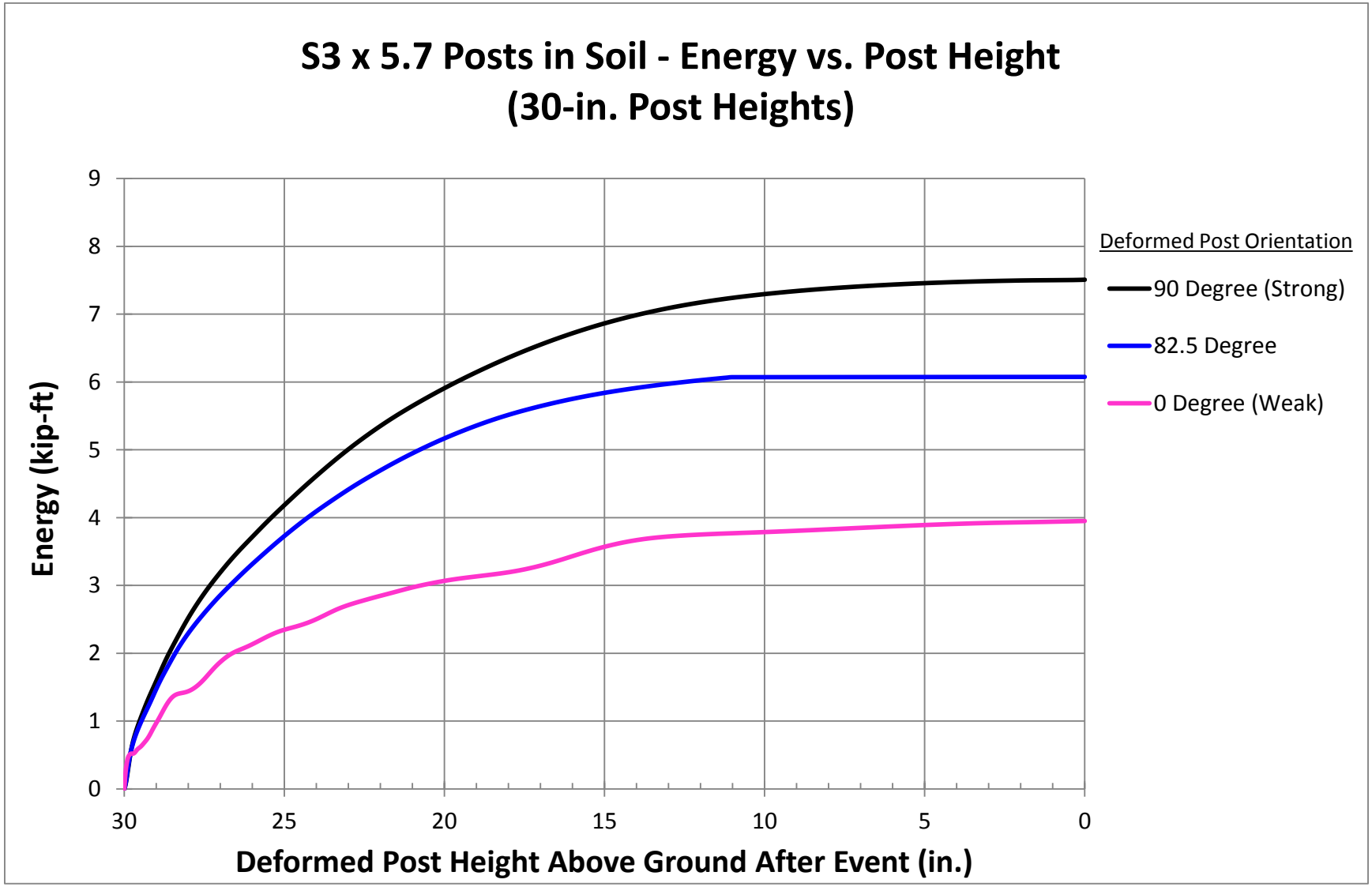

Figure 21. Energy vs. Deformed Post Height – S3x5.7 (S76x8.5) Posts in Soil - Post Height 30 in. (762 mm)

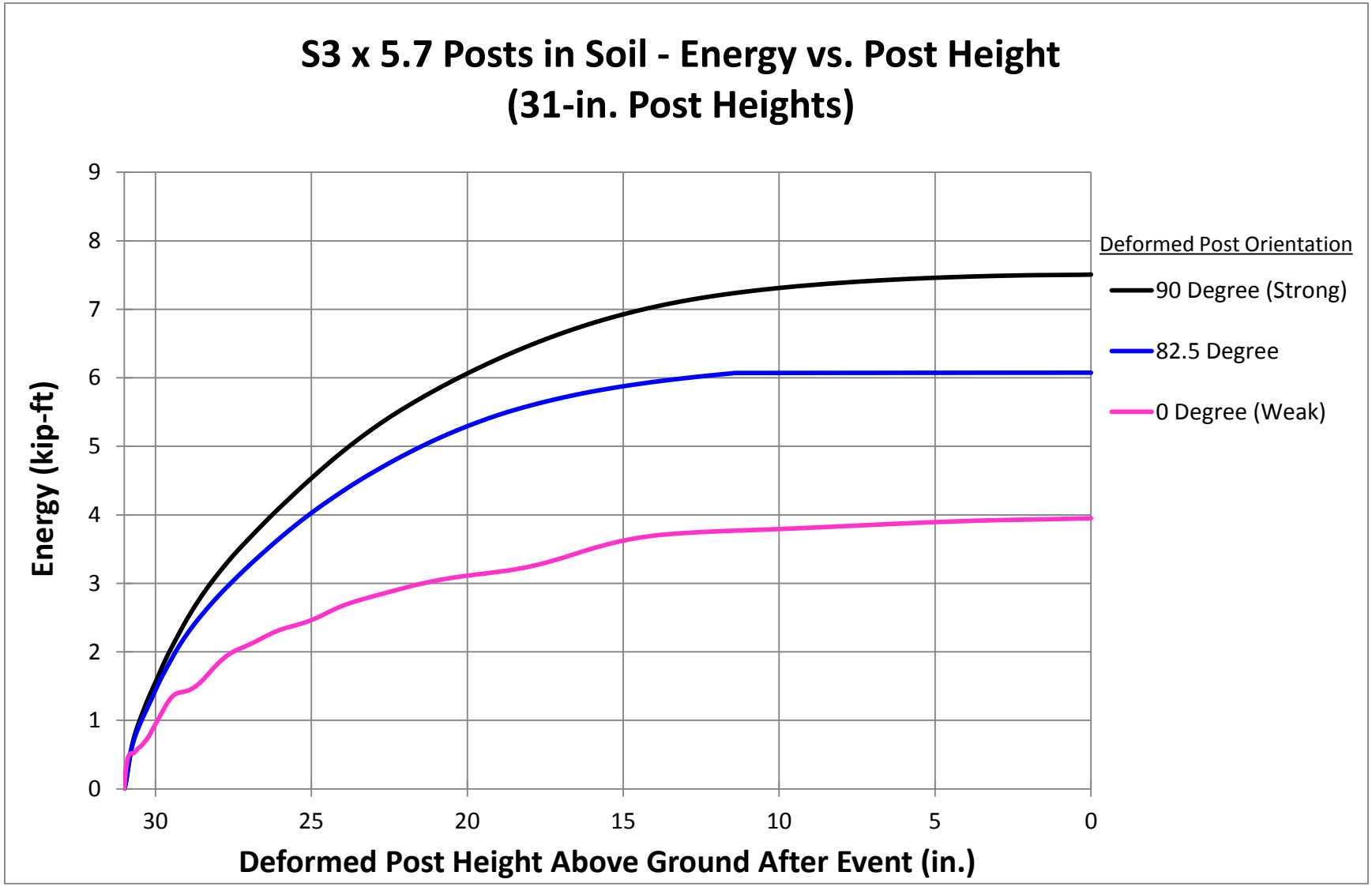

Figure 22. Energy vs. Deformed Post Height – S3x5.7 (S76x8.5) Posts in Soil - Post Height 31 in. (787 mm)

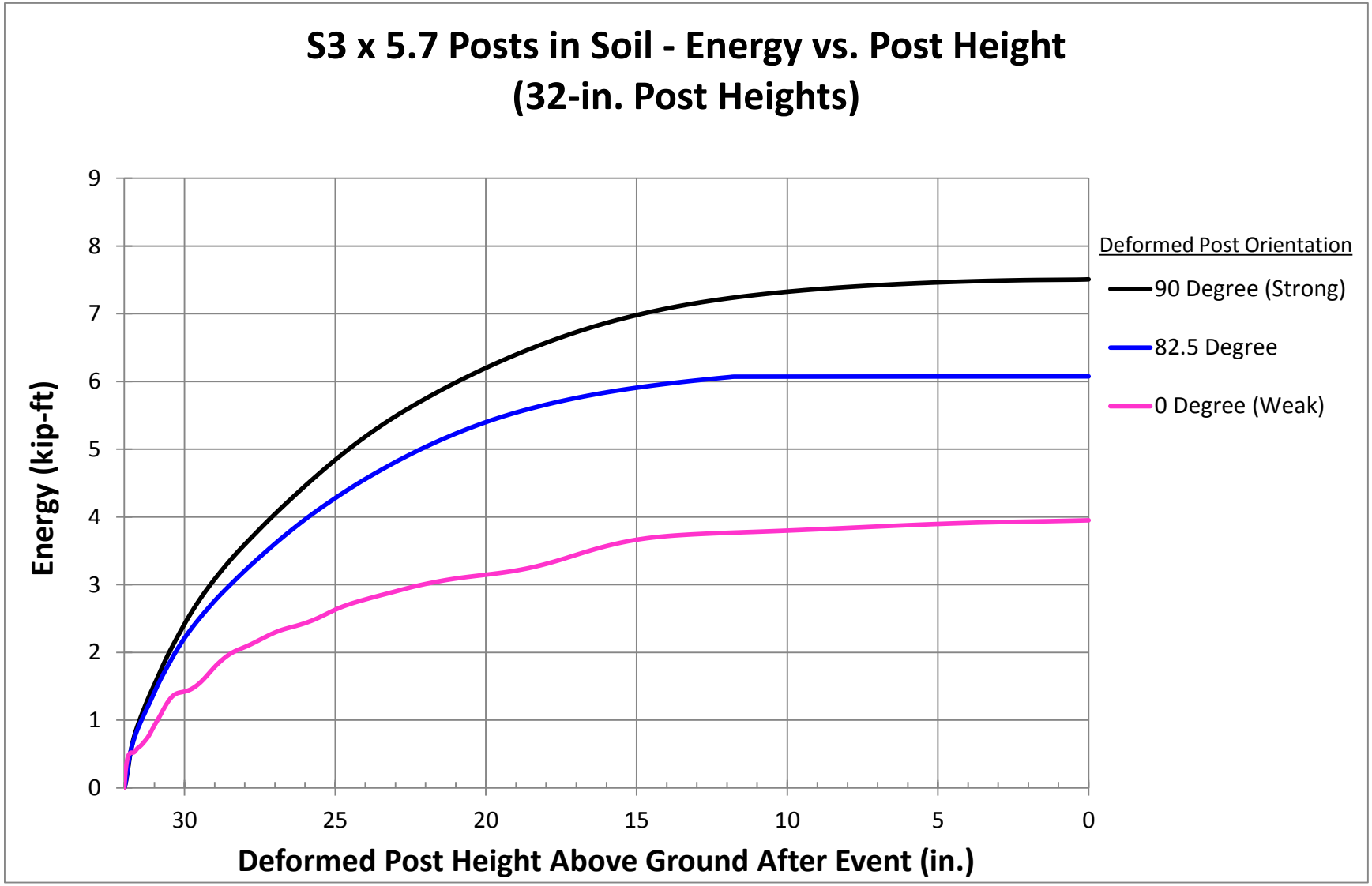

Figure 23. Energy vs. Deformed Post Height – S3x5.7 (S76x8.5) Posts in Soil - Post Height 32 in. (813 mm)

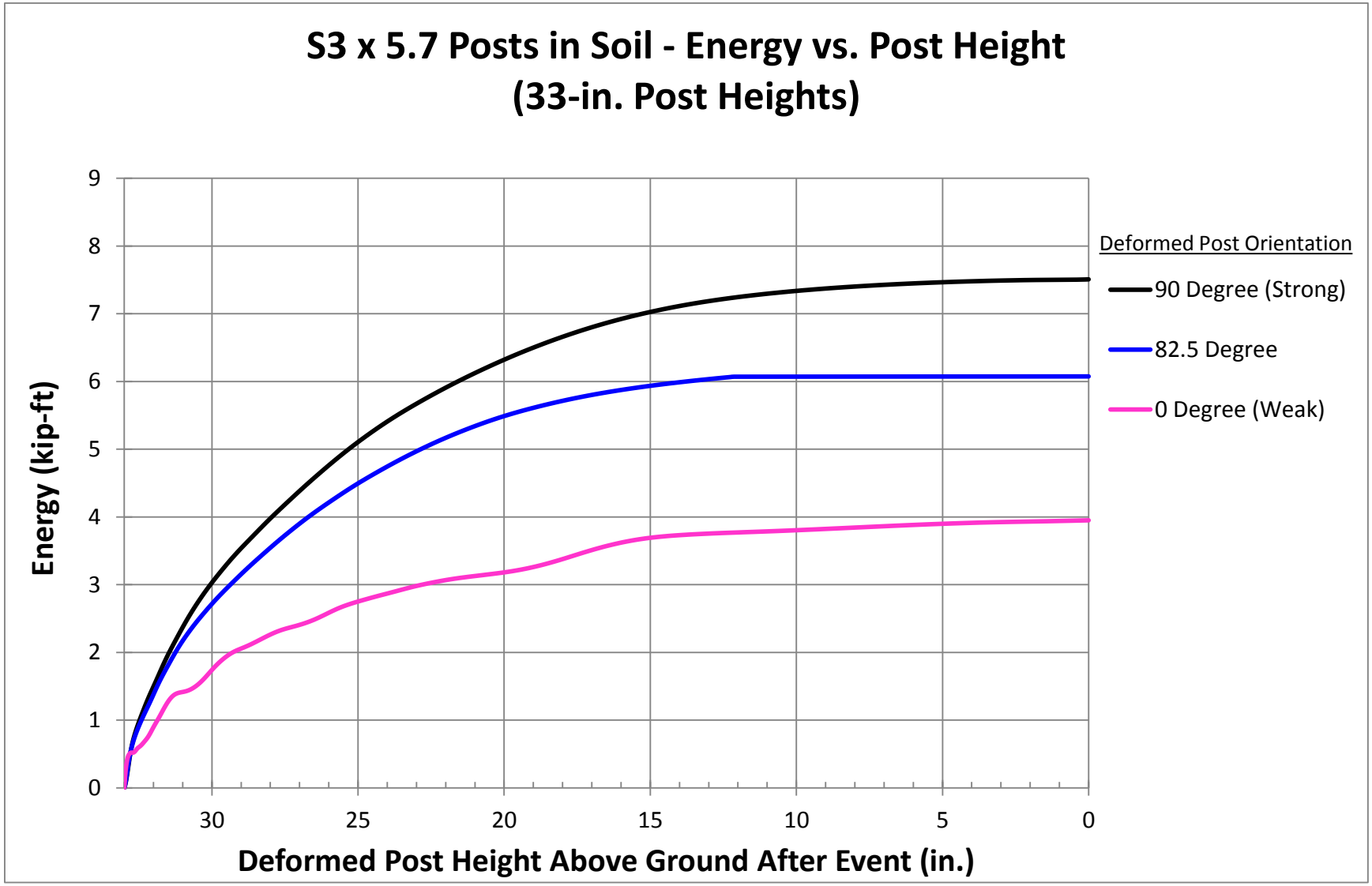

Figure 24. Energy vs. Deformed Post Height – S3x5.7 (S76x8.5) Posts in Soil - Post Height 33 in. (838 mm)

2.2 Vehicle-Ground Interaction

Depending on the site-specific conditions, a vehicle leaving the roadway will encounter a concrete/asphalt surface or a grass/soil surface before impacting a cable barrier system. The energy absorbed by the vehicle-ground interaction is approximated by multiplying the weight of the vehicle by the coefficient of rolling resistance or drag factor between the vehicle and ground and the distance traveled. The distance traveled by the vehicle from impact to system exit should be measured, and the tire marks need to be studied to determine when the vehicle was rolling, sliding, and/or braking per typical accident reconstruction procedures.

When the vehicle is tracking (i.e. tires rolling normally), the coefficient of rolling resistance is small and varies slightly with the road/ground surface. Many times when a vehicle leaves the roadway, the driver will be actively braking, which creates a high drag factor between the skidding tires and the ground surface adjacent to the barrier system. This drag factor is significant, but it is not easy to quantify. Once the vehicle impacts a cable barrier system, the vehicle may transition between tracking and non-tracking (i.e. tires sliding laterally) conditions. Vehicle-ground coefficients for various road/ground surfaces and for different braking/skidding and rolling scenarios are shown in Appendix B [8]. These values were used to estimate the total kinetic energy lost through vehicle-ground interaction during the full-scale crash tests. However, the accident reconstructionist should closely examine the specific site conditions and determine when the vehicle was tracking, non-tracking, and braking. The vehicle-ground coefficients should be determined through skid testing, if available.

2.3 Internal Cable Energy

The tension increases in the cables as a vehicle deflects the cable barrier system during an impact event. The kinetic energy transferred to the barrier is equal to the integral of the lateral force component of the cable tension applied to the vehicle over the lateral deflection of the

barrier. Since only the lateral extent of wheel trajectory marks may be known after an accident, the lateral deflection of the barrier can be approximated by the maximum lateral displacement of the vehicle's wheels. The maximum lateral displacement of the vehicle could switch between the front and rear wheels, but it is not important to discern which part of the vehicle produces the maximum barrier deflection. The dynamic cable tension during an impact varies between straight, exterior-curved, and interior-curved cable barrier systems. The energy absorbed during an impact with a straight system was analyzed in test no. CS-2 [2]. The energy absorbed during an impact with an exterior-curved system was analyzed in test no. NYCC-3 [1]. Full-scale crash testing of an interior-curved system was not available.

The lateral redirective cable force (F_{lat}) was estimated in full-scale crash tests based on the tension (T) as well as the leading and trailing angles (θ_1, θ_2) that are formed by the cable in contact with the vehicle, as shown in Figure 25.

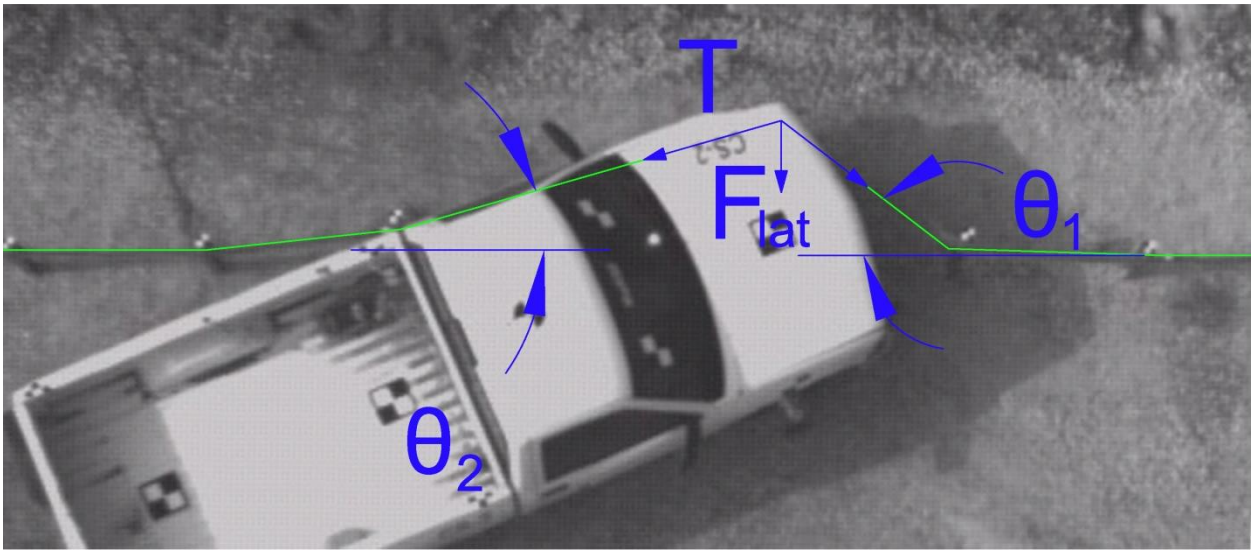

Figure 25. Parameters Associated with Cable Contact with Vehicle

The lateral cable force (F_{lat}) is calculated using the following equation:

$$F_{lat} = T * (\sin\theta_1 + sin\theta_2)$$

The angles vary as the vehicle initially impacts the barrier, becomes parallel to the system, and then redirects away from the barrier system. The leading and trailing angles, the lateral displacement of the vehicle, and the total distance traveled were measured from overhead video using AutoCAD at 30-ms or 50-ms discrete time intervals. These values would not be known during a real-world accident.

Integrating the lateral force vs. lateral wheel trajectory curve (i.e, assumed lateral barrier displacement), the energy absorbed as a function of the lateral wheel trajectory can be found. The calculated energy during loading (up to the maximum deflection) decreases the vehicle's kinetic energy. The calculated energy during unloading (after the maximum deflections) increases the vehicle's kinetic energy. The change in energy between these two curves represents the internal cable energy losses.

Relationships between the lateral force and the lateral wheel trajectory were found for test nos. CS-2 and NYCC-3. Additional full-scale crash testing of cable barrier systems is necessary to determine if the relationships apply to systems with different post spacing, system lengths, curve radii, and impact conditions.

2.3.1 Straight Cable Barrier System – Test No. CS-2 [2]

The combined cable tension of all three cables and lateral deflection during test no. CS-2 is shown in Figure 26. There is a good correlation between the cable tension and lateral deflection. The leading and trailing angles formed by the cables in contact with the vehicle are shown at discrete time intervals in Figure 27. The cable tension, the leading and trailing angles, and lateral deflection were found at 50-ms intervals. The lateral cable force was calculated from the tension and cable angles. The lateral force vs. lateral deflection is shown in Figures 28 and 29 during cable loading and cable unloading, respectively. The kinetic energy absorbed up until maximum deflection is shown in Figure 30. The kinetic energy added back to the vehicle after

maximum deflection is shown in Figure 31. The difference between the maximum of these two curves represents the internal cable energy lost during the impact event, which was 30.6 kip-ft (41.5 kJ) for test no. CS-2.

During a roadside accident, cable tension, leading and trailing angles, and system deflections throughout the impact would not be known. In order to determine the energy absorbed by the cable stretch during an accident, curves were fitted to the data provided in Figures 28 and 29. The fitted curves were integrated, and equations to estimate the energies are contained in Appendix C.

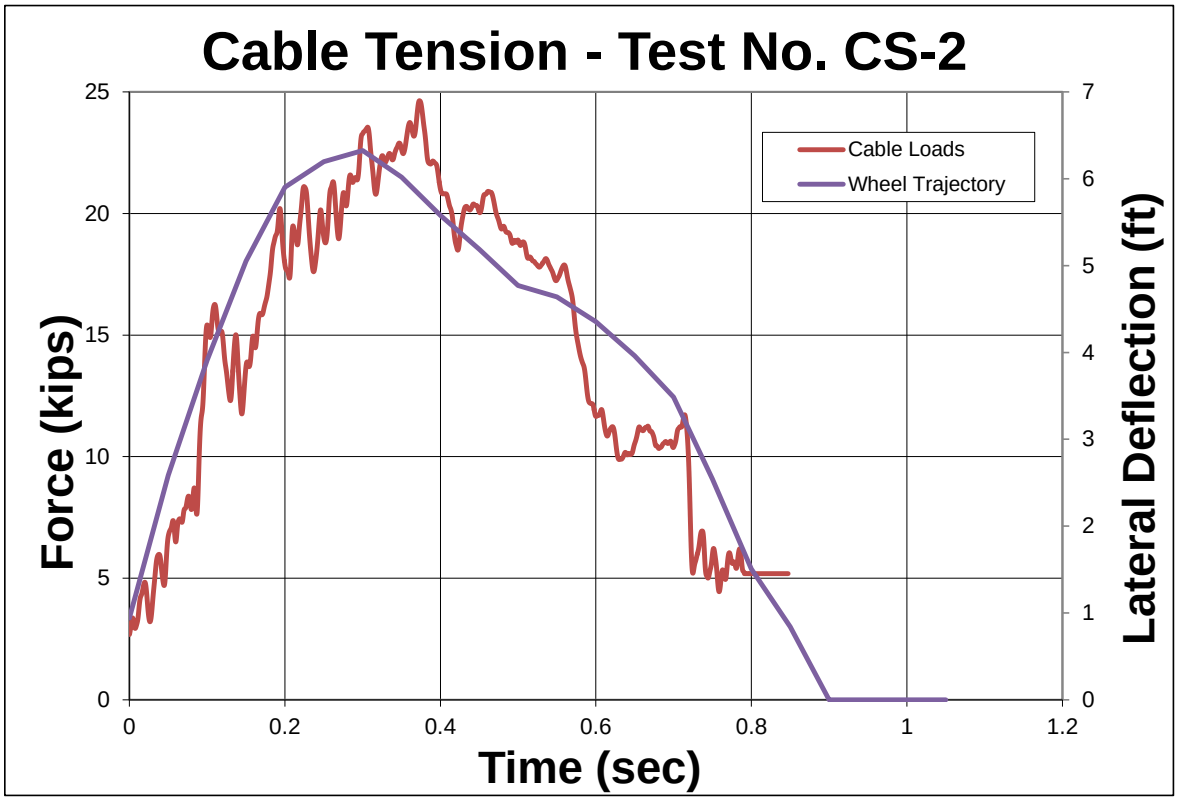

Figure 26. Cable Tension and Lateral Deflection vs. Time – Test No. CS-2

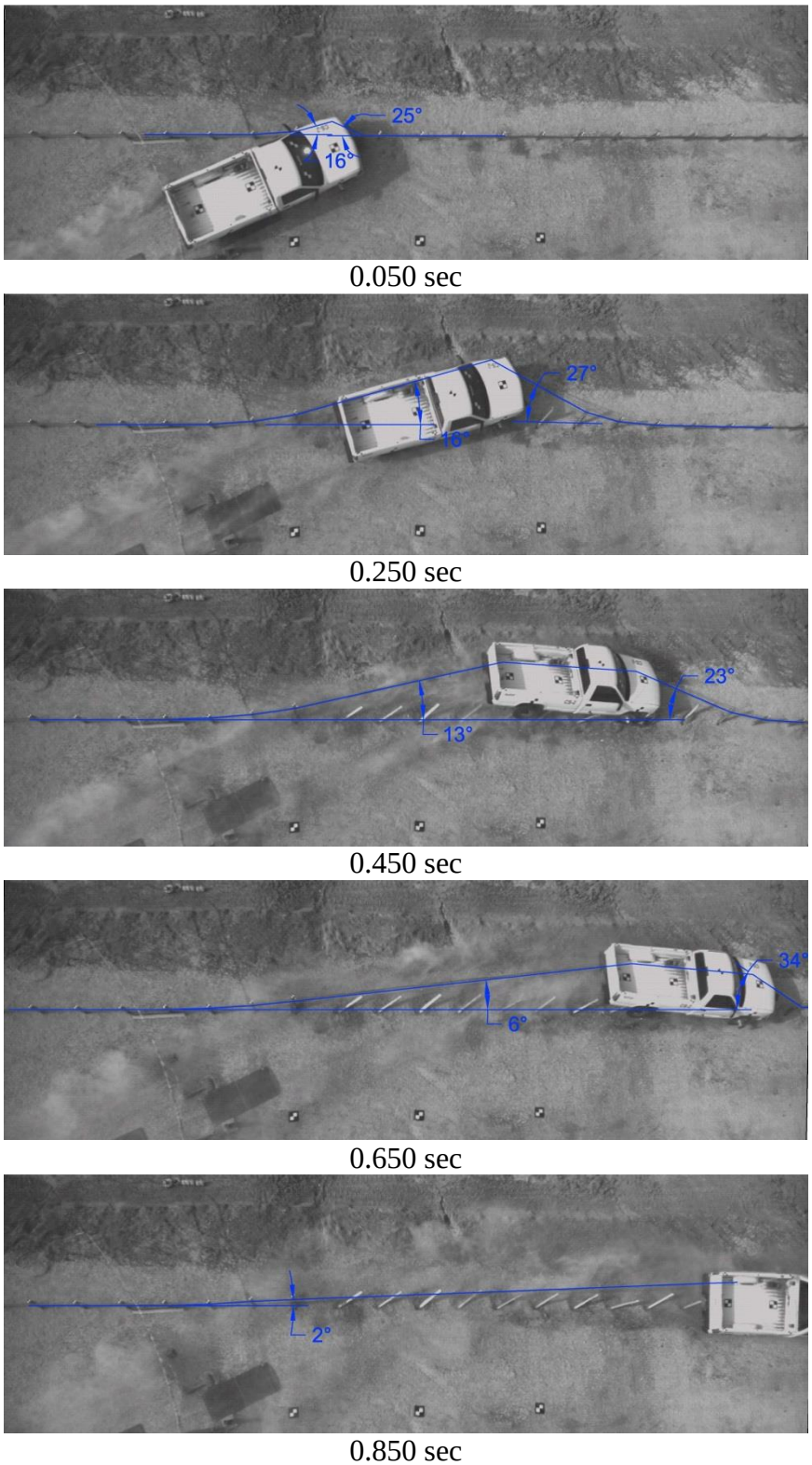

Figure 27. Cable Position and Vehicle Trajectory – Test No. CS-2

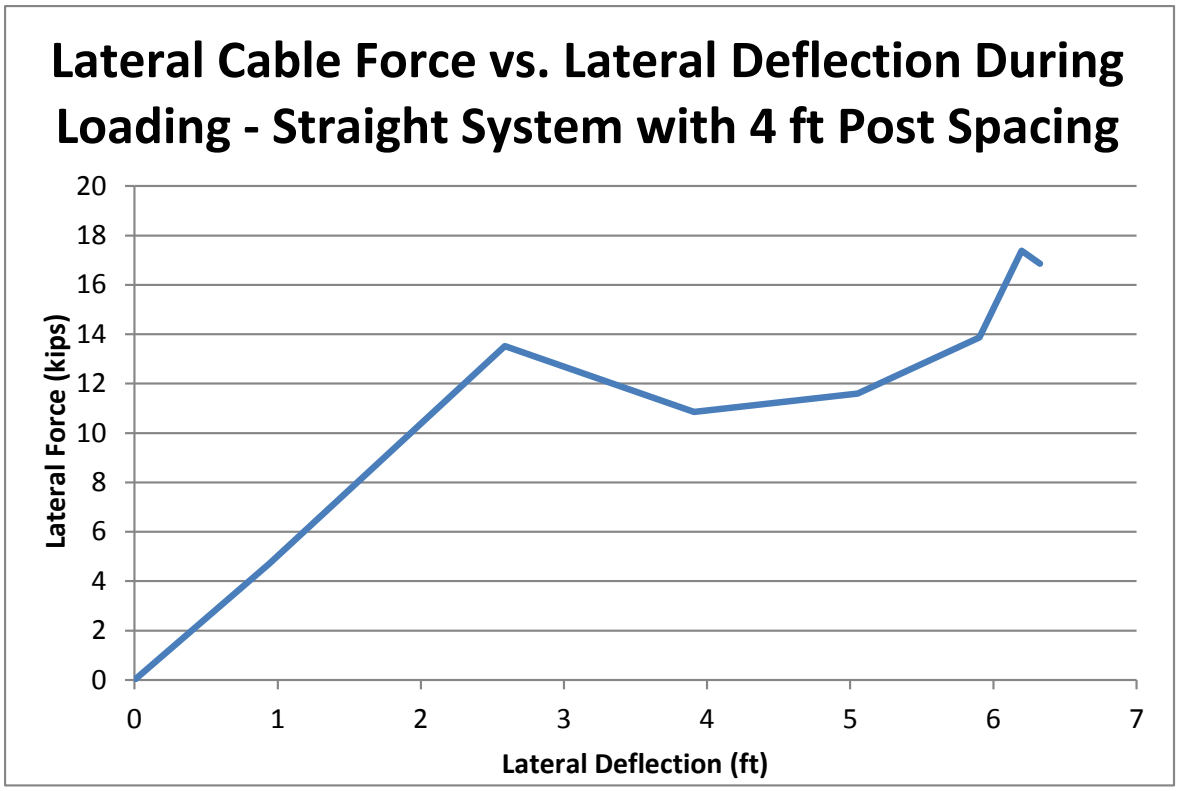

Figure 28. Lateral Cable Force vs. Lateral Deflection During Loading– Test No. CS-2

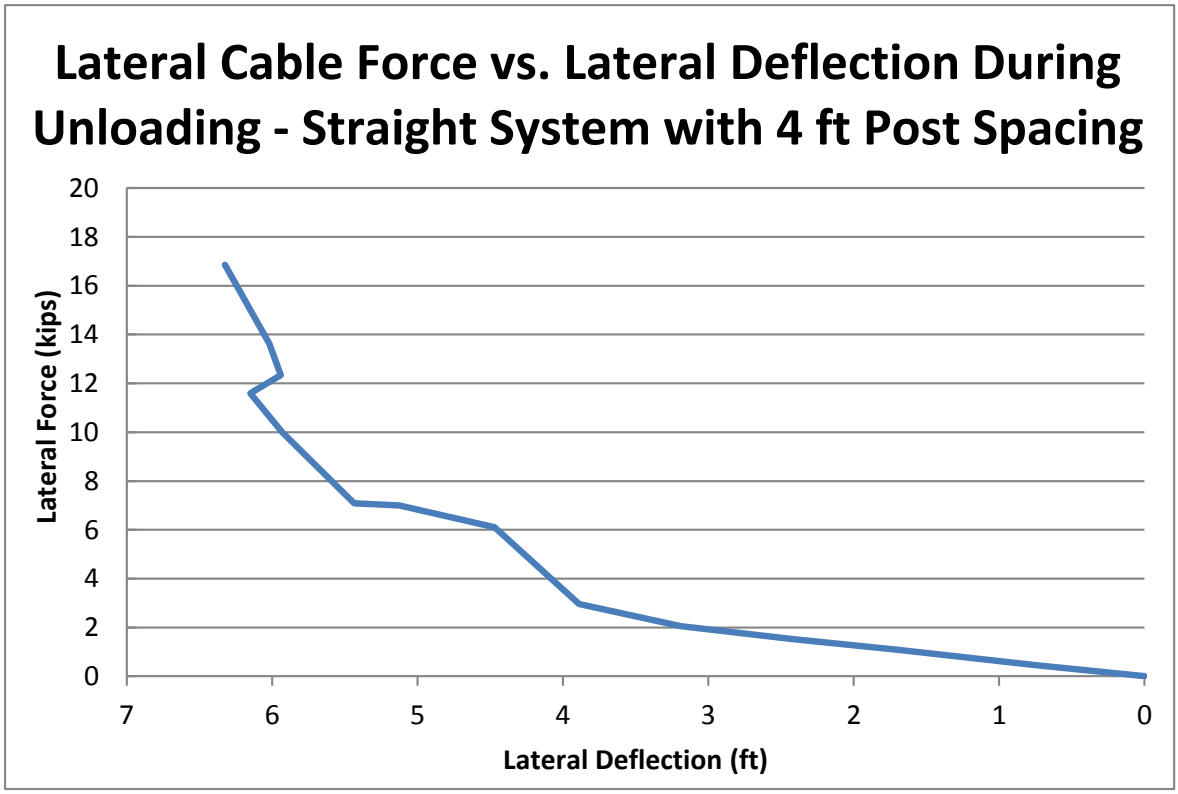

Figure 29. Lateral Cable Force vs. Lateral Deflection During Unloading– Test No. CS-2

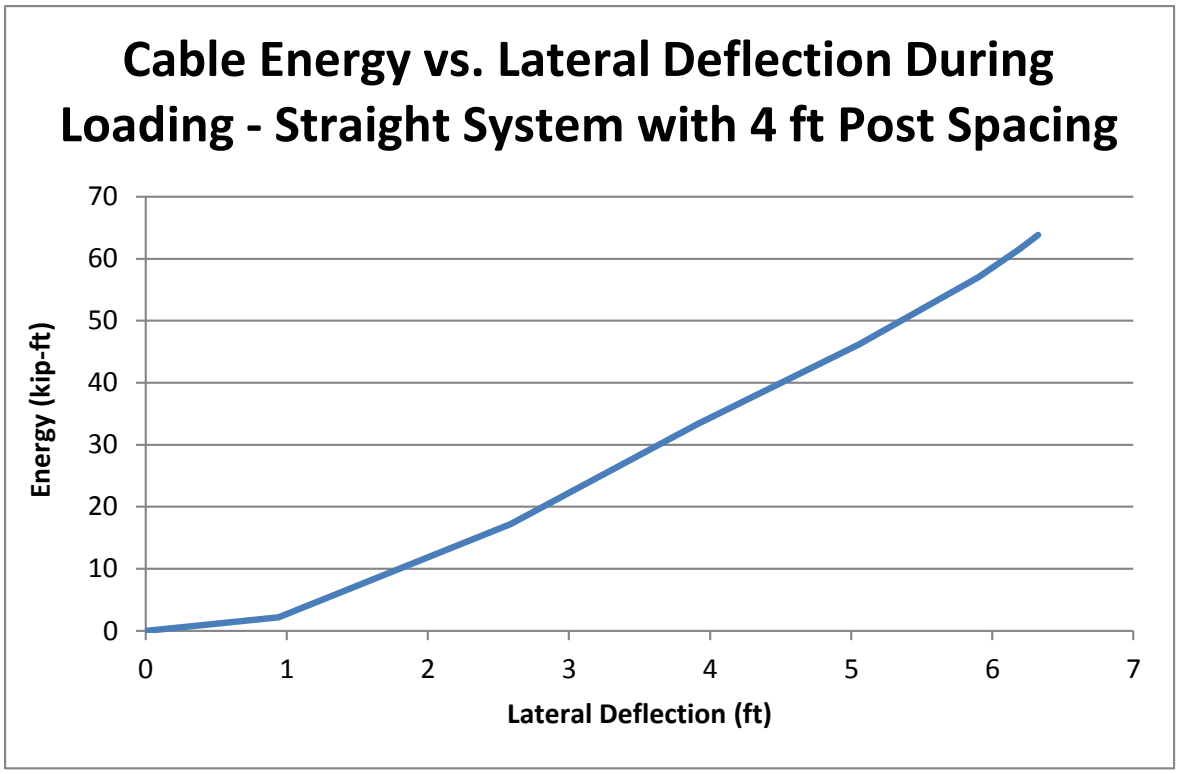

Figure 30. Cable Energy vs. Lateral Deflection During Loading – Test No. CS-2

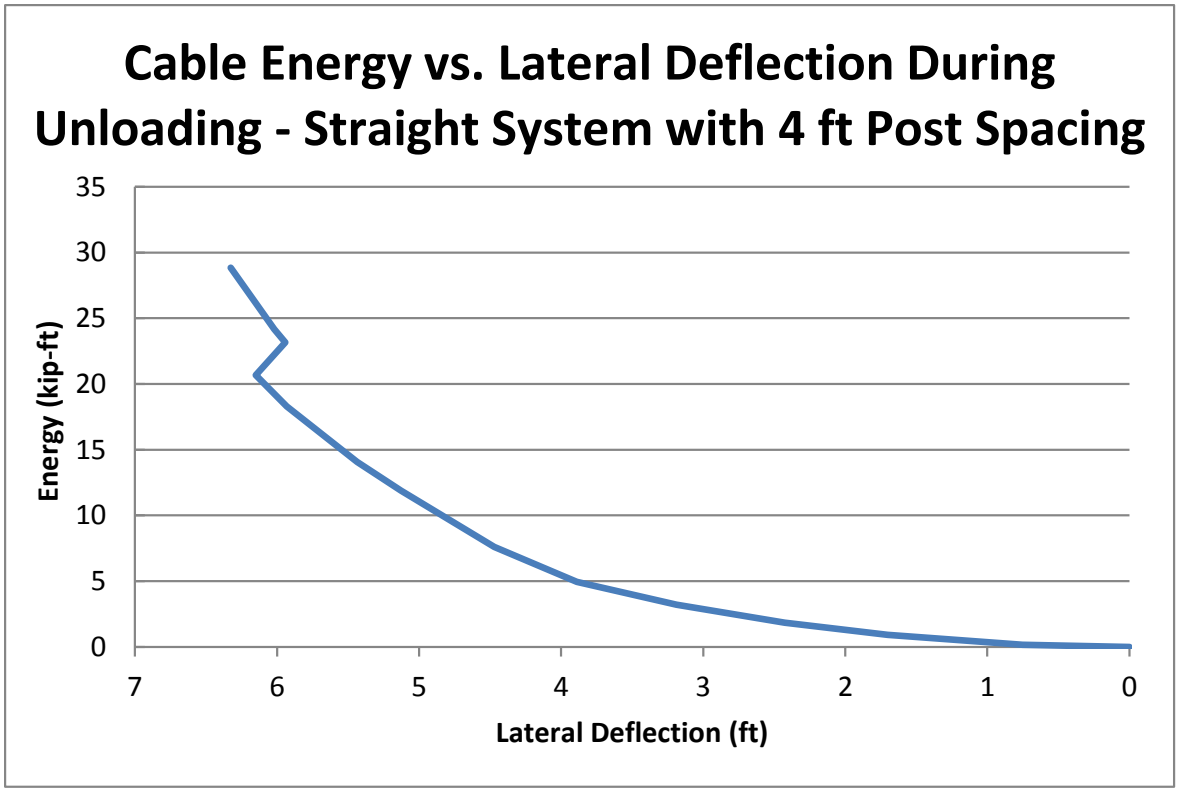

Figure 31. Cable Energy vs. Lateral Deflection During Unloading – Test No. CS-2

2.3.1 Exterior-Curved Cable Barrier System – Test No. NYCC-3 [1]

The combined cable tension of all three cables and lateral deflection during test no. NYCC-3 is shown in Figure 32. The combined cable tension was noisy. A correlation was noted between the cable tension and lateral deflection, but the maximum tension did not coincide with the maximum deflection like in the straight cable barrier system. The leading and trailing angles formed by the cables in contact with the vehicle are shown at discrete time intervals in Figure 33. The cable tension, the leading and trailing angles, and lateral deflection were found at 50-ms intervals. The lateral cable force was calculated from the tension and cable angles. The lateral force vs. lateral deflection is shown in Figures 34 and 35 during cable loading and cable unloading, respectively. The kinetic energy absorbed up until maximum deflection is shown in Figure 36. The kinetic energy added back to the vehicle after maximum deflection is shown in Figure 37. The difference between the maximum of these two curves represents the internal cable energy lost during the impact event, which was 35.7 kip-ft (48.4 kJ) for test no. NYCC-3.

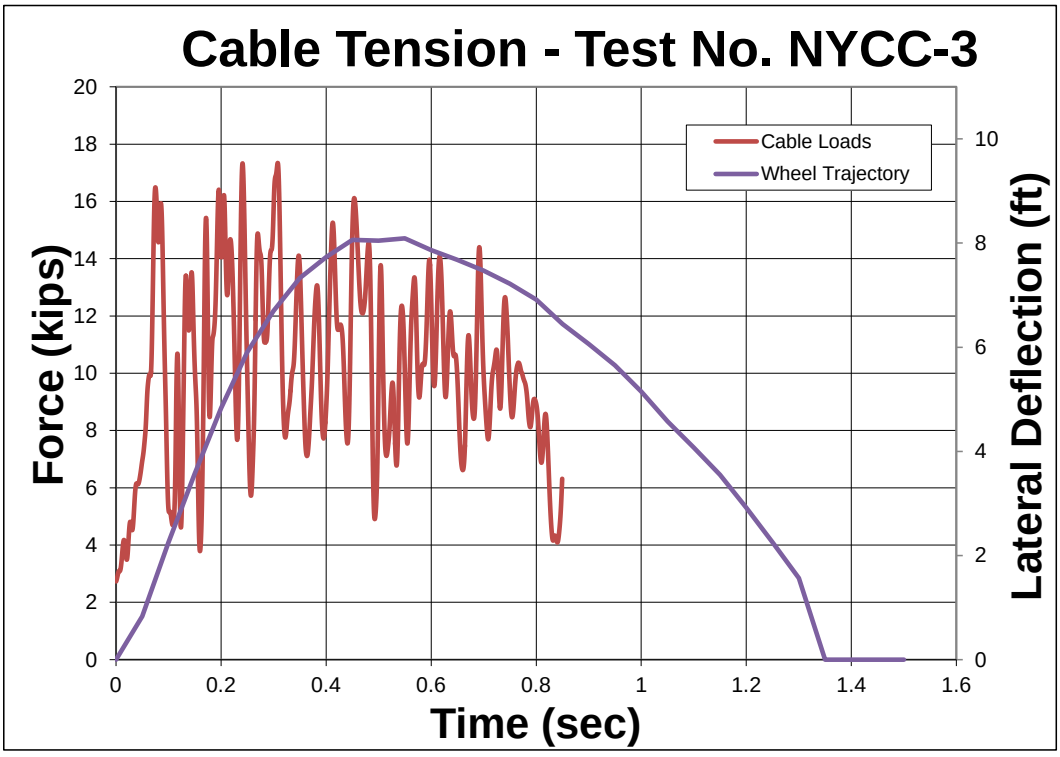

Figure 32. Cable Tension and Lateral Deflection vs. Time – Test No. NYCC-3

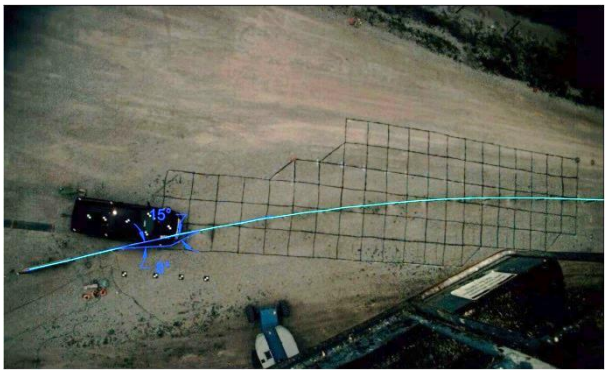
0.050 sec

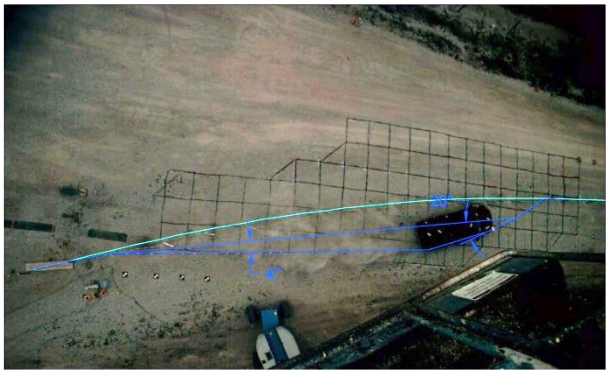
0.850 sec

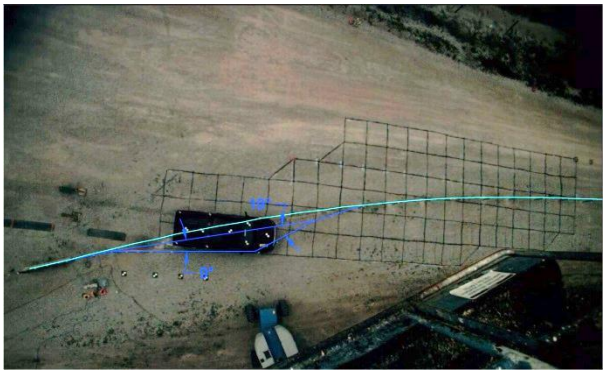
0.250 sec


1.050 sec

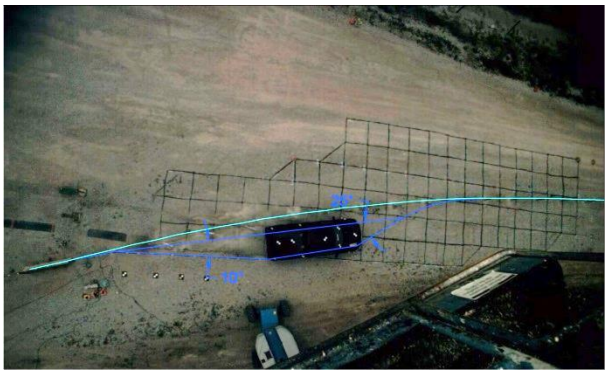
0.450 sec


1.250 sec

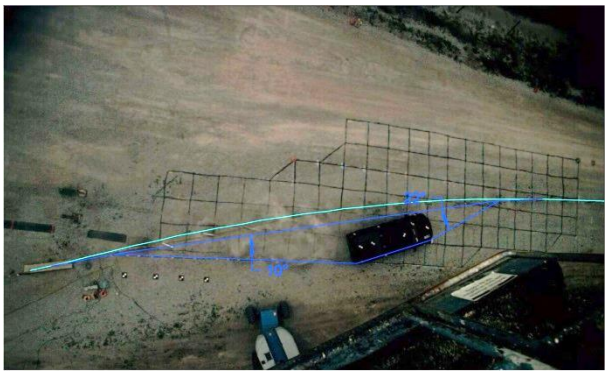
0.650 sec

Figure 33. Cable Position and Vehicle Trajectory – Test No. NYCC-3

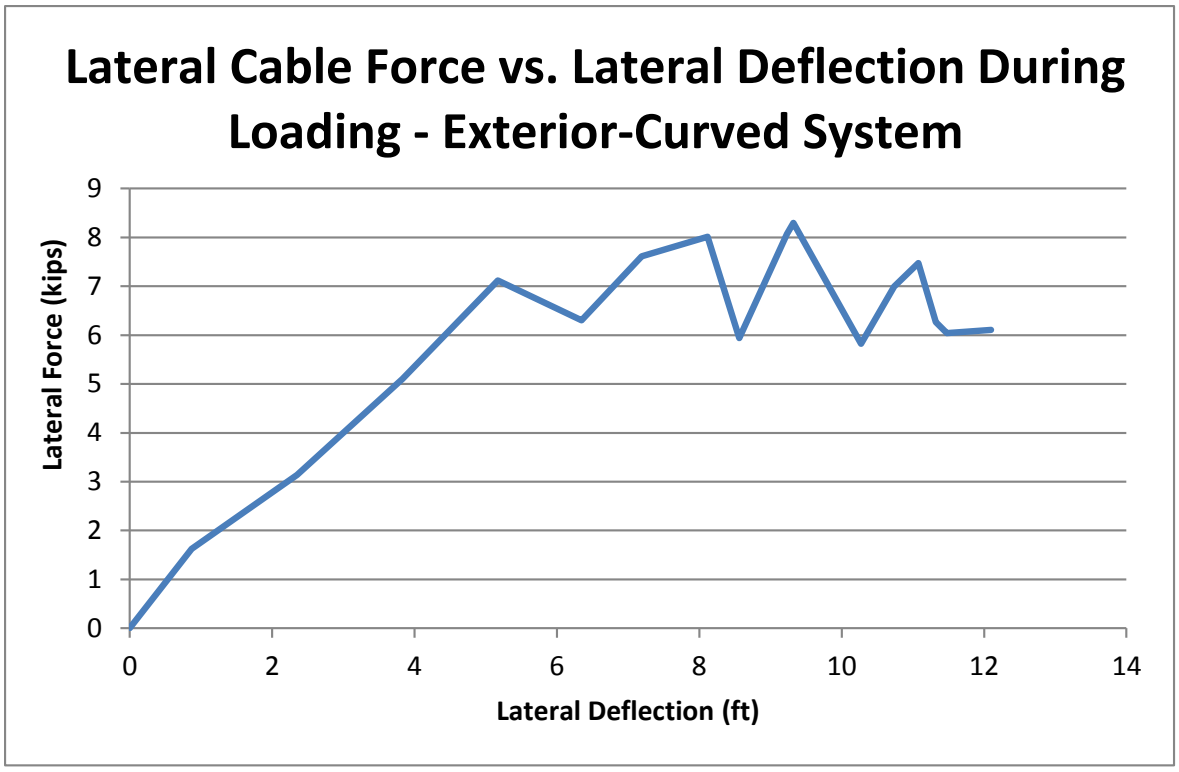

Figure 34. Lateral Cable Force vs. Lateral Deflection During Loading– Test No. NYCC-3

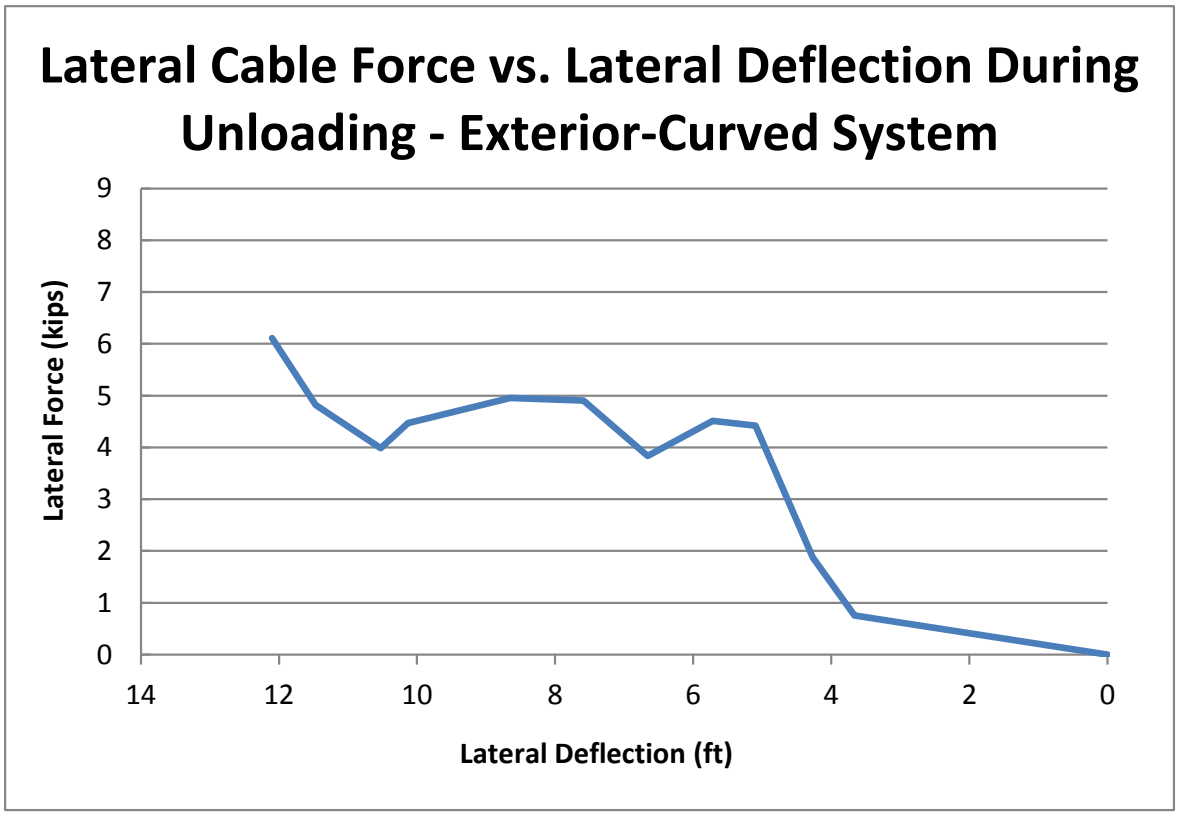

Figure 35. Lateral Cable Force vs. Lateral Deflection During Unloading– Test No. NYCC-3

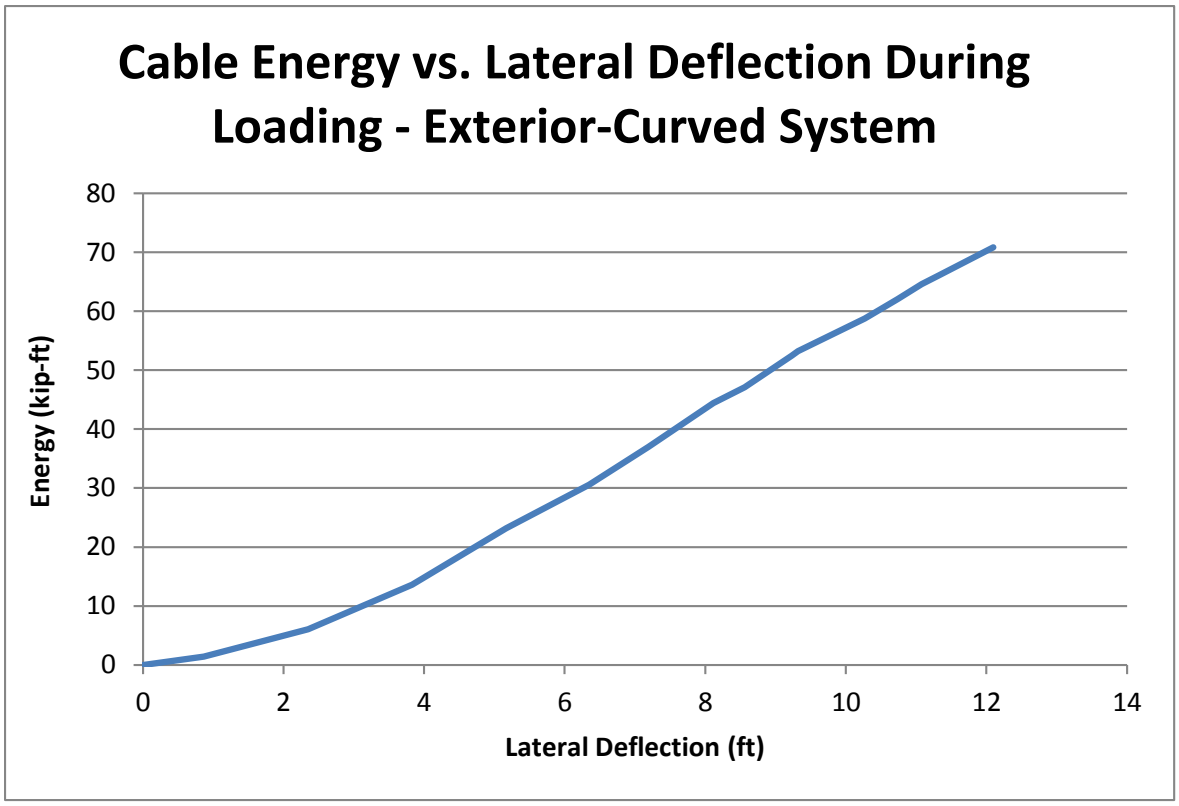

Figure 36. Cable Energy vs. Lateral Deflection During Loading – Test No. NYCC-3

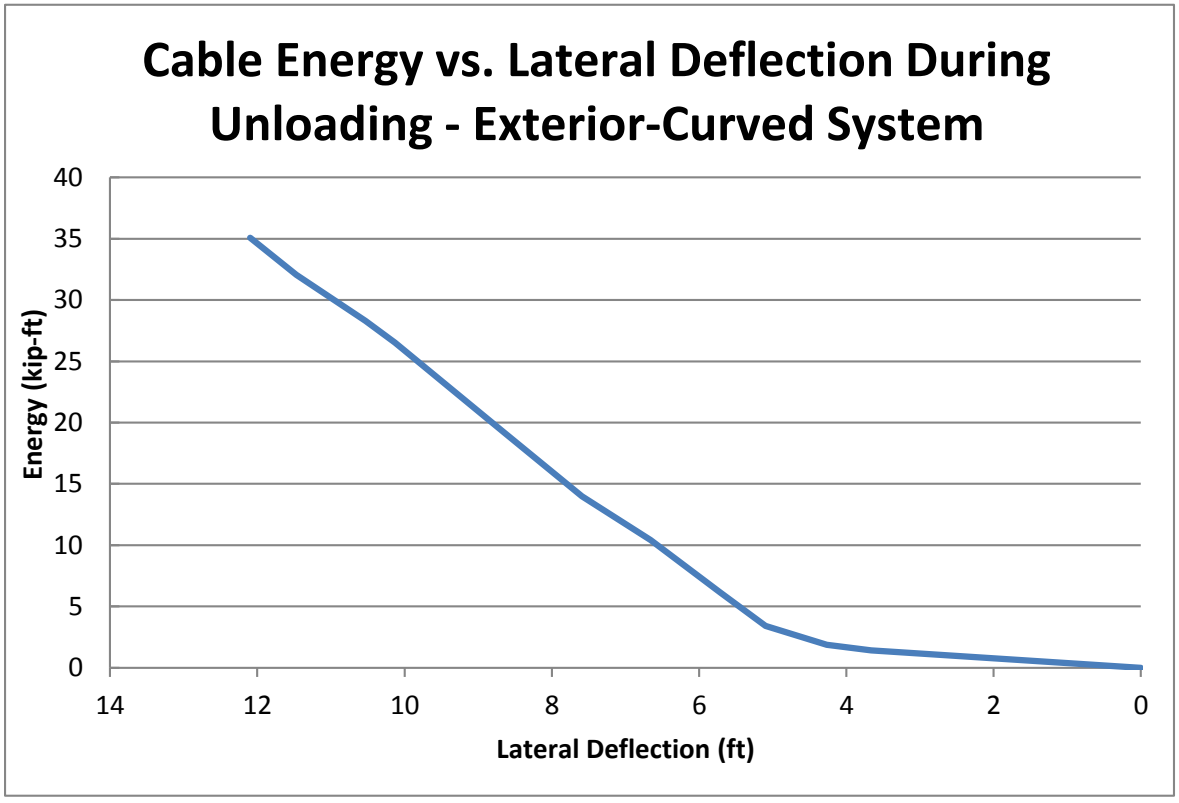

Figure 37. Cable Energy vs. Lateral Deflection During Unloading – Test No. NYCC-3

2.4 Vehicle-Barrier Frictional Interaction

The energy absorbed due to vehicle-barrier friction is equal to the integral of lateral cable force found in Section 2.3 multiplied by the coefficient of friction between the vehicle and barrier over the distance the vehicle traveled. Previous simulation of cable barrier system impacts has shown that a coefficient of friction of 0.08 has been used in validated cable barrier system models [7]. Therefore, the vehicle-barrier coefficient of friction was estimated to be in the range from 0.08 to 0.12. The upper range was established and may be applicable when there is very apparent vehicle damage due to cables sliding along the sheet metal. Since there has not been any physical testing known to date of cable to sheet metal contact friction, a larger range of coefficients may need to be used during accident reconstructions. The vehicle-barrier frictional energy vs. the total distance traveled was found for both a straight cable system (test no. CS-2) and an exterior-curved cable system (test no. NYCC-3), as shown in Figures 38 and 39, respectively. Additional full-scale crash testing of cable barrier systems is necessary to determine if the relationships apply to systems with different post spacing, system lengths, curve radii, and impact conditions.

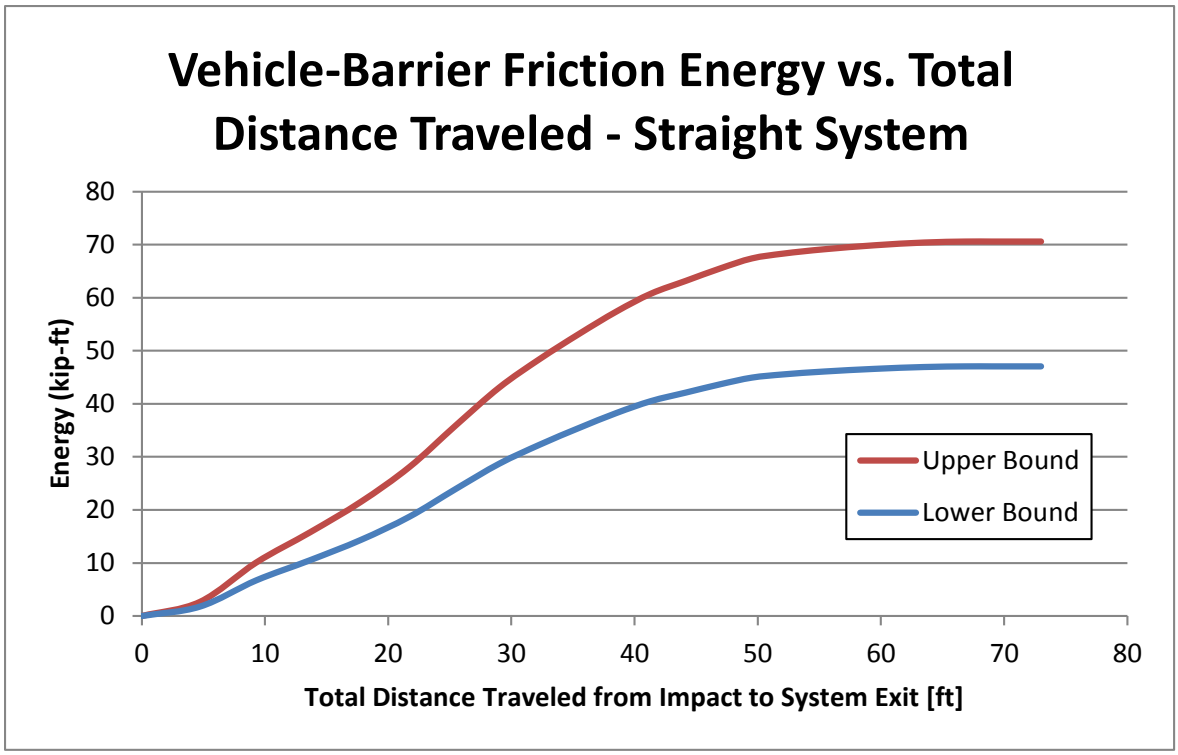

Figure 38. Vehicle-Barrier Frictional Energy vs. Total Distance Traveled – Test No. CS-2

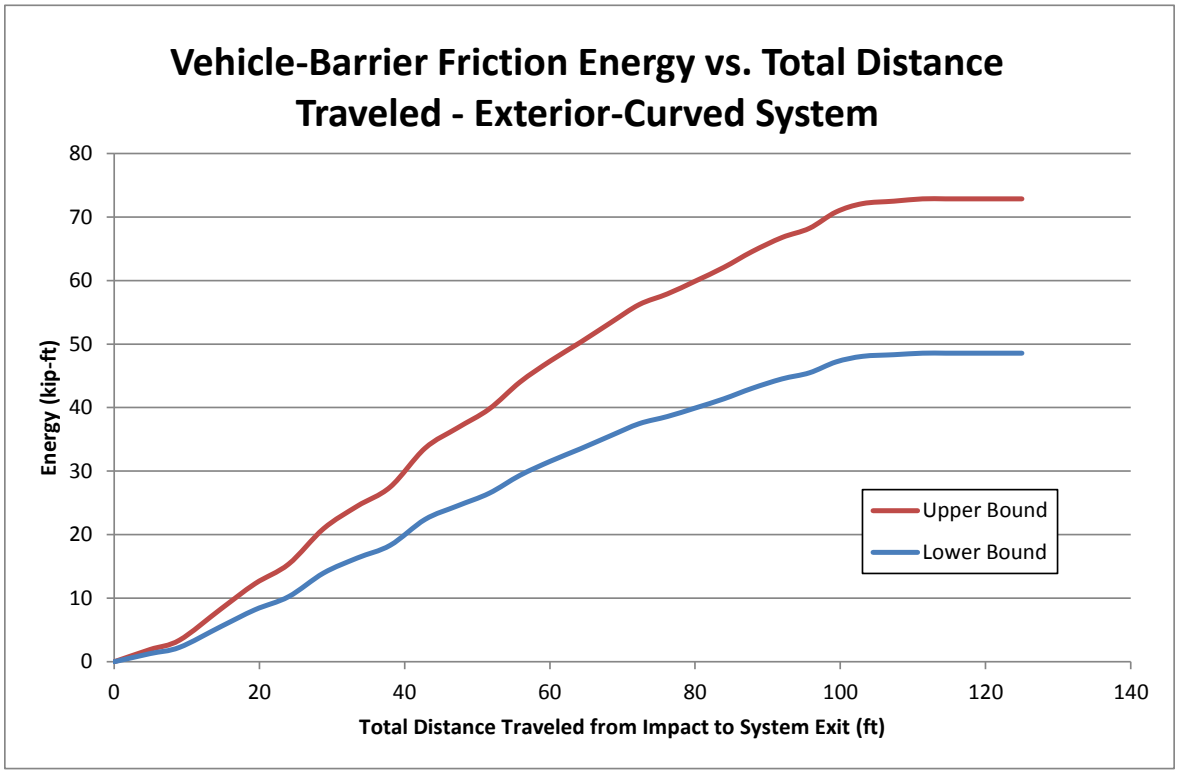

Figure 39. Vehicle-Barrier Friction Energy vs. Total Distance Traveled – Test No. NYCC-3

2.5 J-Bolt Deformation

The energy absorbed through the deformation of the 5/16-in. (7.9-mm) J-bolts, which retain the cable guardrail to the posts, was investigated. MwRSF completed a component testing program in which 5/16-in. (7.9-mm) J-bolts were loaded vertically and horizontally [6]. A simulated cable, which was a ¾-in. (19-mm) diameter steel bar, was mounted in an MTS machine to load the J-bolts in three configurations: (1) a vertical load to simulate a cable pulling the J-bolt upward; (2) a vertical load to simulate a cable pulling the J-bolt downward; and (3) a horizontal load to simulate a cable pulling the J-bolt away from a post.

The energy vs. displacement curves for each of the 5/16-in. (7.9-mm) J-bolt loading cases are shown in Figures 40 through 42, respectively. For the upward direction loading, the total energy absorbed was 0.035 kip-ft (0.047 kJ). For the downward direction loading, the total energy absorbed was 0.19 kip-ft (0.258 kJ). For the horizontal direction loading, the total energy absorbed averaged 0.09 kip-ft (0.122 kJ). The greatest energy dissipation occurred when the J-bolt was loaded vertically downward. If all three cables on a single post were pulled downward, 0.57 kip-ft (0.773 kJ) of energy would be dissipated. However, the cables commonly release from the posts during an impact in the upward or horizontal direction, so the energy due to J-bolt deformation is likely to be much smaller than 0.57 kip-ft (0.773 kJ) per post. The inaccuracies in the energy dissipated by a single post deforming are believed to be greater than the total energy absorbed by the J-bolts deforming. Therefore, the energy dissipated by the J-bolts was not included in the calculation of the total energy dissipated in the full-scale test analyses in this report.

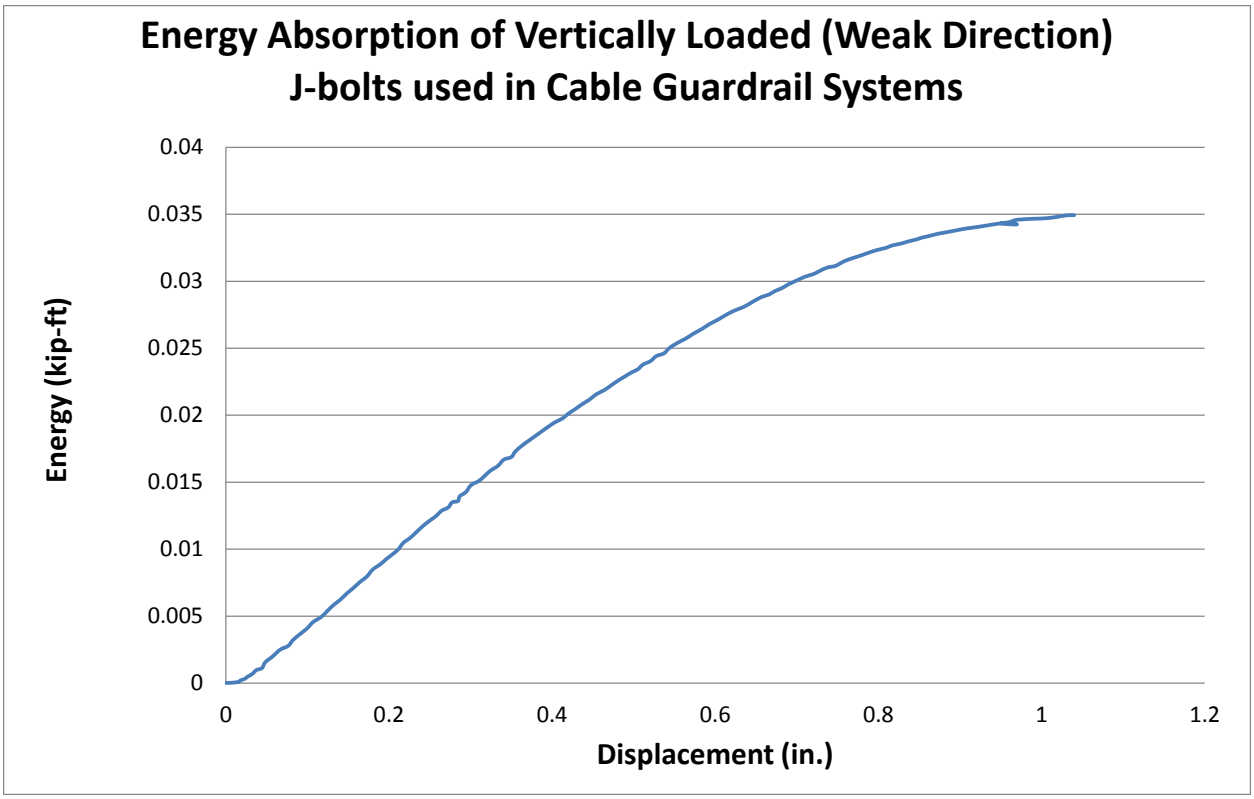

Figure 40. Energy vs. Displacement – J-bolt Loaded Vertically in an Upward Direction [6]

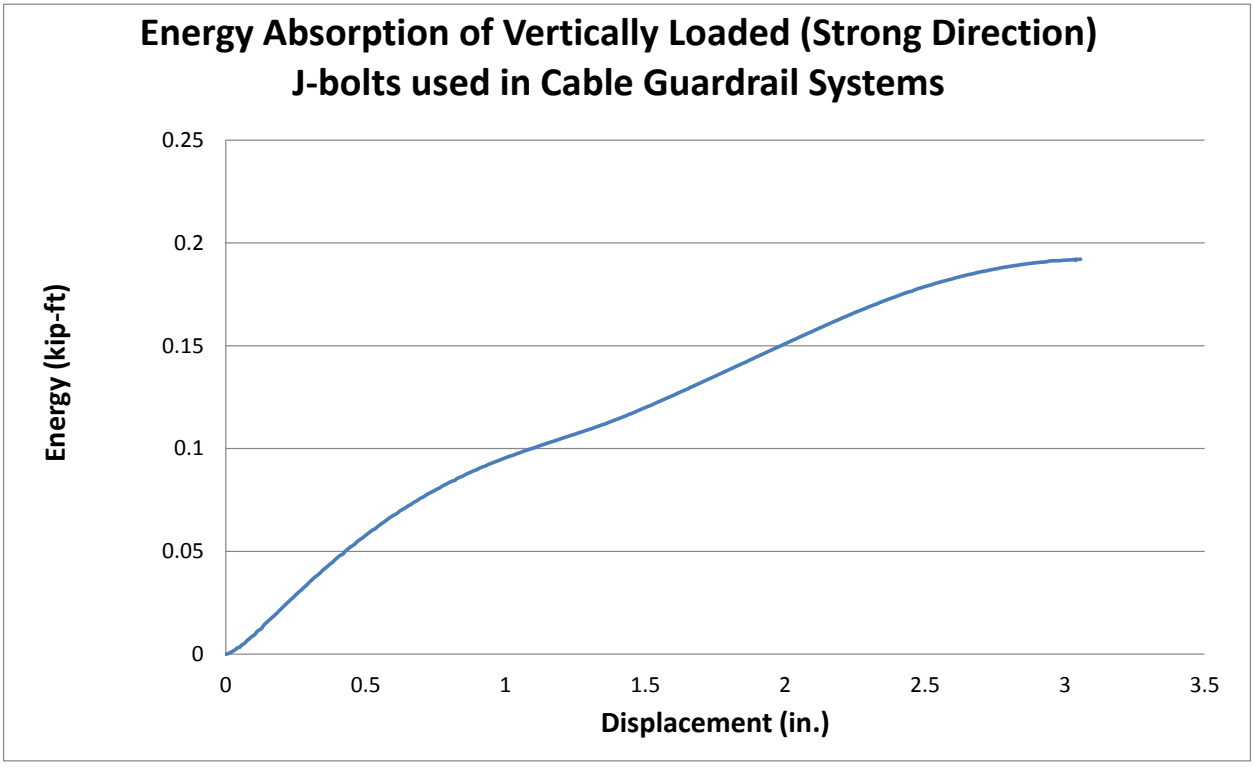

Figure 41. Energy vs. Displacement – J-bolt Loaded Vertically in a Downward Direction [6]

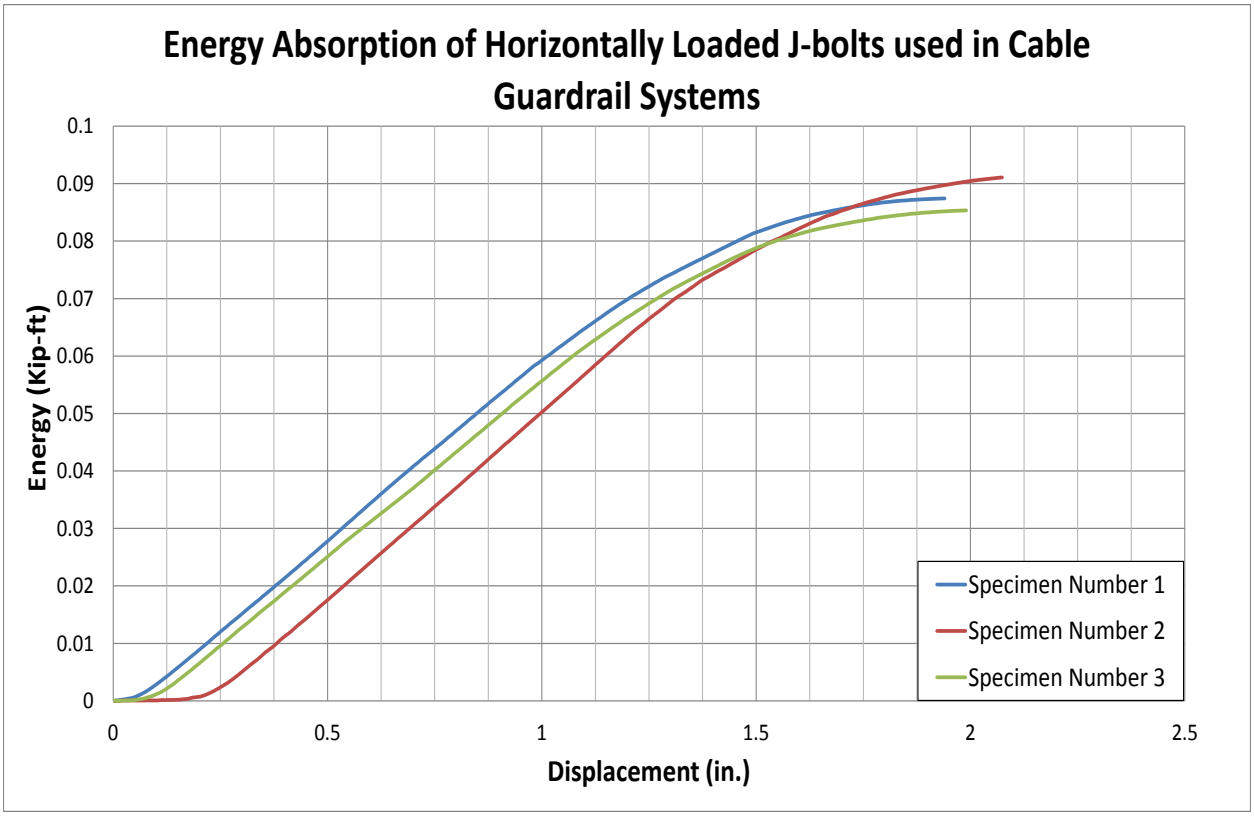

Figure 42. Energy vs. Displacement – J-bolt Loaded Horizontally Away from the Post [6]

3 RECONSTRUCTION TECHNIQUE

The summation of the energy absorbed by each of the energy components is the total kinetic energy lost during a cable barrier system impact. These components include the plastic deformation/rotation of posts, vehicle-ground interaction, internal cable energy, vehicle-barrier interaction, and J-bolt deformation. The quantity of energy absorbed by each of the previously discussed components are added to find the total energy lost from the initial impact of a cable barrier system until the vehicle exited the system. It is assumed that the velocity of the vehicle when it exited the system is known from other accident reconstruction techniques. Since the mass of the vehicle is also known, the vehicle's kinetic energy upon exiting the system is known. The kinetic energy upon existing the system is added to the total energy lost during the impact to estimate the kinetic energy of the vehicle at the initial impact. The initial velocity of the vehicle can then be determined. This technique was evaluated using three full-scale crash tests found in the following chapters.

4 RECONSTRUCTION TECHNIQUE - TEST NO. CS-2

Test no. CS-2 was conducted with a 4,481-lb (2,033-kg) pickup truck impacting a straight, low-tension, three-cable barrier system at 61.6 mph (99.1 km/h) and at an angle of 25 degrees [2]. The S3x5.7 (S76x8.5) posts were spaced 4 ft (1.2 m) on center. The total length of the system was 494 ft (150.6 m). Since vehicle accelerometer data was not available, video analysis was used to determine the time when the vehicle exited the system and the corresponding velocity. The velocity of the pickup truck was approximately 32.8 mph (52.8 km/h) when the vehicle exited the system. The kinetic energy of the pickup truck at impact was approximately 568.2 kip-ft (770.4 kJ). The kinetic energy of the pickup truck when it exited the system was approximately 161.3 kip-ft (218.8 kJ). Therefore, 406.9 kip-ft (551.6 kJ) of energy was absorbed during the impact with the cable barrier system. Each energy absorbing component is discussed in detail in the following sections. Since the J-bolt deformation is minimal and hard to determine for previous crash tests, it was excluded from this analysis.

4.1 Plastic Deformation/Rotation of Posts

The energy absorbed by the components identified in Chapter 2 were quantified for test no. CS-2. The S3x5.7 (S76x8.5) posts were fabricated from ASTM A36 steel. Eighteen posts plastically deformed during the impact. The posts had an initial height of 33 in. (838 mm) and were installed in soil. Therefore, the energy absorbed by each post was estimated from Figure 24. The deformed post orientation and deformed post height were estimated from high-speed video and post-test photographs. The estimated deformed post orientation, deformed post height, and energy absorbed for each post is shown in Table 3. A total of 63.4 kip-ft (86.0 kJ) of energy was absorbed through the deformation/rotation of the S3x5.7 (S76x8.5) posts.

Table 3. Energy Absorbed by S3x5.7 (S76x8.5) Posts – Test No. CS-2

Post No.	Post No. from CAD	Deformed Post Orientation (degrees)	Height from Ground (in.)	Energy Absorbed (k-ft)
1	32	90	32	1.4
2	33	30	15	4.1
3	34	30	20	3.7
4	35	30	22	3.5
5	36	45	15	4.3
6	37	70	18	4.7
7	38	70	25	3.6
8	39	70	23	4
9	40	70	18	4.7
10	41	70	19	4.6
11	42	70	22	4.3
12	43	45	24	3.4
13	44	45	24	3.4
14	45	45	27	2.7
15	46	15	20	3.2
16	47	15	18	3.4
17	48	15	15	3.7
18	49	0	32	0.7
			Total Energy Absorbed by all Posts	**63.4**

4.2 Vehicle-Ground Interaction

The weight of the vehicle without any occupants was 4,481 lb (2,033 kg). The distance the vehicle traveled over 50-ms intervals was measured from the overhead high-speed video with the use of AutoCAD. The vehicle was also determined to be either rolling or sliding from the high-speed video. During the times when the vehicle was rolling, the vehicle-ground coefficient range was 0.01 to 0.0375 for new, sharp concrete to sandy dirt, as determined from Appendix B. During the times when the vehicle was sliding or non-tracking, the vehicle-ground coefficient range was 0.4 to 0.7 for dry loose gravel at a velocity greater than 30 mph (48 km/h), as determined from Appendix B. The upper and lower ranges for the energy absorbed by the vehicle-ground interaction at each time interval as well as the total energy absorbed are shown in

Table 4. The estimated energy absorbed by the vehicle-ground interaction ranged from 99.8 kip-ft to 176.2 kip-ft (135.3 kJ to 238.9 kJ).

Table 4. Energy Absorbed by Vehicle-Ground Interaction – Test No. CS-2

Time (sec)	Distance Traveled (ft)	Vehicle is	Vehicle-Ground Coefficient		Energy Absorbed	
			Lower Range	Upper Range	Lower (kip-ft)	Upper (kip-ft)
0	0	rolling	0.01	0.0375	0	0
0.05	4.7	rolling	0.01	0.0375	0.2	0.8
0.1	9.3	rolling	0.01	0.0375	0.2	0.8
0.15	13.6	rolling	0.01	0.0375	0.2	0.7
0.2	17.8	rolling	0.01	0.0375	0.2	0.7
0.25	21.7	rolling	0.4	0.7	7.1	12.4
0.3	25.5	sliding	0.4	0.7	6.7	11.8
0.35	29.0	sliding	0.4	0.7	6.4	11.2
0.4	32.3	sliding	0.4	0.7	5.9	10.4
0.45	35.5	sliding	0.4	0.7	5.6	9.9
0.5	38.5	sliding	0.4	0.7	5.4	9.5
0.55	41.3	sliding	0.4	0.7	5.0	8.8
0.6	44.2	sliding	0.4	0.7	5.1	8.9
0.65	46.9	sliding	0.4	0.7	5.0	8.7
0.7	49.5	sliding	0.4	0.7	4.7	8.2
0.75	52.1	sliding	0.4	0.7	4.6	8.0
0.8	55.4	sliding	0.4	0.7	5.9	10.4
0.85	59.5	sliding	0.4	0.7	7.4	12.9
0.9	63.5	sliding	0.4	0.7	7.1	12.5
0.95	66.9	sliding	0.4	0.7	6.0	10.6
1	(69.0)	sliding	0.4	0.7	3.8	6.7
1.05	(71.0)	sliding	0.4	0.7	3.6	6.3
1.1	(73.0)	sliding	0.4	0.7	3.6	6.3
	(estimated)			**Total**	**99.8**	**176.2**

4.3 Internal Cable Energy

The lateral deflection, leading and trailing angles, and the tension in the cables were determined at 50-ms time intervals using AutoCAD, as shown in Chapter 2. The kinetic energy absorbed by the cables during loading is shown in Figure 43. The kinetic energy released to the vehicle by the cables during unloading is shown in Figure 44. The maximum lateral deflection

was found to be 6.3 ft (1.9 m). The difference between the energies at maximum lateral deflection was the energy absorbed by the cables, which was approximately 35.0 kip-ft (47.4 kJ).

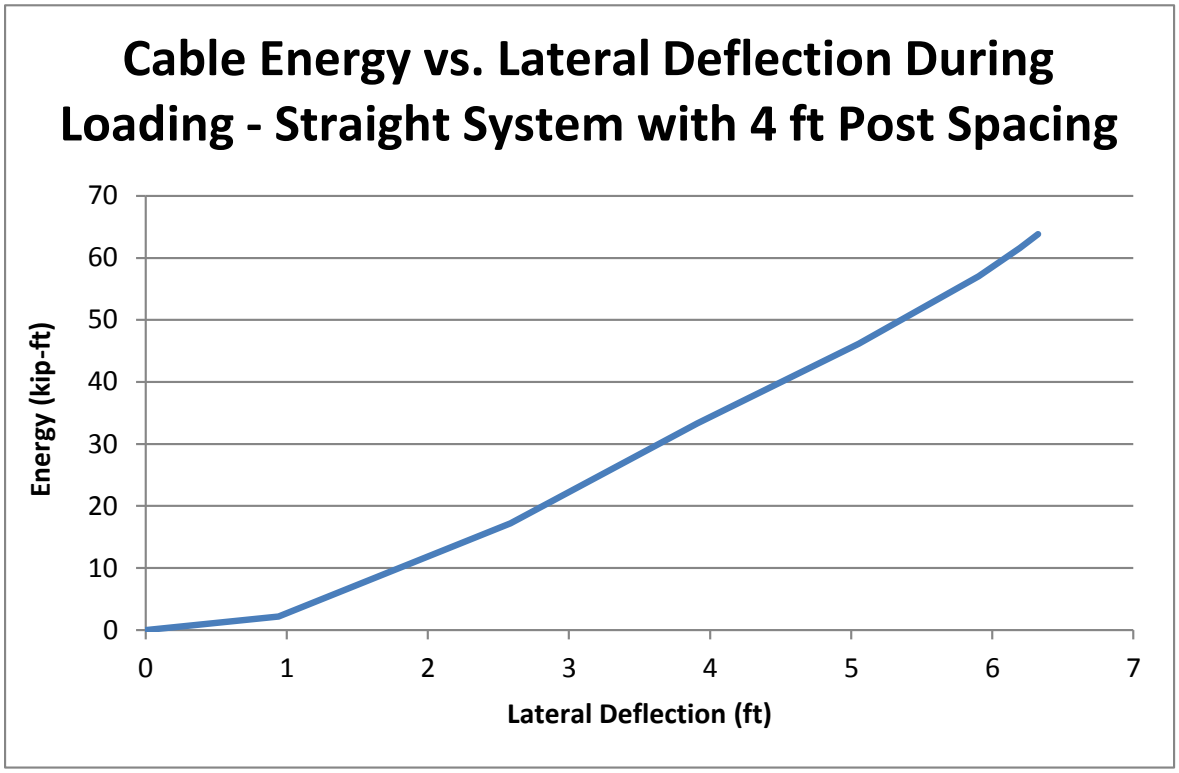

Figure 43. Cable Energy vs. Lateral Deflection During Loading – Test No. CS-2

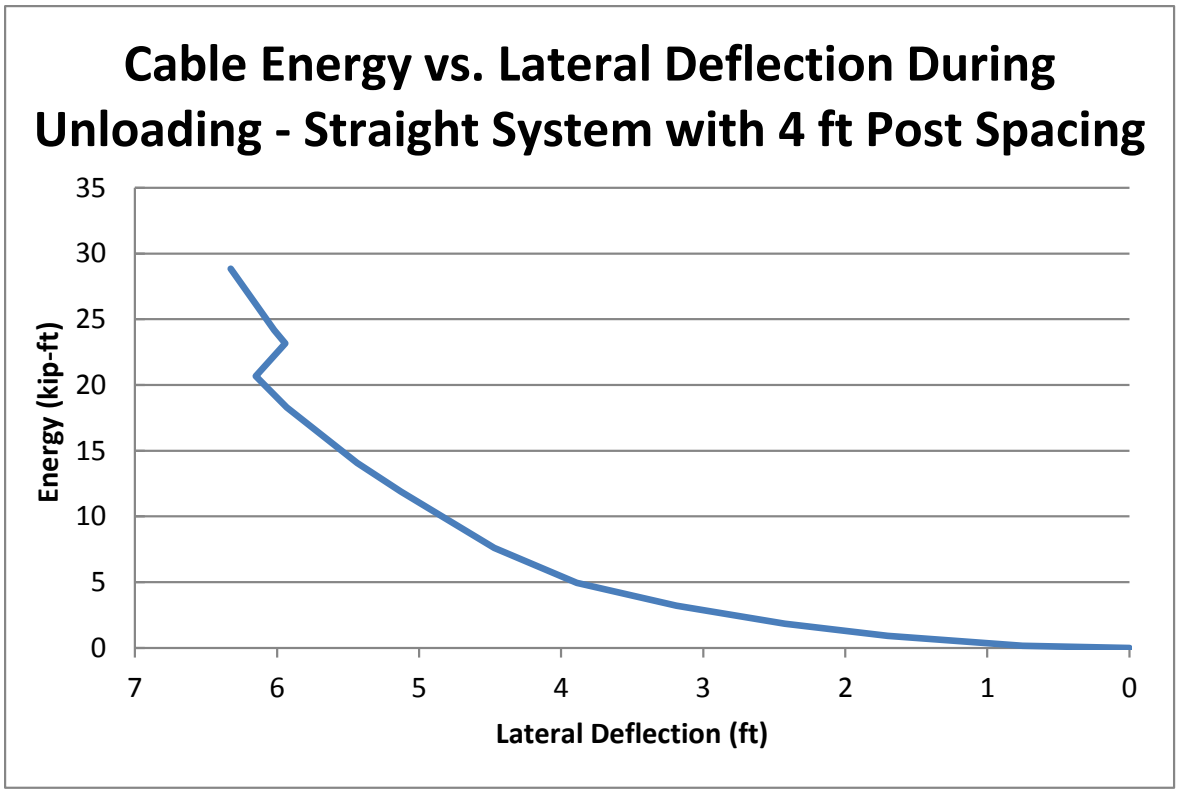

Figure 44. Cable Energy vs. Lateral Deflection During Unloading – Test No. CS-2

4.4 Vehicle-Barrier Frictional Interaction

Friction occurred between the vehicle and the cables due to the lateral cable loading. The coefficient of friction between the vehicle and cables ranged from 0.08 to 0.12, as mentioned in Chapter 2. The distance traveled and the lateral cable loading were found at 50-ms intervals. The upper and lower bounds of the energy absorbed by the vehicle-barrier interaction are shown in Figure 45. The total energy absorbed by the vehicle-barrier friction through the traveled distance from impact to system exit ranged from 47.1 kip-ft to 70.6 kip-ft (63.8 kJ to 95.7 kJ).

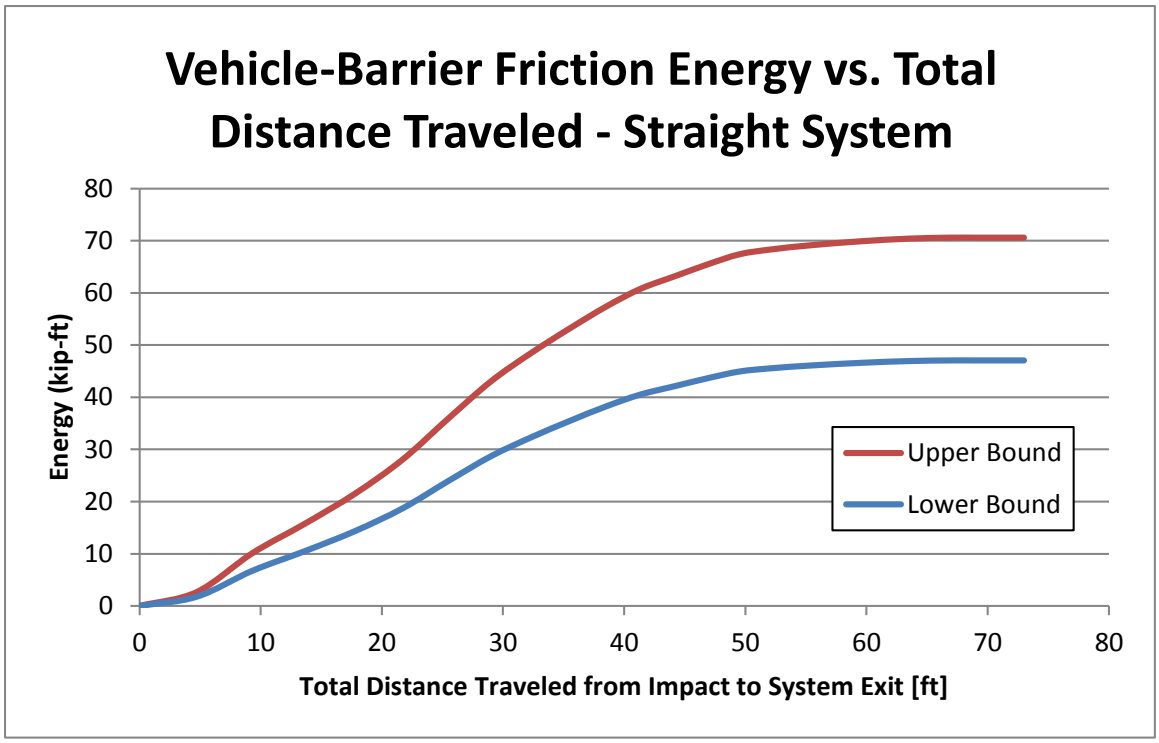

Figure 45. Vehicle-Barrier Interaction Energy vs. Distance Traveled – Test No. CS-2

4.5 Total Energy and Initial Velocity

The energy of all components is summarized in Table 5. The actual kinetic energy of the vehicle when it exited the system was 161.3 kip-ft (218.8 kJ). The sum of the component energies which was 295.2 kip-ft ± 50.0 kip-ft (400. kJ ± 67.8 kJ) was added to the kinetic energy when the vehicle exited. Therefore, the estimate of the vehicle's initial kinetic energy was 456.6 kip-ft ± 50.0 kip-ft (619.0 kJ ± 67.8 kJ). The vehicle's estimated initial velocity was 55.1 mph ± 3.0 mph (88.7 km/h ± 4.9 km/h). The actual velocity of the vehicle was 61.6 mph (99.1 km/h), which is higher than the reconstruction technique predicted range. This potentially could be due to the other energy components that were unaccounted for, underestimated coefficients of vehicle-ground and vehicle-barrier interaction, contributions of the sloped soil region behind the barrier, or inaccuracies in estimating deformed post height and orientations.

Table 5. Summary of Energy Components – Test No. CS-2

Component	Lower Bound (kip-ft)	% total
Posts	63.4	26%
Vehicle-Ground	99.8	41%
Cable Redirection	35.0	14%
Vehicle-Barrier	47.1	19%
Total Energy of Components	**245.2**	
Velocity Before Impact (mph)	**52.1**	

Component	Upper Bound (kip-ft)	% total
Posts	63.4	18%
Vehicle-Ground	176.2	51%
Cable Redirection	35.0	10%
Vehicle-Barrier	70.6	20%
Energy Change Observed	**345.2**	
Velocity Before Impact (mph)	**58.1**	

5 RECONSTRUCTION TECHNIQUE - TEST NO. NYCC-1

Test no. NYCC-1 was conducted with a 5,020-lb (2,277-kg) pickup truck impacting a curved, low-tension, three-cable barrier system at a speed of 61.6 mph (99.1 km/h) and at an angle of 19.9 degrees [1]. The S3x5.7 (S76x8.5) posts were spaced at 8 ft (2.4 m) on center along a 360 ft (109.7 m) radiused curve. The total length of the system was 400 ft (122 m). The top cable snagged on the front of the vehicle and the threaded cable end fractured 300 ms after the initial impact. Therefore, the energy absorption was analyzed only over the first 300 ms of the impact event. The velocity of the vehicle versus time from the accelerometer data as well as overhead video analysis is shown in Figure 46. Since the values followed the same trend and were within a 2 mph (3.2 km/h) range, the velocity from the accelerometer data was selected for use in the analysis. The velocity of the pickup truck after 300 ms was approximately 57.2 mph (92 km/h). The kinetic energy of the pickup truck at impact was approximately 636.4 kip-ft (862.9 kJ). The kinetic energy of the pickup truck after 300 ms was approximately 548.2 kip-ft (734.2 kJ). Therefore, 88.3 kip-ft (119.7 kJ) of energy was absorbed during the first 300 ms of the impact with the cable barrier system. Each energy absorbing component is discussed in detail in the following sections. Since the J-bolt deformation is minimal and hard to determine for previous crash tests, it was excluded from this analysis.

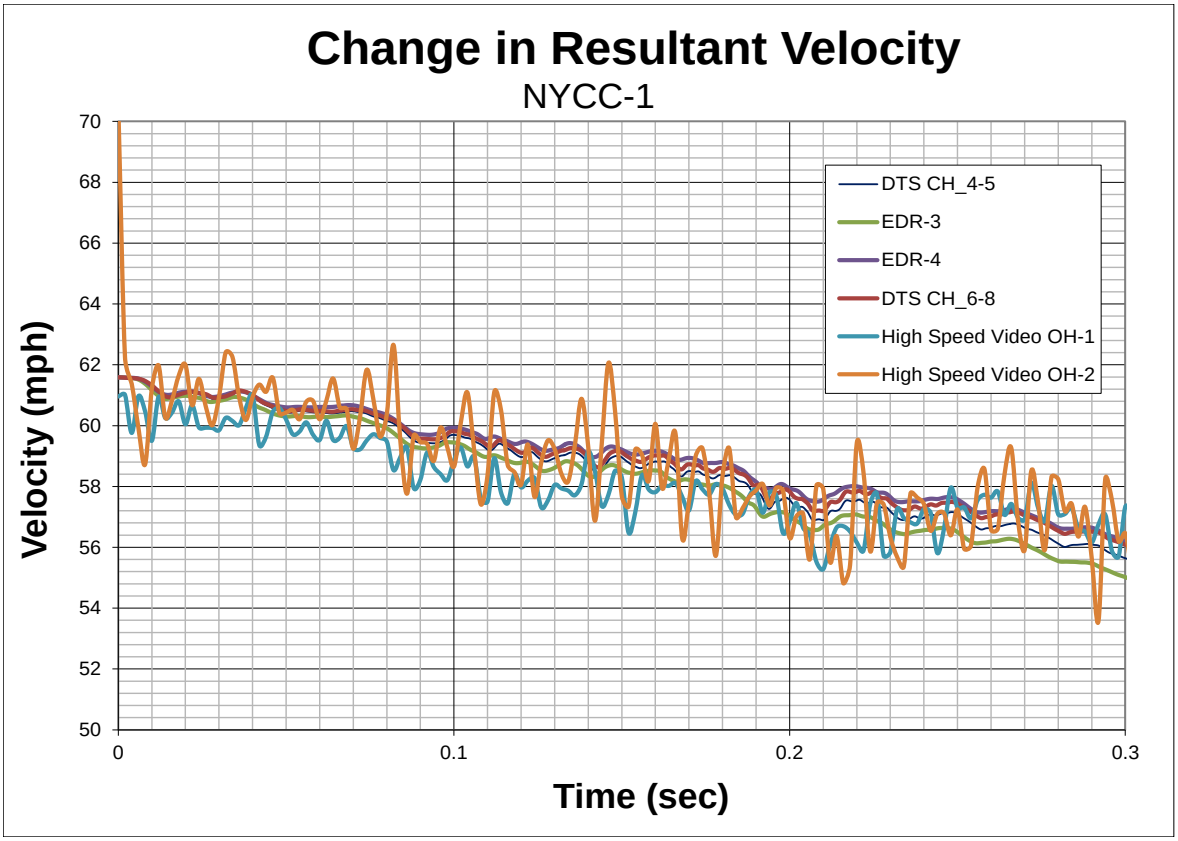

Figure 46. Change in Vehicle Velocity – Test No. NYCC-1

5.1 Plastic Deformation/Rotation of Posts

The S3x5.7 (S76x8.5) posts were fabricated from ASTM A992 steel. Five posts plastically deformed during the first 300 ms of the impact, as determined from high-speed video. The posts had an initial height of 30 in. (838 mm) and were installed in soil. Therefore, the energy absorbed by each post was determined from Figure 21. Since this impact was analyzed only through the first 300 ms, the deformed post orientation and deformed post orientation were estimated from only high-speed video. The height of some of the posts could not be estimated from post-test photographs, because they had only partially deformed up through 300 ms. Therefore for those posts, the lateral deflection of the post was measured from overhead video using AutoCAD and the energy was determined from lateral deflection instead of deformed post height. The deformed post orientation, deformed post height, lateral deflection, and energy

absorbed for each post is shown in Table 6. A total of 18.1 kip-ft (24.5 kJ) of energy was absorbed through the deformation/rotation of the five deformed S3x5.7 (S76x8.5) posts.

Table 6. Energy Absorbed by S3x5.7 (S76x8.5) Posts – Test No. NYCC-1

Post No.	Post No. from CAD	Deformed Post Orientation (degrees)	Height from Ground (in.)	Deflection (in.)	Energy Absorbed (k-ft)
1	17	20	8	-	4.1
2	18	20	15	-	3.9
3	19	20	15	-	3.9
4	20	70	-	16	3.1
5	21	70	-	16	3.1
				Total Energy Absorbed by Posts	**18.1**

5.2 Vehicle-Ground Interaction

The distance the vehicle traveled over 30-ms intervals was measured from the overhead high-speed video with the use of AutoCAD. Since the vehicle was rolling through the first 300 ms, the vehicle-ground coefficient range was 0.01 to 0.0375 for new, sharp concrete to sandy dirt, as determined from Appendix B. The upper and lower ranges for the energy absorbed by the vehicle-ground interaction at each time interval as well as the total energy absorbed are shown in Table 7. The estimated energy absorbed by the vehicle-ground interaction ranged from 1.4 kip-ft to 5.2 kip-ft (1.9 kJ to 7.0 kJ).

Table 7. Energy Absorbed by Vehicle-Ground Interaction – Test No. NYCC-1

Time (sec)	Distance Traveled (ft)	Vehicle is	Vehicle-Ground Coefficient		Energy Absorbed	
			Lower Range	Upper Range	Lower (kip-ft)	Upper (kip-ft)
0	0	rolling	0.01	0.0375	0.0	0.0
0.03	2.8	rolling	0.01	0.0375	0.1	0.5
0.06	5.7	rolling	0.01	0.0375	0.1	0.5
0.09	8.4	rolling	0.01	0.0375	0.1	0.5
0.12	11.2	rolling	0.01	0.0375	0.1	0.5
0.15	14.0	rolling	0.01	0.0375	0.1	0.5
0.18	16.9	rolling	0.01	0.0375	0.1	0.5
0.21	19.6	rolling	0.01	0.0375	0.1	0.5
0.24	22.4	rolling	0.01	0.0375	0.1	0.5
0.27	25.0	rolling	0.01	0.0375	0.1	0.5
0.3	27.6	rolling	0.01	0.0375	0.1	0.5
				Total	1.4	5.2

5.3 Internal Cable Energy

The lateral deflection, leading and trailing angles, and the tension in the cables were determined at 30-ms time intervals using AutoCAD. The kinetic energy absorbed by the cables during loading is shown in Figure 47. Since the tension in the cables was never unloaded during the first 300 ms, all of the work done by the cables absorbed kinetic energy. The maximum lateral deflection the vehicle reached was 7.0 ft (2.1 m). The estimated kinetic energy absorbed by the cables was 38.1 kip-ft (51.6 kJ).

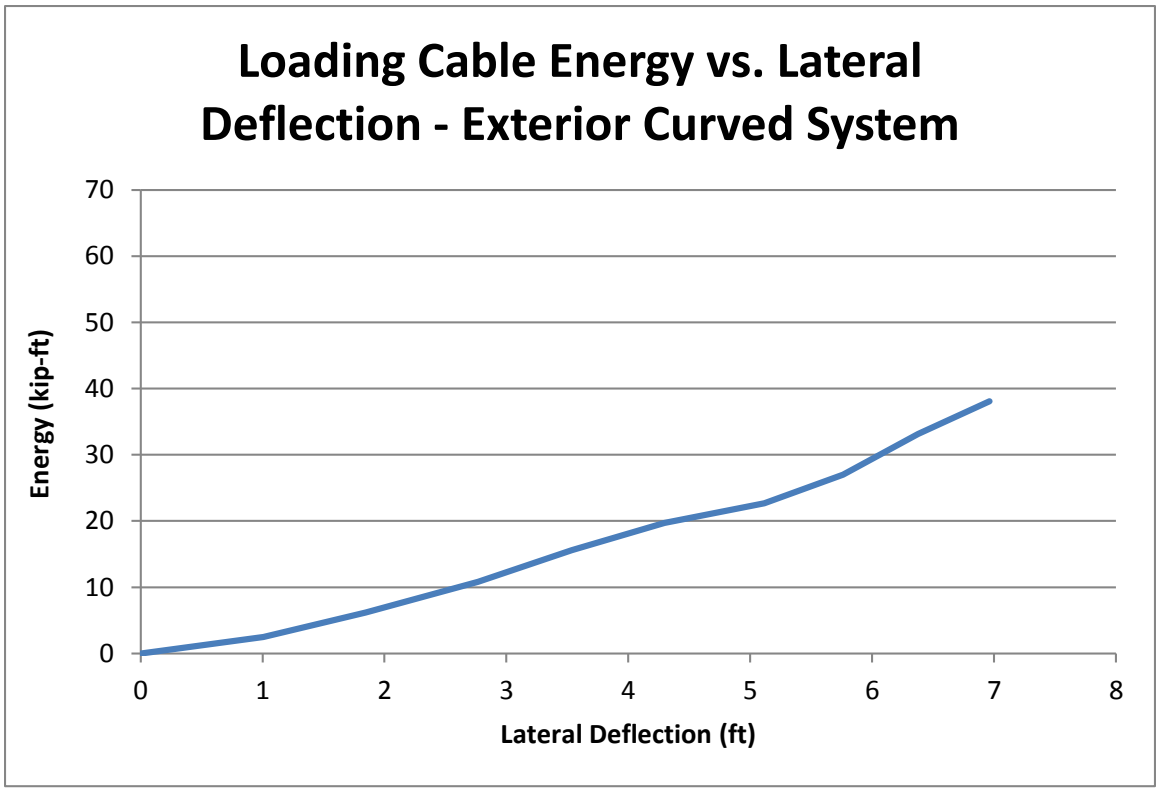

Figure 47. Cable Energy During Loading vs. Lateral Deflection – Test No. NYCC-1

5.4 Vehicle-Barrier Frictional Interaction

Friction occurred between the vehicle and the cables due to the lateral cable loading. The coefficient of friction between the vehicle and cables ranged from 0.08 to 0.12, as mentioned in Chapter 2. The distance traveled and the lateral cable loading were found at 30-ms intervals. The upper and lower bounds of the energy absorbed by the vehicle-barrier interaction are shown in Figure 45. The total energy absorbed by the vehicle-barrier friction through the traveled distance from impact to 300 ms into the impact ranged from 12.3 kip-ft to 18.4 kip-ft (16.6 kJ to 25.0 kJ).

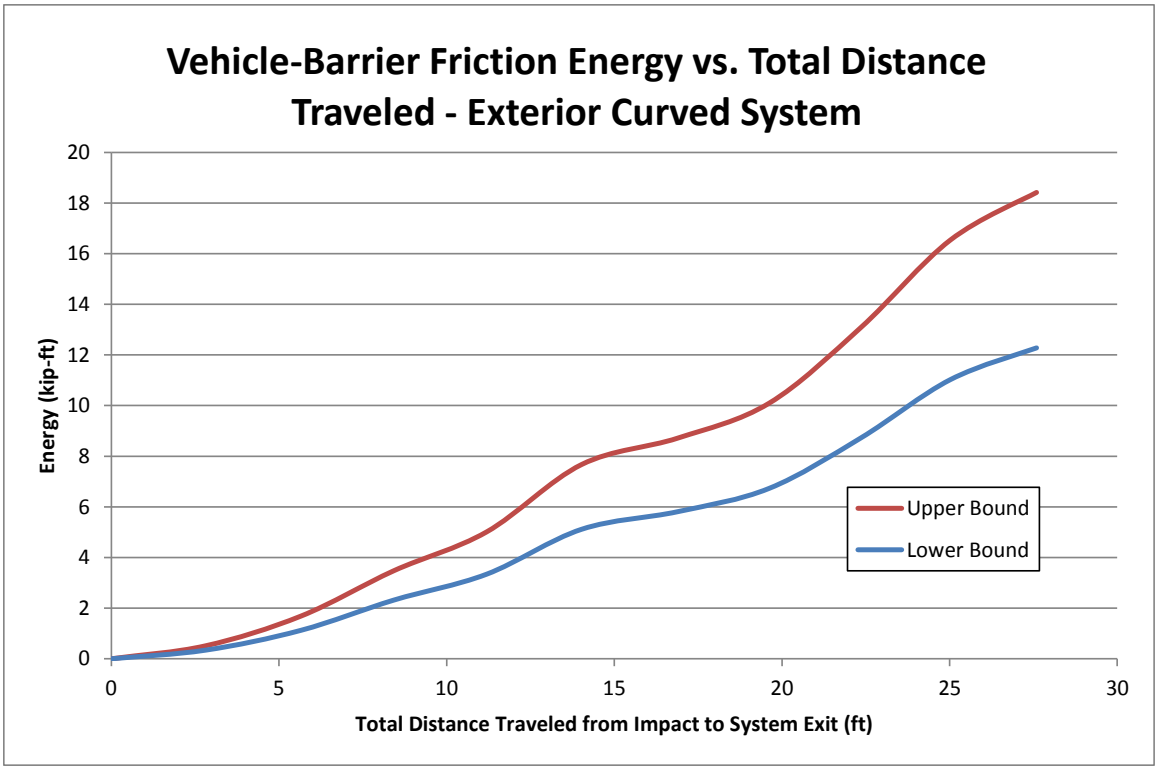

Figure 48. Vehicle-Barrier Interaction Energy vs. Distance Traveled – Test No. NYCC-1

5.5 Total Energy and Initial Velocity

The energy of all components is summarized in Table 8. The actual kinetic energy of the pickup truck after 300 ms was 548.2 kip-ft (734.2 kJ). The sum of the component energies was 74.8 kip-ft ± 5.0 kip-ft (101.5 kJ ± 6.8 kJ) and was added to the kinetic energy at 300 ms. Therefore, the estimate of the vehicle's initial kinetic energy was 623.0 kip-ft ± 5.0 kip-ft (844.7 kJ ± 6.8 kJ). The vehicle's estimated initial velocity was 61.0 mph ± 0.3 mph (98.1 km/h ± 0.4 km/h). The actual velocity of the vehicle was 61.6 mph (99.1 km/h), which is slightly higher but very close to the reconstruction technique predicted velocity. Differences potentially could be due to the other energy components that were unaccounted for, the ASTM A992 steel post material, underestimated coefficients of vehicle-ground and vehicle-barrier interaction, or inaccuracies in estimating deformed post height and orientations.

Table 8. Summary of Energy Components – NYCC-1

Component	Lower Bound (kip-ft)	% total
Posts	18.1	30%
Vehicle-Ground	1.4	2%
Cable Redirection	30.7	51%
Vehicle-Barrier	9.9	17%
Total Energy of Components	**60.1**	
Velocity Before Impact (mph)	**60.2**	

Component	Upper Bound (kip-ft)	% total
Posts	18.1	26%
Vehicle-Ground	5.2	8%
Cable Redirection	30.7	45%
Vehicle-Barrier	14.9	22%
Total Energy of Components	**68.8**	
Velocity Before Impact (mph)	**60.6**	

6 RECONSTRUCTION TECHNIQUE - TEST NO. NYCC-3

Test no. NYCC-3 was conducted with a 4,998-lb (2,267-kg) pickup truck impacting a curved, low-tension, three-cable barrier system at a speed of 63.1 mph (101.6 km/h) and at an angle of 21.6 degrees [1]. The S3x5.7 (S76x8.5) posts were spaced 8 ft (2.4 m) on center along a 440 ft (134.1 m) radiused curve. The total length of the system was 389 ft - 4 in. (118.7 m). Video analysis was used to determine the time when the vehicle exited the system. Since the accelerometer and video analysis values in test no. NYCC-1 were similar, accelerometer data was used to determine the velocity of the pickup truck when the vehicle exited the system. The velocity of the pickup truck as determined from the accelerometer data analysis was approximately 50.0 mph (80.5 km/h) when the vehicle exited the system. The kinetic energy of the pickup truck at impact was approximately 627.3 kip-ft (850.5 kJ). The kinetic energy of the pickup truck when it exited the system was approximately 398.4 kip-ft (540.2 kJ). Therefore, 228.8 kip-ft (310.3 kJ) of energy was absorbed during the impact with the cable barrier system. Each energy absorbing component is discussed in detail in the following sections. Since the J-bolt deformation is minimal and hard to determine for previous crash tests, it was excluded from this analysis.

6.1 Plastic Deformation/Rotation of Posts

Sixteen S3x5.7 (S76x8.5) posts plastically deformed during the impact. Post nos. 17 through 25 were fabricated from ASTM A36 steel, and post nos. 26 through 30 were fabricated from ASTM A992 steel. The posts had an initial height of 32 in. (813 mm) and were installed in soil. Therefore, the energy absorbed by each post was determined from Figure 23. The deformed post orientation and deformed post height were estimated from high-speed video and post-test photographs. The deformed post orientation, deformed post height, and energy absorbed for each

post is shown in Table 9. A total of 47.5 kip-ft (64.4 kJ) of energy was absorbed through the deformation/rotation of the S3x5.7 (S76x8.5) posts.

Table 9. Energy Absorbed by S3x5.7 (S76x8.5) Posts – Test No. NYCC-3

Post No.	Post No. from CAD	Deformed Post Orientation (degrees)	Height from Ground (in.)	Energy Absorbed (k-ft)
1	17	15	6	3.9
2	18	25	15	4
3	19	25	18	3.7
4	20	25	21	3.4
5	21	90	31	1.5
6	22	75	30	2
7	23	75	30	2
8	24	75	30	2
9	25	75	30	2
10	26	75	15	5.3
11	27	45	9	4.9
12	28	45	15	4.6
13	29	0	18	3.3
14	30	45	9	4.9
			Total Energy Absorbed by Posts	**47.5**

6.2 Vehicle-Ground Interaction

The distance the vehicle traveled over 50-ms intervals was measured from the overhead high-speed video with the use of AutoCAD. The vehicle was also determined to be either rolling or sliding from the high-speed video. During the times when the vehicle was rolling, the vehicle-ground coefficient range was 0.01 to 0.0375 for new, sharp concrete to sandy dirt, as determined from Appendix B. During the times when the vehicle was sliding or non-tracking, the vehicle-ground coefficient range was 0.4 to 0.7 for dry loose gravel at a velocity greater than 30 mph (48 km/h), as determined from Appendix B. From 0.8 to 1.05 sec, the vehicle was redirecting out of the system. The vehicle was still sliding sideways, but also rolling a lot more than previously, so coefficients of 0.2 and 0.35, which were half of the sliding coefficients, were used. The upper

and lower ranges for the energy absorbed by the vehicle-ground interaction at each time interval as well as the total energy absorbed are shown in Table 10. The estimated energy absorbed by the vehicle-ground interaction ranged from 87.7 kip-ft to 160.6 kip-ft (119.0 kJ to 217.8 kJ).

Table 10. Energy Absorbed by Vehicle-Ground Interaction – Test No. NYCC-3

Time (sec)	Distance Traveled (ft)	Vehicle is	Vehicle-Ground Coefficient		Energy Absorbed	
			Lower Range	Upper Range	Lower (kip-ft)	Upper (kip-ft)
0	0.0	rolling	0.01	0.0375	0	0
0.05	5.0	rolling	0.01	0.0375	0.2	0.9
0.1	9.0	rolling	0.01	0.0375	0.2	0.8
0.15	14.7	rolling	0.01	0.0375	0.3	1.1
0.2	19.4	rolling	0.01	0.0375	0.2	0.9
0.25	24.0	rolling	0.01	0.0375	0.2	0.9
0.3	28.8	rolling	0.01	0.0375	0.2	0.9
0.35	33.5	rolling	0.01	0.0375	0.2	0.9
0.4	38.0	rolling	0.01	0.0375	0.2	0.8
0.45	42.8	sliding	0.4	0.7	9.6	16.7
0.5	47.2	sliding	0.4	0.7	8.9	15.5
0.55	51.6	sliding	0.4	0.7	8.8	15.4
0.6	55.9	sliding	0.4	0.7	8.5	14.8
0.65	60.1	sliding	0.4	0.7	8.4	14.7
0.7	64.2	sliding	0.4	0.7	8.2	14.3
0.75	68.4	sliding	0.4	0.7	8.3	14.6
0.8	72.3	rolling/sliding	0.2	0.35	3.9	6.9
0.85	76.2	rolling/sliding	0.2	0.35	3.9	6.8
0.9	80.0	rolling/sliding	0.2	0.35	3.8	6.7
0.95	84.0	rolling/sliding	0.2	0.35	3.9	6.9
1	87.8	rolling/sliding	0.2	0.35	3.9	6.8
1.05	92.0	rolling/sliding	0.2	0.35	4.1	7.2
1.1	95.7	rolling	0.01	0.0375	0.2	0.7
1.15	99.4	rolling	0.01	0.0375	0.2	0.7
1.2	103.1	rolling	0.01	0.0375	0.2	0.7
1.25	107.4	rolling	0.01	0.0375	0.2	0.8
1.3	111.3	rolling	0.01	0.0375	0.2	0.7
1.35	(114.5)	rolling	0.01	0.0375	0.2	0.6
1.4	(118.0)	rolling	0.01	0.0375	0.2	0.7
1.45	(121.5)	rolling	0.01	0.0375	0.2	0.7
1.5	(125.0)	rolling	0.01	0.0375	0.2	0.7
	(estimated)			**Total**	87.7	160.6

6.3 Internal Cable Energy

The lateral deflection, leading and trailing angles, and the tension in the cables were determined at 50-ms time intervals using AutoCAD, as shown in Chapter 2. The kinetic energy absorbed by the cables during loading is shown in Figure 49. The kinetic energy released to the vehicle by the cables during unloading is shown in Figure 50. The maximum lateral deflection was found to be 12.1 ft (3.7 m). The difference between the energies at maximum lateral deflection was the energy absorbed by the cables, which was approximately 35.7 kip-ft (48.4 kJ).

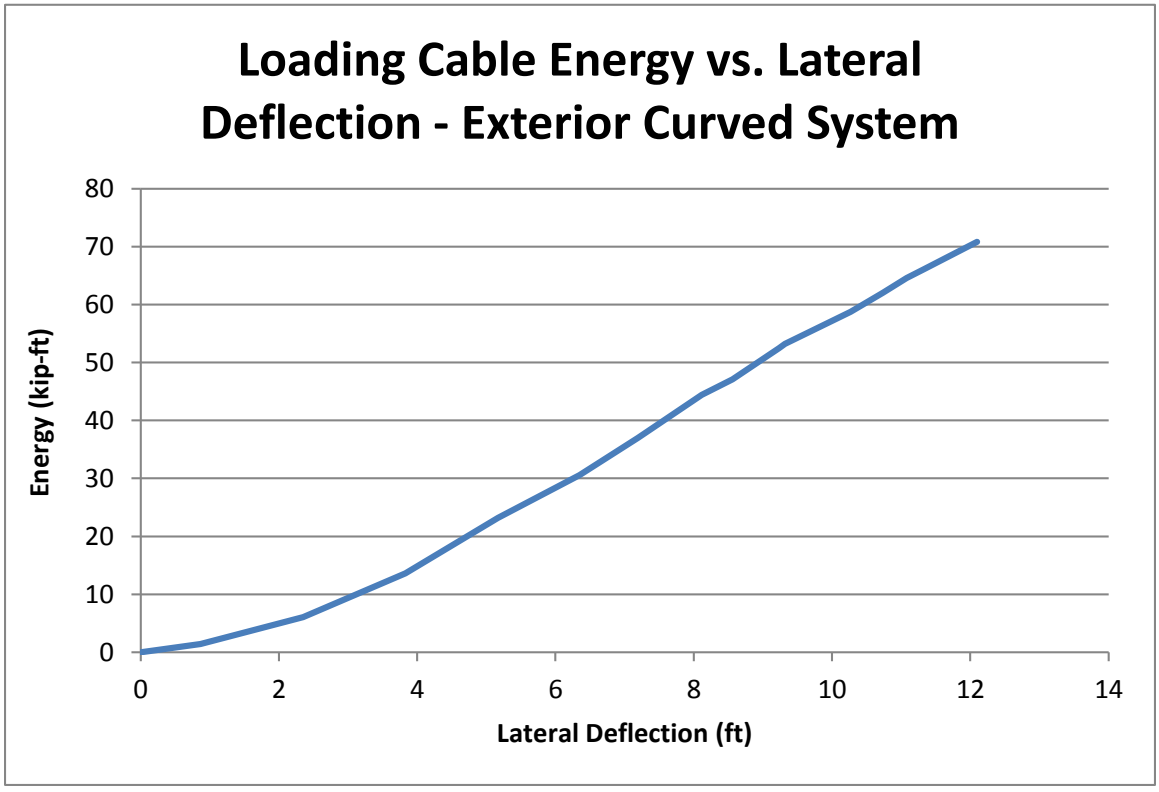

Figure 49. Cable Energy During Loading vs. Lateral Deflection – Test No. NYCC-3

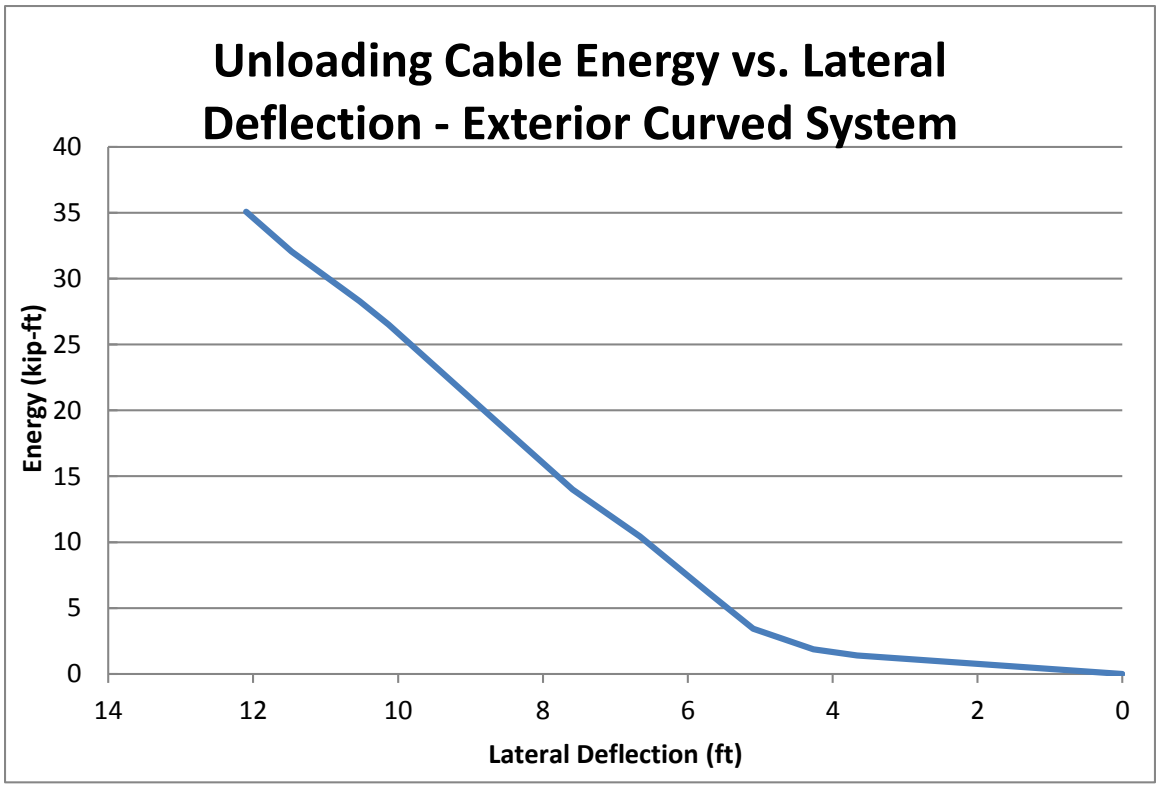

Figure 50. Cable Energy During Unloading vs. Lateral Deflection – Test No. NYCC-3

6.4 Vehicle-Barrier Frictional Interaction

Friction occurred between the vehicle and the cables due to the lateral cable loading. The coefficient of friction between the between the vehicle and cables ranged from 0.08 to 0.12, as mentioned in Chapter 2. The distance traveled and the lateral cable loading were found at 50-ms intervals. The upper and lower bounds of the energy absorbed by the vehicle-barrier interaction are shown in Figure 51. The total energy absorbed by the vehicle-barrier friction ranged from 48.6 kip-ft to 72.9 kip-ft (65.8 kJ to 98.8 kJ).

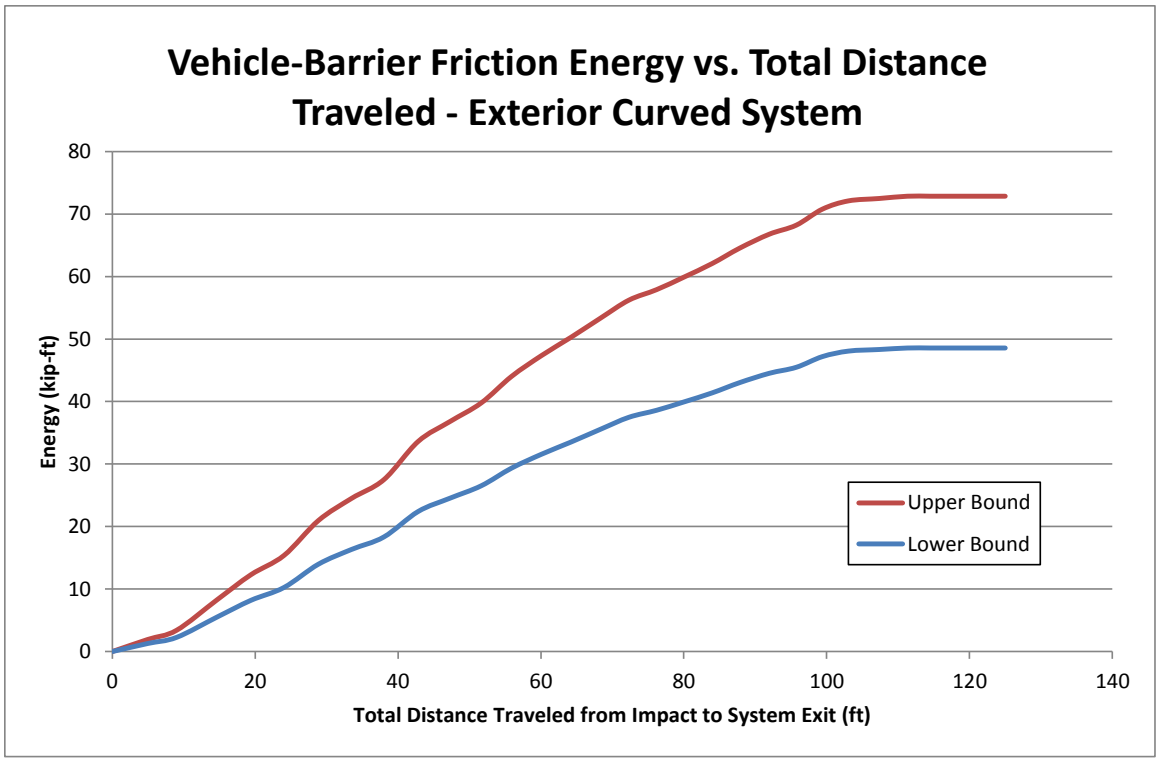

Figure 51. Vehicle-Barrier Interaction Energy vs. Distance Traveled – Test No. NYCC-3

6.5 Total Energy and Initial Velocity

The energy of all components is summarized in Table 11. The actual kinetic energy of the vehicle when it exited the system was 398.4 kip-ft (540.2 kJ). The sum of the component energies was 268.1 kip-ft ± 48.6 kip-ft (903.7 kJ ± 65.9 kJ) was added to the kinetic energy when the vehicle exited. Therefore, the estimate of the vehicle's initial kinetic energy was 666.6 kip-ft ± 48.6 kip-ft (903.7 kJ ± 65.9 kJ). The vehicle's estimated initial velocity was 63.2 mph ± 2.4 mph (101.6 km/h ± 3.7 km/h). The actual velocity of the vehicle was 63.1 mph (101.6 km/h), which is within the bounds of the estimated reconstructed velocity.

Table 11. Summary of Energy Components – Test No. NYCC-3

Component	Lower Bound (kip-ft)	% Total
Posts	47.5	23%
Vehicle-Ground	87.7	42%
Cable Redirection	32.3	15%
Vehicle-Barrier	41.3	20%
Total Energy of Components	**208.8**	
Velocity Before Impact (mph)	**60.3**	

Component	Upper Bound (kip-ft)	% Total
Posts	47.5	16%
Vehicle-Ground	160.6	53%
Cable Redirection	32.3	11%
Vehicle-Barrier	62.0	20%
Total Energy of Components	**302.4**	
Velocity Before Impact (mph)	**64.8**	

7 SUMMARY, CONCLUSIONS, AND RECOMMENDATIONS

7.1 Summary

A procedure was developed for estimating the energy absorbed during an impact with a cable barrier system and initial impact velocity. The energy absorbed during a cable barrier system impact was divided into several components: (1) plastic deformation/rotation of posts; (2) vehicle-ground interaction; (3) internal cable energy; (4) vehicle-barrier frictional interaction; and (5) J-bolt deformation. The energy absorbed by deforming the J-bolt cable clips was analyzed and determined to be negligible for this study. The energy absorption per foot during distinct segments of the event could not be found simply due to the overlap of each energy absorption component.

Charts were constructed to determine the energy absorbed by deformed S3x5.7 (S76x8.5) cable posts. The charts were developed based on the ground condition: (1) in a rigid sleeve and (2) in a compacted, crushed limestone soil. The rigid sleeve charts represent a ground surface that does not allow the post to rotate at groundline. The soil charts represent a ground surface that allows the post to rotate at groundline. Each set of charts has initial post heights that vary from 28 in. to 33 in. (711 mm to 838 mm) above the ground. The deformed post orientation and deformed post height above the ground need to be determined and documented at an accident site. The deformed post orientation should be estimated based on the angle of the base of post from its normal position. A 0-degree orientation (weak axis) would typically occur from an impact of a vehicle parallel to the system. A 90-degree orientation (strong axis) would typically occur from the cable pulling the posts backward.

Charts were also developed from test data of ASTM A36 S3x5.7 (S75x8.5) steel posts with unknown yield strengths. Since ASTM A992 rolled shapes have become more common than ASTM A36 rolled shapes, many new S3x5.7 (S76x8.5) steel posts may be fabricated with

ASTM A992 steel. The ASTM A992 material has a higher minimum yield strength than the ASTM A36 material. The energy absorbed by the post will increase when the yield strength of the steel is higher. However, the exact yield strengths of line posts installed in cable barrier system installations would be difficult to determine and energy vs. deflection information for ASTM A992 S3x5.7 (S76x8.5) steel posts at different impact angles is currently unavailable.

The energy absorbed by the vehicle-ground interaction is approximated by multiplying the weight of the vehicle by the coefficient of rolling resistance or drag factor between the vehicle and ground and the distance traveled. The distance traveled by the vehicle from impact to system exit should be measured. Vehicle-ground coefficients for various road/ground surfaces and for different braking/skidding and rolling scenarios are shown in Appendix B. However, the accident reconstructionist should closely examine the specific site conditions and determine when the vehicle was tracking, non-tracking, and braking and the road/ground surface during those times. The vehicle-ground coefficients should be determined through skid testing, if available.

The tension increases in the cables as a vehicle deflects the cable barrier system during an impact event The kinetic energy transferred to the barrier by the membrane action of the tension in the cables is equal to the integral of the lateral component of the cable force applied to the vehicle over the lateral deflection of the barrier. The cable tension varies between straight, exterior-curved, and interior-curved cable barrier systems. The lateral cable force can be found at any point in time based on the tension and leading and trailing angles that are formed by the cable in contact with the vehicle. These angles vary as the vehicle initially impacts, becomes parallel to the system, and then redirects away from the barrier system. Charts of the energy dissipated as a function of the lateral wheel trajectory were created by integrating the lateral force vs. lateral wheel trajectory curve. The difference between the maximum kinetic energy

absorbed and the maximum kinetic energy added back to the vehicle represents the internal cable energy absorbed. Unfortunately, only the lateral deflection of the vehicle could be estimated based on tire marks during a real-world accident and the other values are unknown. Additional full-scale crash testing of cable barrier systems is necessary to determine if the lateral cable force and deflection relationships apply to systems with different post spacing, system lengths, curve radii, and impact conditions.

The energy absorbed due to vehicle-barrier friction is equal to the integral of lateral cable force multiplied by the coefficient of friction between the vehicle and barrier over the distance the vehicle traveled. The distance the vehicle traveled should be determined from the accident site. The lateral cable force is not known for a real-world accident. Therefore, additional full-scale crash testing of cable barrier systems is necessary to determine if the vehicle-barrier friction relationships apply to systems with different post spacing, system lengths, curve radii, and impact conditions.

The summation of the energy absorbed by each of the energy components is the total kinetic energy lost during a cable barrier system impact. It is assumed that the velocity of the vehicle when it exited the system can be estimated from other accident reconstruction techniques. Since the mass of the vehicle is also known, the vehicle's kinetic energy upon exiting the system can also be estimated. The kinetic energy upon existing the system is added to the total energy lost during the impact to estimate the kinetic energy of the vehicle at the initial impact. The initial velocity of the vehicle can then be estimated. This technique was evaluated using three full-scale crash tests.

In test no. CS-2, the vehicle's estimated initial velocity was 55.1 mph ± 3.0 mph (88.7 km/h ± 4.9 km/h). The actual velocity of the vehicle was 61.6 mph (99.1 km/h), which is higher than the reconstruction technique predicted range. This potentially could be due to the other

energy components that were unaccounted for, underestimated coefficients of vehicle-ground and vehicle-barrier interaction, contributions of the sloped soil region behind the barrier, or inaccuracies in estimating deformed post height and orientations.

In test no. NYCC-1, the vehicle's estimated initial velocity ranged 61.0 mph ± 0.3 mph (98.1 km/h ± 0.4 km/h). The actual velocity of the vehicle was 61.6 mph (99.1 km/h), which is slightly higher but very close to the reconstruction technique predicted range. This potentially could be due to the other energy components that were unaccounted for, the ASTM A992 steel post material, underestimated coefficients of vehicle-ground and vehicle-barrier interaction, or inaccuracies in estimating deformed post height and orientations. The reconstruction technique was only applied for the first 300 ms of the impact event.

In test no. NYCC-3, the vehicle's estimated initial velocity ranged from 63.2 mph ± 2.4 mph (101.6 km/h ± 3.7 km/h). The actual velocity of the vehicle was 63.1 mph (101.6 km/h), which is within the bounds of the estimated reconstructed velocity.

The reconstruction technique provided initial velocity estimates very close to what the actual initial velocity was for both full-scale crash tests on the curved barrier systems. Additional crash testing on both curved and straight barrier systems is recommended to determine if there is additional unaccounted for energy that might occur in an impact with a straight cable barrier system versus a curved cable barrier system or if the analysis needs to be modified. The reconstruction technique should be applied with caution to real-world vehicular impacts with cable barrier systems due to the limitations outlined in this study.

7.2 Future Research Improvements

Several future research improvements were identified throughout this study that could enhance and/or eliminate the limitations of the reconstruction technique developed.

- Additional full-scale crash testing is necessary to determine if the internal cable losses and vehicle-barrier friction relationships can be applied to systems with different post spacing, system lengths, curve radii, and impact conditions. If not, a new procedure should be developed that can be used to reconstruct accidents with a wide variety of systems and impacts.
- Since ASTM A992 steel has become more common than ASTM A36 steel, accurate post data should be obtained for ASTM A992 (50 ksi) S3x5.7 (S76x8.5) steel posts. The effects of yield strength on the post behavior and energy absorption should also be determined through additional component tests.
- Since most impact angles are from 0 to 30 degrees, additional post testing at lower impact angles in both a rigid foundation and soil would provide more comprehensive data for the energy absorbed by deforming posts.
- The smaller energy components that were excluded from these analyses should be quantified in future studies to determine if they would contribute to more accurate velocity predictions.
- The overall accident reconstruction technique should be simplified if accurate results can still be obtained. Minimizing the efforts of the accident reconstructionist will save both time and money.

7.3 Recommendations

The energy absorbed by the plastic deformation/rotation of posts in both rigid sleeves and soil is believed to be accurate and can be used during accident reconstructions of cable barrier system impacts. Depending on the S3x5.7 (S76x8.5) steel post material specification (ASTM A36 or ASTM A992) and the actual yield strength of the posts, the energy absorbed by a deformed post may differ from the data obtained during post testing. The yield strength varies

within the same material specification as well. However, it would be difficult to determine yield strengths in cable barrier system installations, so the charts provided are sufficiently accurate and should be used until further updates are warranted. The initial post height, deformed post height, and deformed post orientation should be determined for each S3x.5.7 (S76x8.5) post that is deformed during a vehicle impact.

The energy absorbed through vehicle-ground interaction is one of the most fundamental energy absorption mechanisms employed in accident reconstructions. The total distance traveled by the vehicle, weight of vehicle, and coefficients of rolling resistance and/or drag factor must be appropriately selected, per standard accident reconstruction techniques. The trajectory marks need to be closely studied to determine if the vehicle was tracking or non-tracking over various segments of the trajectory to apply the correct coefficient between the vehicle-ground surface. The procedure for vehicle-ground interaction is fairly straightforward because agencies already determine this information for other accident reconstructions.

The energy absorbed by J-bolt deformation is believed to be accurate and can be used during accident reconstructions of cable barrier system impacts. The energy was considered negligible and difficult to determine for the full-scale crash tests analyzed in this study. However, the energy could be found during an accident reconstruction by determining the loading direction and displacement of each J-bolt.

The internal cable energy absorbed is believed to be accurate for the specific systems and impacts analyzed in this study. However, it has yet to be determined if the vehicle-barrier procedure can be applicable to other systems and impacts. Therefore, the accident reconstructionist should determine how to analyze the internal cable energy component.

The energy absorbed through vehicle-barrier frictional interaction is believed to be accurate for the specific systems and impacts analyzed in this study. However, it has yet to be

determined if the vehicle-barrier procedure can be applicable to other systems and impacts. Therefore, the accident reconstructionist should determine how to analyze the vehicle-barrier frictional interaction component.

8 REFERENCES

1. Schmidt, T.L., Lechtenberg, K.A., Meyer, C.L., Faller, R.K., Bielenberg, R.W., and Reid, J.D., *Evaluation of the New York Low-Tension Curved Three-Cable Barrier*, Final Report to the New York State Department of Transportation, MwRSF Research Report No. TRP-03-263-12, Project No. TPF-5(193) Supplement #130, Midwest Roadside Safety Facility, University of Nebraska-Lincoln, Lincoln, Nebraska, February 19, 2013.

2. Terpsma, R.J., Polivka, K.A., Sicking, D.L., Rohde, J.R., Reid, J.D., and Faller, R.K., *Evaluation of a Modified Three Cable Guardrail Adjacent to Steep Slope*, Final Report to the Midwest States' Regional Pooled Fund Program, MwRSF Research Report No. TRP-03-192-08, Project No. SPR-03(017), Midwest Roadside Safety Facility, University of Nebraska-Lincoln, Lincoln, Nebraska, March 4, 2008.

3. Kuipers, B.D. and Reid, J.D., *Testing of M203x9.7 (M8x6.5) and S76x8.5 (S3x5.7) Steel Posts – Post Comparison Study for the Cable Median Barrier*, MwRSF Research Report No. TRP-03-143-03, Midwest Roadside Safety Facility, University of Nebraska-Lincoln, Lincoln, Nebraska, October 24, 2003.

4. Lutting, M. and Lechtenberg, K.A., *Cut Cable Post Bogie Testing Test Nos. CCP-1 through CCP-11*, Internal Report, Midwest Roadside Safety Facility, University of Nebraska-Lincoln, Lincoln, Nebraska, February 19, 2012.

5. Fating, R.M. and Reid, J.D., *Dynamic Impact Testing of S75x8.5 Steel Posts (Cable Barrier Posts)*, MwRSF Research Report No. TRP-03-117-02, Midwest Roadside Safety Facility, University of Nebraska-Lincoln, Lincoln, Nebraska, November 15, 2002.

6. Reid, J.D. and Coon, B.A., *Finite Element Modeling of Cable Hook Bolts*, 7th International LS-DYNA Users Conference, Simulation 2002, Dearborn, Michigan, May 19-21, 2002.

7. Reid, J.D., Lechtenberg, K.A., and Stolle, C.S., *Development of Advanced Finite Element Material Models for Cable Barrier Wire Rope*, MATC-UNL Report No. 220, MwRSF Reasearch Report No. TRP-03-233-10, Midwest Roadside Safety Facility, University of Nebraska-Lincoln, Lincoln, Nebraska, August 2, 2010.

8. Trantham, N., *Post Impact Drag Factor*, Technical Accident Investigation, Nebraska Law Enforcement Training Center, May 2009.

9 APPENDICES

Appendix A. Post Testing Setup and Methodology

The post testing setup, methodology, and data processing in this appendix were compiled and adapted from previous post testing reports [3-5].

A.1 Equipment and Instrumentation

Several post tests were conducted during three separate testing series: CMPB [3], CCP [4], and CPB [5]. A variety of equipment and instrumentation were used to record and collect data. The main equipment and instruments used for the tests were:

- Bogie
- Accelerometer
- Pressure Tape Switches
- Photography Cameras

A.1.1 Bogie

A rigid frame bogie was used to impact the posts. An impact head, made of an 8 in. (203 mm) standard steel pipe, was mounted to the bogie at the height of 21.65 in. (550 mm) above the ground. Neoprene belting, 3/4 in. (19 mm) thick, was attached to the steel pipe to minimize the local damage to the post from the impact. The bogie weight was 1,353 lb (613.7 kg) in the CMPB and CCP test series, and the bogie is shown in Figure A-1. The bogie weight was 2,237 lb (1,014 kg) in the CPB test series, and the bogie is shown in Figure A-2.

Figure A-1. Bogie and Test Setup – CMBP and CCP Test Series

Figure A-2. Bogie and Test Setup – CPB Series

A.1.2 Accelerometer

One tri-axial piezo-resistive accelerometer system with a range of ± 200 g's was mounted on the frame of the bogie at approximately the center of gravity in the CCP and CPB test series. It measured the accelerations in the longitudinal direction at a sample rate of 3200 Hz. The accelerometer system known as the Model EDR-3 developed by the Instrumented Sensor Technology (IST) of Okemos, Michigan. The EDR-3 is a self-contained, user-programmable acceleration sensor/recorder with a 74dB dynamic range. During active recording, acceleration signals are digitized to 10-bit resolution and stored in digital memory onboard the unit. Configured with 256 KB of RAM and a 1120 Hz filter, the EDR-3 offers recording capability from six input channels simultaneously. Analog low-pass filtering was used internally in the EDR-3 to condition the input signal. A Butterworth low-pass filter with a –3dB cut-off frequency of 1120 Hz was used for anti-aliasing. The EDR-3 had a maximum cross axis sensitivity of ±3%.

One tri-axial piezo-resistive accelerometer system with a range of ± 200 G's was used to measure the acceleration in the longitudinal, lateral, and vertical and was mounted on the frame of the bogie near its center of gravity in the CMPB test series. The environmental shock and vibration sensor/recorder system, known as the Model EDR-4, was developed by Instrumented Sensor Technology (IST) of Okemos, Michigan and includes three differential channels as well as three single-ended channels. The EDR-4 is a self-contained, user-programmable acceleration sensor/recorder. During testing, the EDR-4 was configured with 6 MB of RAM memory and was set to sample data at 10,000 Hz. A Butterworth low-pass filter with a –3dB cut-off frequency of 1500 Hz was used for anti-aliasing.

Although the accelerometer was located at the center of gravity and measured the acceleration of the bogie's center of gravity, the sampled data was used to approximate the bogie/post forces at the point of impact using Newton's Second Law. A laptop computer

downloaded the raw acceleration data immediately following each test. The computer made the use of "DynaMax 1.75" accelerometer software (6) and then loaded into "DADiSP 4.0" data processing program. The data is processed as per the SAE J211/1 specifications.

A.1.3 Pressure Tape Switches

Three pressure tape switches, spaced at a 3.3-ft (1-m) intervals, were used to determine the speed of the bogie before the impact. As the front left tire of the bogie passed over each tape switch, a strobe light was fired, sending an electronic timing signal to the data acquisition system. Test speeds were determined by knowing the time between these signals from the data acquisition system and the distance between the switches.

A.1.4 Photography Cameras

High-speed Red Lake E/cam video cameras, with an operating speed of 500 frames/sec, and Canon digital video cameras, with an operating speed of 29.97 frames/sec, were used to film the crash tests. The cameras were placed perpendicular to the direction of the bogie. The film was analyzed using the Vanguard Motion Analyzer. Actual camera speed and camera divergence factors were considered in the analysis of the high-speed film.

A.2 Methodology of Testing

Two types of tests were conducted to obtain a complete understanding of the dynamic behavior of the post: 1) posts in a concrete sleeve and 2) posts in soil. The test parameters can be seen in Table A-1.

Table A-1. CMPB Test Parameters

Parameter	CMPB	CCP	CPB
Accelerometer	EDR-4	EDR-3	EDR-3
Bogie Weight	1,353 lb (614 kg)	1,353 lb (614 kg)	2,237 lb (1,014 kg)
Embedment Length	30 in. (762 mm)	30 in. (762 mm)	38 in. (965 mm)

A weak-axis impact is one in which the bogie impacts perpendicular to the web of the post. A strong-axis impact is one in which the bogie impacts parallel to the web of the post. When the bogie impacted the post at an angle, the impact angle was measured from the axis of a weak-axis impact.

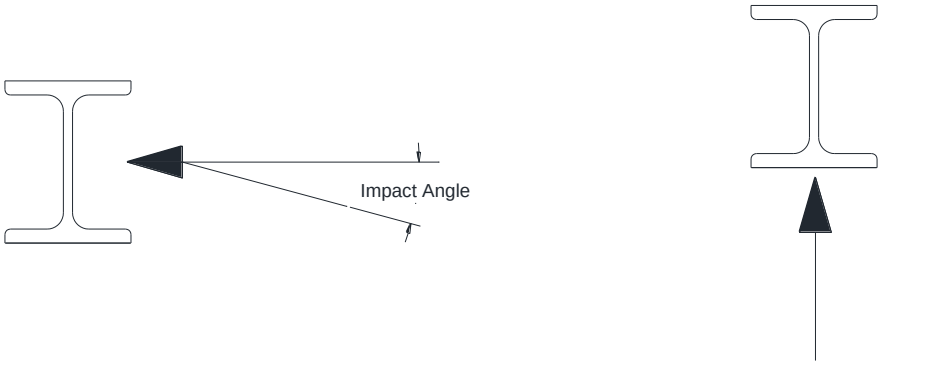

Figure A-3. Weak- and Strong-Axis Impacts

In all tests, a reverse cable tow and guide rail system was used to propel the test vehicle. The bogie was accelerated towards the post along the 98.4 ft (30-m) long tracking system, which consisted of a steel pipe anchored 3.94 in. (100 mm) above the tarmac. Rollers attached to the bogie straddled the pipe, and ensured the proper direction and position of the bogie. The tow cable was released just prior to impact, which allowed the bogie to be free of all external constraints. The bogie positioned on the guide rail can be seen in Figure A-3.

In all of the tests conducted, the bogie wheels were aligned for caster and toe-in values of zero so that the bogie would track properly along the guidance system. A remote braking system was installed on the bogie to allow the bogie to be brought safely to a stop after the test. Accelerometers located at the bogie's center of gravity recorded lateral, horizontal, and vertical acceleration data.

Figure A-4. Bogie Positioned on the Guide Track

A.2.1 Posts in a Concrete Sleeve

For tests CMPB-4, CMPB-5, CMPB-6, and CCP-5, a rectangular hole was cut out in the tarmac to house the post. The hole was lined with a mild steel tube, approximately 10.0 in. x 8.75 in. (254 mm x 222.25 mm) and 10 mm (0.394 in.) thick, to prevent spalling of the concrete around the hole. The post was fitted into the steel lined hole with a block of wood to keep it upright and rigidly hold the post against the casing. A soil plate was attached to the S3x5.7 (S76x8.5) posts and was flush with the wood blocks. An effort was also made to minimize the slop in the posts by inserting an additional steel plate or a piece of plywood to fill the gaps. Neoprene was also added between the post and casing to prevent damage from the impact that may have affected the post properties subsequently determined. The installation setup for test no. CMPB-4 is shown in Figure A-4. The other tests had the same setup only with the wood oriented at different angles.

Figure A-5. Typical Post and Wood Block Setup

A.2.2 Posts in Soil

Test nos. CMPB-14, CMPB-15, and CPB-6 were carried out along and at angles to the strong axis of impact and at different embedment depths in standard NCHRP 350 soil.

A plan view of the test setup and the post-testing pit is shown in Figure A-5. The pit was located at a sufficient distance from the edge of the concrete apron so as not to interfere with the soil response during the impact.

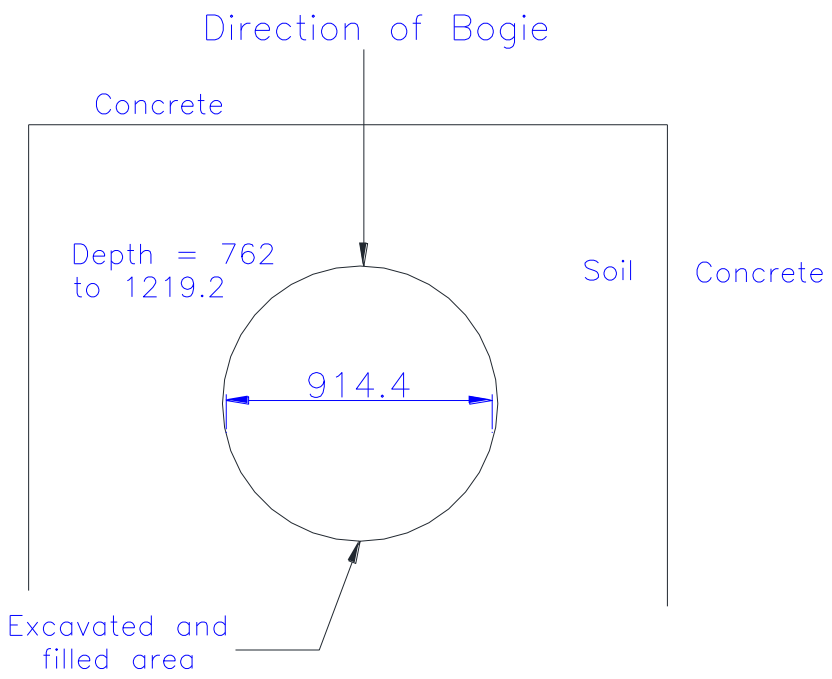

(dimensions in mm)

Figure A-6. Plan View of the Post Testing Area

For the tests, holes measuring 36 in. (0.914 m) in diameter and 30 to 48 in. (0.762 to 1.219 m) in depth were dug out in the test area. The holes were filled with soil meeting the AASHTO "Standard Specification for Materials and Aggregate and Soil-Aggregate Subbase, Base and Surface Courses," designation M147-65 (1990), grading A or B and compacted in accordance with AASHTO guide specifications for highway construction, section 304.05 and 304.07. The moisture content was relatively dry (4% - 6%) with the primary considerations being the homogeneity, consistency and the ease of compaction.

A.3 End of Test Determination

When the bogie overrides the post, the end of the test cannot be the entire duration of the contact between the post and the bogie head, because a portion of the force is consumed to lift the bogie in the vertical direction. When the bogie head initially impacts the post, the force exerted by the bogie is directed perpendicular to the face of the post. As the post begins to rotate

and/or form a plastic hinge, the bogie head is no longer perpendicular to the face of the post and begins to slide along the face of the post as shown in the Figure A-6.

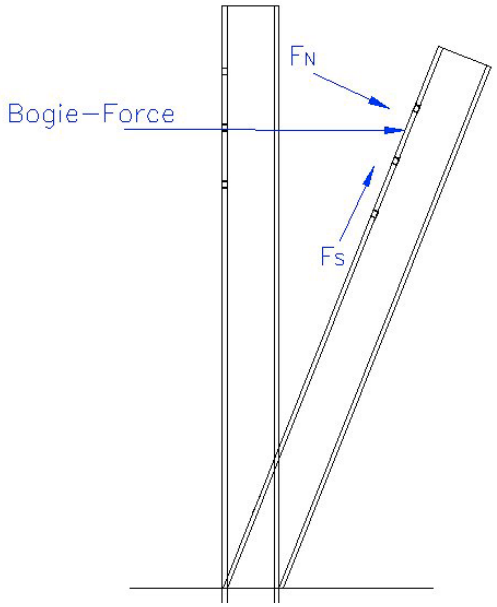

Figure A-7. Various Forces Acting on the Post in Soil and Their Orientations

The S3x5.7 (S76x8.5) posts will form plastic hinges at groundline in both the concrete sleeve and soil. In addition to the variation due to the changing angle of impact, the neoprene on the bogie head, used to minimize the local stress concentration at the point of impact, increases the frictional forces acting on the surface of the post. Additionally, since the accelerometer was used to represent the contact forces rather than the actual center of gravity forces it truly observes, additional error was added to the data. This required that only the initial portion of the accelerometer trace be used. This is because the variations in the data start to become more significant as the post rotates. The bogie, in each case, continued to travel forward after the impact and after clearing the post. The bogie was stopped when the onboard braking system was activated.

A.4 Data Processing

The data was filtered using the SAE Class 60 Butterworth filter conforming to the SAE J211/1 specifications. Pertinent acceleration signal was extracted from the bulk of the data. The processed acceleration data is then multiplied by the mass of the bogie to get the impact force using Newton's Second Law. Next, the acceleration trace was integrated to find the rate of change of velocity. Initial velocity of the bogie, calculated using the data from the pressure tape switches, was then used to determine the bogie velocity. The calculated velocity trace was integrated to find the displacement. Subsequently, using the previous results, the force deflection curve was plotted for each test. Finally, integration of the force-deflection curve provides the energy-displacement curve for each test.

Appendix B. Vehicle-Ground Coefficients

DESCRIPTION OF ROAD SURFACE	DRY	< 48 kph < 30 mph	DRY	> 48 kph > 30 mph	WET	< 48 kph < 30 mph	WET	> 48 kph > 30 mph
	From	To	From	To	From	To	From	To
PORTLAND CEMENT								
New, Sharp	0.80	1.20	0.70	1.00	0.50	0.80	0.40	0.75
Traveled	0.60	0.80	0.60	0.75	0.45	0.70	0.45	0.65
Traffic Polished	0.55	0.75	0.50	0.65	0.45	0.65	0.45	0.60
ASPHALT or TAR								
New, Sharp	0.80	1.20	0.65	1.00	0.50	0.80	0.45	0.75
Traveled	0.60	0.80	0.55	0.70	0.45	0.70	0.40	0.65
Traffic Polished	0.55	0.75	0.45	0.65	0.45	0.65	0.40	0.60
Excess Tar	0.50	0.60	0.35	0.60	0.30	0.60	0.25	0.55
GRAVEL								
Packed, Oiled	0.55	0.85	0.50	0.80	0.40	0.80	0.40	0.60
Loose	0.40	0.70	0.40	0.70	0.45	0.75	0.45	0.75
CINDERS								
Packed	0.50	0.70	0.50	0.70	0.65	0.75	0.65	0.75
ROCK								
Crushed	0.55	0.75	0.55	0.75	0.55	0.75	0.55	0.75
ICE								
Smooth	0.10	0.25	0.07	0.20	0.05	0.10	0.05	0.10
SNOW								
Packed	0.30	0.55	0.35	0.55	0.30	0.60	0.30	0.60
Loose	0.10	0.25	0.10	0.20	0.30	0.60	0.30	0.60
OPEN METAL GRID	0.70	0.90	0.55	0.75	0.25	0.45	0.20	0.35

SLIDING ON ROOF OR SIDE	
Concrete	0.30
Asphalt	0.30 - 0.40
Gravel	0.50 - 0.70
Dry Grass	0.50
Dirt	0.20

Retrieved from reference [8]

ROLLING RESIST.	
Drive Axle	0.10 - 0.20
Non Drive Axle	
Norm Inflation	0.01
Partial Inflation	0.013
Flat Tire	0.017
ENGINE BRAKING	
Low Gear	0.20 - 0.40
High Gear	0.20
BRAKING	
Light Braking	0.10 - 0.20
Normal Braking	0.20 - 0.40
LATERAL ACCEL.	0.20 - 0.30
ROTATIONAL ACCELERATION	
Long Post Travel	0.20 - 0.30
Short Post Travel	0.35 - 0.50
ROLLOVER	0.38 - 0.53
PEDESTRIAN (Sliding)	
Grass	0.45 - 0.70
Asphalt	0.45 - 0.60
Concrete	0.40 - 0.65
MOTORCYCLE REAR WHEEL	
Clean, Dry Surface	0.35 - 0.40
Sand	0.90 - 1.20
Dirt	0.70
FRONT WHEEL	
Max w/ Rear Brake	0.90 - 0.95
Free Rolling	0.01 - 0.02
MC ON SIDE	
Asphalt	0.50 - 0.80
Portland Cement	0.40 - 0.75
Concrete	0.45 - 0.65
Gravel	0.65 - 1.05
Sand	1.50 - 1.60
Hard Soil	0.70
Light Scratching	0.30 - 0.40
Heavy Scratching	0.45 - 0.55
Lube by Fluids	0.20

Retrieved from reference [8]

Coefficients of Rolling Friction of Various Roadway Surfaces

DESCRIPTION OF ROAD SURFACE	fg
CONCRETE	
New, Sharp	0.01
Good	0.015
Worn	0.02
ASPHALT or TAR	
New, Sharp	0.0125
Good	0.0175
Worn	0.0225
GRAVEL (Macadam)	
Good	0.015
Fair	0.0225
Poor	0.0375
PEA GRAVEL (truck ramp)	0.25 - 0.35
DIRT	
Smooth	0.025
Sandy	0.0375
SAND (level, soft)	0.06-0.15
MUD	0.0375 - 0.15
SNOW	
2 inches (5.08 cm)	0.025
4 inches (10.16 cm)	0.0375

Retrieved from reference [8]

Appendix C. Energy Relationships – Test No. CS-2

In test no. CS-2, the relationship between the cable tension and lateral deflection appeared to be almost linear, as shown in Figure 26. However, the lateral component of the cable tension is needed to calculate energy in the cable. The cable tension is multiple by the sine of the leading and trailing angles to find the lateral component, and then the relationship between lateral cable force and lateral deflection is no longer linear, as shown in Figures C-1 and C-2. The relationship between the lateral cable force and total distance traveled is also not linear, as shown in Figure C-3. The actual data could be approximated with a linear relationship, but it would not be very accurate to use in accident reconstructions. The data could also be approximated by a series of linear relationships, but that also adds another degree of complexity as to where each linear segment begins and ends. Therefore, Microsoft Excel was used to fit polynomial curves to the actual data. The data and fitted curves are shown in Figures C-1 through C-3.

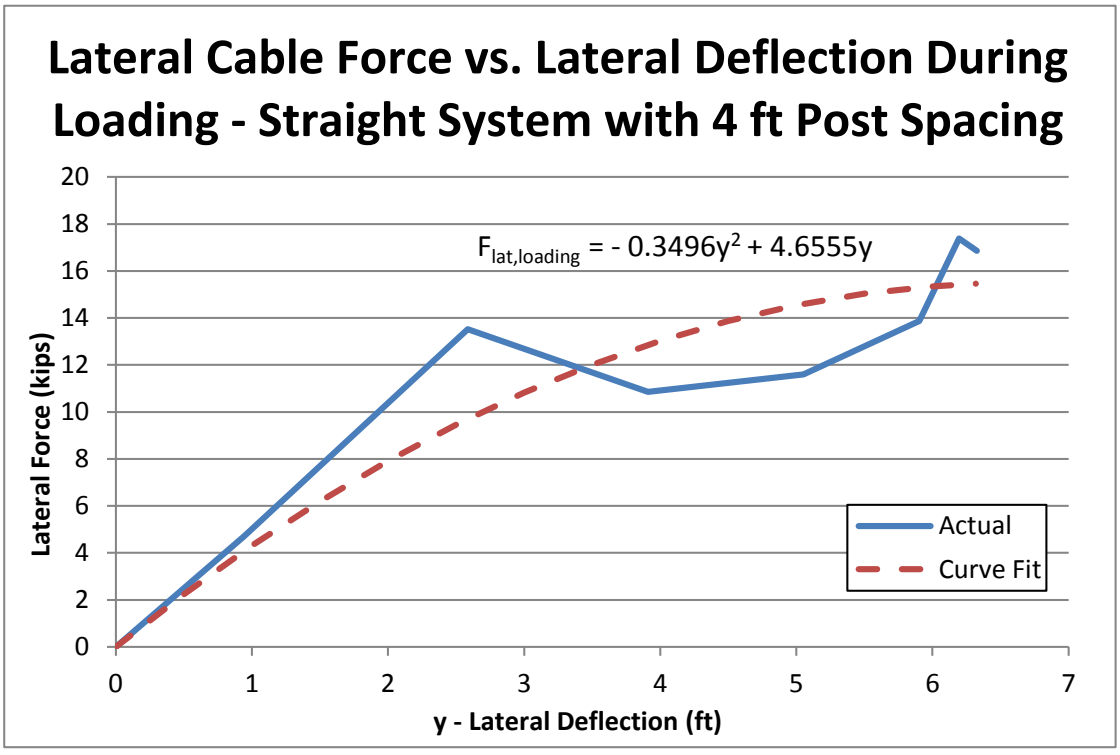

Figure C-1. Lateral Cable Force vs. Lateral Deflection Loading Fitted Curve. – Test No. CS-2

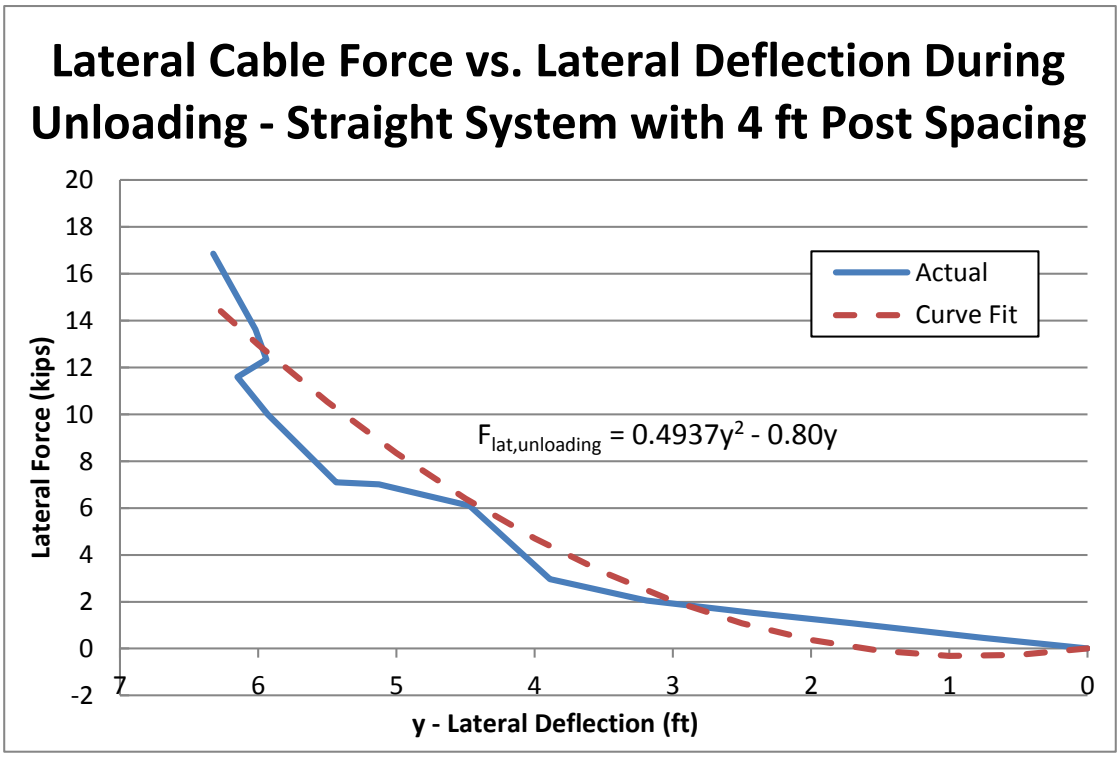

Figure C-2. Lateral Cable Force vs. Lateral Deflection Unloading Fitted Curve. – Test No. CS-2

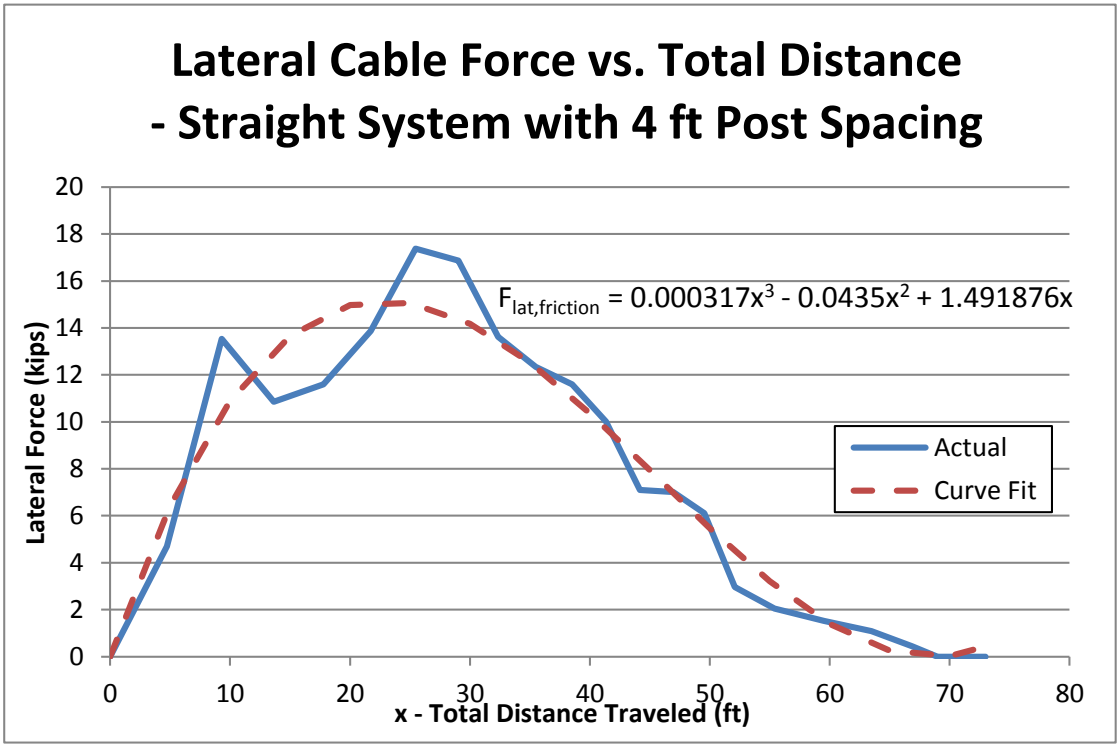

Figure C-3. Lateral Cable Force vs. Total Distance Fitted Curve. – Test No. CS-2

To find the energy absorbed through the internal energy in the cables, the equations for F_{lat} were integrated with respect to the lateral deflection (y) The energy during the loading of the cables ($E_{loading}$ in kip-ft) up to maximum lateral deflection (y_{max} in ft) is:

$$E_{loading} = \int_0^{y_{max}} F_{lat,loading}\, dy$$

$$E_{loading} = \int_0^{y_{max}} (-0.3496y^2 + 4.6555y)\, dy$$

$$E_{loading} = -0.1165y^3 + 2.3278y^2 + C]_0^{y_{max}}$$

$$E_{loading} = -0.1165{y_{max}}^3 + 2.3278{y_{max}}^2$$

From test no. CS-2, when $y_{max} = 6.32$ ft, then $E_{loading} = 63.6$ kip-ft. The actual loading energy was 63.8 kip-ft. The energy during the unloading of the cables ($E_{unloading}$ in kip-ft) from maximum lateral deflection is:

$$E_{unloading} = \int_0^{y_{max}} F_{lat,unloading}\, dy$$

$$E_{unloading} = \int_0^{y_{max}} (0.4937y^2 - 0.80y)\, dy$$

$$E_{unloading} = 0.1646y^3 - 0.40y^2 + C]_0^{y_{max}}$$

$$E_{unloading} = 0.1646{y_{max}}^3 - 0.40{y_{max}}^2$$

From test no. CS-2, when $y_{max} = 6.32$ ft, then $E_{unloading} = 25.6$ kip-ft. The actual loading energy was 28.8 kip-ft. The difference between $E_{loading}$ and $E_{unloading}$ is the energy absorbed during the entire impact. Therefore, 38.2 kip-ft of energy was estimated due to the internal energy in the cables. The actual energy was 35 kip-ft.

The frictional energy due to the interaction of the vehicle and cables ($E_{friction}$ in kip-ft) over the total vehicle distance traveled (x_{max} in ft) is:

$$E_{friction} = \mu \int_0^{x_{max}} F_{lat,friction}\, dy$$

$$E_{friction} = \mu \int_0^{x_{max}} (0.000317x^3 - 0.0435x^2 + 1.4919x)\, dx$$

$$E_{friction} = \mu[0.00007925x^4 - 0.0145x^3 + 0.746x^2 + C]_0^{x_{max}}$$

$$E_{friction} = \mu[0.00007925{x_{max}}^4 - 0.0145{x_{max}}^3 + 0.746{x_{max}}^2]$$

Where μ is the coefficient of friction between the cables and vehicle.

In test no. CS-2, when $x_{max} = 73$ ft and $\mu = 0.08$, then the lower bound for $E_{friction} =$ 46.8 kip-ft. When $x_{max} = 73$ ft and $\mu = 0.12$, then the upper bound for $E_{friction} = 70.2$ kip-ft. The actual lower and upper bounds for the frictional energy between the cables and vehicle were 47.1 kip-ft and 70.6 kip-ft.

These equations give estimations of the internal cable and frictional cable-to-vehicle energies when only x_{max} and y_{max} are known. However, these equations are only applicable to straight, 3-cable, low-tension cable systems with a 4-ft (1.2-m) post spacing. Additional verification and validation is needed to determine if they can be applied to other cable systems.

END OF DOCUMENT